National Diagnostic Working Group (NDWG) for ICF/ HED: The Whole Exceeds the Sum of Its Parts

J. D. Kilkenny,[a] W. W. Hsing,[c] S. Batha,[b] G. A. Rochau,[d] T. C. Sangster,[e] P. M. Bell,[c] D. K. Bradley,[c] H. Chen,[c] J. A. Frenje,[f] M. Gatu-Johnson,[f] V. Yu Glebov,[e] R. J. Leeper,[b] A. J. Mackinnon,[c] S. P. Regan,[e] J. S. Ross.[c]

a) General Atomics, San Diego, California 92186, USA
b) Los Alamos National Laboratory, Los Alamos, New Mexico 87545, USA
c) Lawrence Livermore National Laboratory, Livermore, California 94551-0808, USA
d) Sandia National Laboratory, Livermore, California 94551, USA
e) Laboratory for Laser Energetics, University of Rochester, Rochester, New York 14623, USA
f) Plasma Science and Fusion Center, Massachusetts Institute of Technology, Cambridge, Massachusetts 2139, USA

This work performed under the auspices of the U.S. Department of Energy by General Atomics under Contract 89233119CNA000063 and by Lawrence Livermore National Laboratory under Contract DE-AC52-07NA27344. IM release number is: LLNL-JRNL-840087-DRAFT.

ABSTRACT

The National Diagnostic Working Group (NDWG) has led the effort to fully exploit the major inertial confinement fusion (ICF)/high energy density (HED) facilities in the US with the best available diagnostics. These diagnostics provide key data used to falsify early theories for ignition and suggest new theories recently leading to an experiment that exceeds the Lawson condition required for ignition. The factors contributing to the success of the NDWG, collaboration and scope evolution, and the methods of accomplishment of the NDWG are discussed in this paper. Examples of collaborations in neutron and gamma spectroscopy, x-ray and neutron imaging, x-ray spectroscopy, and deep-ultraviolet Thomson scattering are given. An abbreviated history of the multi-decade collaborations and the present semi-formal management framework is given together with the latest National Diagnostic Plan (NDP).

CONTENTS

To update a TOC: press left click, put cursor in table, choose update table.
To update table and figure numbers, left click on (e.g.) Figure 1 and choose update field.
If heading numbering disappears, send to me, trivial to fix.

1. INTRODUCTION: COLLABORATION ON DIAGNOSTICS FOR HED SCIENCE 5

2. TECHNICAL EXAMPLES OF SUCCESSES OF THE NDWG 6

2.1 Gated X-Ray Imaging with Microchannel Plates (MCP) 6

2.2 Neutron Spectroscopy 12

2.2.1 Neutron Time-of-Flight Diagnostic for OMEGA, NIF (and Z) 15

2.2.2 Neutron Spectroscopy with Magnetic Recoil Spectrometer and Time Resolution 19

2.3 The "SLOS/hCMOS" Work of the NDWG 20

2.3.1 Multiple Time-Gated Hybridized CMOS Arrays 21

2.3.2 Gated Laser Entrance Hole Imager Application of hCMOS FPA on NIF and LMJ 22

2.3.3 Time-Resolved X-Ray Diffraction And Opacity Diagnostics Using hCMOS FPAs on NIF 24

2.3.4 Pulse- DIlation Technology: Application to Dilation X-Ray Imager (DIXI) 24

2.3.5 Pulse Dilation Technology: Application to World's Fastest Photomultiplier 25

2.3.6 Pulse Dilation and hCMOS Applied to a SLOS Detector 25

2.4 X-Ray Spectroscopy 27

2.4.1 Collaborations in X-Ray Spectroscopy: Early Days 27

2.4.2 High-Resolution X-Ray Spectroscopy: X-Ray Streak Cameras, hCMOS, and SLOS 28

2.5 VISAR (Velocity Interferometer System for Any Reflector) 31

2.6 Wolter X-Ray Imager for Z and NIF 33

2.7 Neutron Imaging 34

2.8 Ultraviolet Optical Thomson Scattering (UVTS) 36

3. EARLY DAYS: COLLABORATIVE HED DIAGNOSTICS 1993–2008 37

3.1 The High-Temperature Plasma Diagnostic Conference and Proceedings of SPIE 37

3.2 Diagnostics for the NIF Conceptual Design Review (CDR). 39

3.3 Post-CDR NIF Diagnostic Activities 40

3.4 Diagnostic Vacuum Insertors and Manipulators 42

4. THE NIF DIAGNOSTIC WORKING GROUP, 2009–2014 44
4.1 Diagnostic Status at start of NIF Operations: A Need to Evolve 44
4.2 National Diagnostic Meetings, 2009–2014 44
4.3 Overview of Non-Ignition HED-Based Diagnostics 47
4.4 Commissioning the Set of NIF Diagnostics Installed by 2014 50
4.4.1 Directly Driven Capsules: "Exploding Pushers" 50
4.4.2 Indirectly-Driven Single-Shock Implosions 52
4.4.3 4.4 List of Diagnostics Operational by ~ 2014, ... 53
4.5 The National Diagnostic Plan (NDP): 2015 55
4.6 Expert Review of the NDP 2015 56

5. NDWG MEETINGS 2015–2021 57
5.1 The Tenth National Diagnostic Working Group Meeting 57
5.2 The Eleventh National Diagnostic Working Group Meeting 57
5.3 The Twelfth NDWG Meeting 58
5.4 The Thirteenth National Diagnostics Working Group Meeting 58
5.5 The Fourteenth National Diagnostics Working Group Meeting 59
5.6 The Fifteenth National Diagnostic Working Group Meeting 59

6. THE NATIONAL DIAGNOSTIC PLAN (NDP) FOR HED SCIENCE, SEPTEMBER 2021 59

7. CONCLUSION 62

ACKNOWLEDGEMENTS 65

APPENDIX A. DIAGNOSTIC ACRONYMS 66

1. INTRODUCTION: COLLABORATION ON DIAGNOSTICS FOR HED SCIENCE

The National Nuclear Security Administration (NNSA) has made significant investments in major facilities and high-performance computing to successfully execute NNSA's Stockpile Stewardship Program (SSP) and exceed the Lawson criterion required for ignition.[1] Sophisticated diagnostics provide the connection between the experiments done on the facilities and the simulations done on the supercomputers. It is essential to continuously advance these diagnostic capabilities to improve the detail and accuracy of the data to not only reveal new, previously unknown information about complex systems, but also to provide the information needed to truly advance learning through the falsification of hypotheses.[2] Indeed, data acquired from the continuous improvement of diagnostics on the National Ignition Facility (NIF) falsified early theories for ignition and aided in the development of new theories.

High-energy density (HED) diagnostics on the three major US inertial-confinement fusion (ICF) facilities—NIF, OMEGA, and Z—have benefited from multi-decade inter-laboratory collaborations, enhanced by numerous publications mainly in this journal. Apart from meeting at the High Temperature Plasma Diagnostic (HTPD) conference, the genesis of these collaborations came in 1993, when the so-called Joint Central Diagnostic Team (JCDT) took responsibility for the initial diagnostics plan in the NIF conceptual design report (CDR). A decade and a half later, a limited and clearly inadequate set of diagnostics, approximating those in the CDR, was in use when NIF started full operations in 2009.

To respond to the increasing sophistication of ICF and HED experiments on the NIF, the expert scientific community undertook national cooperative diagnostics, with major significant assignments agreed to by an inter-laboratory team calling itself the NIF Diagnostic Working Group. In 2015, to formalize the collaboration and expand the scope of this work to other major ICF facilities in the US and France, the NNSA directed the formation and scope of the National Diagnostics Working Group for HED Science (NDWG). The NDWG is a patently successful, multi-institutional alignment of the HED diagnostic development effort with over a dozen institutions, including three in Europe, and involving well over 100 diagnostic experts. The group has met at least annually from 2009 to 2021; a leadership team with the authority to make institutional commitments meets multiple times per year to plan and track progress. The purpose of the NDWG is to encourage inter-laboratory cooperation and innovation and develop and steward a coordinated national diagnostic plan (NDP). The NDP defines diagnostic-development activities across the major ICF facilities, identifies technical challenges and opportunities, and schedules developments. The NDP is endorsed and funded by NNSA through the ICF and assessment-science program elements within the Office of Experimental Sciences and is reassessed annually to adjust to technical progress and the evolving needs of the national HED program. Version releases are published online.

The NDWG is a remarkable achievement in cooperation, showing that the whole is more than the sum of its parts. This paper comments on the NDWG and its predecessor, the Joint Central Diagnostic Team (JCDT).

Section 2 lists some NDWG achievements commenting on success factors, as shown in Table I. First and foremost is collaboration: agreed diagnostic responsibilities, coordinated schedules, attracting outsiders including industry result. Second a flexible scope especially as ideas and theory are falsified and new/better diagnostics are invented. Third copious publication to share data and criticism. About three generations of

scientists and engineers have worked these HED diagnostics.

Section 3 summarizes diagnostic collaborations from 1993–2008.

Section 4 describes the formative years of the NDWG, 2009–2014, covering the formalization of the NDWG and its NDP.

Section 5 covers subsequent work up to the NDWG's 15th plenary meeting in December 2021. The methods of accomplishment, in the generation of a living National Diagnostic Plan are described as indicated in Table I.

Section 6 summarizes the National Diagnostic Plan for HED science as of September 2021

Section 7 reviews and concludes the paper.

Factor	Attribute
Collaborations: NNSA Labs, Industry, University, Europe	Best facility for the job Agreed diagnostic responsibilities Coordination Attracts outside experts
	Coordination
	Attract
Scope expands with time	Falsifiability–upgrade, new diagnostics Copious publications
Methods of accomplishing a living National Diagnostic Plan	Targeted NDWG parallel sessions Large NDWG plenary meeting Management resources NDWG management group

Table I. Factors and Attributes for NDWG success.

2. TECHNICAL EXAMPLES OF SUCCESSES OF THE NDWG

This section provides examples of highly successful collaborations on HED diagnostic development, several instances of falsification of theories, and cases of unanticipated science leading to further development of diagnostics.

2.1 Gated X-Ray Imaging with Microchannel Plates (MCP)

Because a picture is worth a thousand words, gated microchannel plate (MCP) x-ray imaging is now used at nearly every HED facility worldwide. The history of this technology, which arose from the HTPD, is

an excellent example of collaboration, especially with industry. The origins of this story precede the NDWG but set the model for NDWG collaboration. Notably, MCP development has continued for three decades by LLNL, LANL, LLE, SNL and industry as can be seen in Table II. Faster x-ray gating is now done by pulse-dilation (PD) technology (Section 2.3.4), but gated MCP technology is adequate for most HED experiments and is more used for HED measurements than any other diagnostic.

Year	Technology	Instruments	
		Nova/NIF	Omega/Z
1983	MCP Coating		
1985	Microstrip on MCP Auston switch Solid state pulser Pulse forming module 6 ohm pulsers	4 open strips 4 strips	
1990	MCP temporal model Long pulse theory	MAX module	Serpentine MCP 30 psec MCP
1995	UV laser calibration CCD readout	Flexible gated MCP	MCP on Kirkpatrick-Baez (KB)
2000	Airbox technology Monte Carlo modeling	2x engineered GXD	Gated MCP spectrometer
2005	Microprobe/modeling Long pulse validation	4x engineered GXD	4x XRFC
2010	NIF calibration Microstrip crosstalk	4x engineered hGXI	4x Sydor framing camera
2015	ERASER		

Table II. The three-decade development effort on gated microchannel plates by LLNL, LANL, LLE, SNL, and industry. Time goes down.

Gated MCPs were investigated in the early 80s to record soft x-ray spectra.[3] The technology for coating the surface of MCPs to form electrical microstrips was critical.[4, 5] With this technology push, the experimentalists on Nova fielded, in SIMs (Section 3.4), gated MCPs to record pinhole images of HED plasmas.[4] This was made possible by a company[6] supplying a high power, jitter-free, compact, and reliable pulse generator for the MCP.[7] A subsequent series of papers in the late 80s demonstrated this capability.[8]

LLNL benefitted greatly from collaborating with LLE and OMEGA's much higher shot rate[9] and was able to demonstrate a seminal result in Figure 1, where an implosion on OMEGA was followed in time as the voltage pulse swept along the length of the meander microstrip coated on a microchannel.[10] This data is so spectacular that a senior HED experimentalist asked if it were a simulation upon seeing it. An elegant feature of this design is that although the stagnation of the implosion is much brighter than early emission from the laser as it lights up the glass capsule in x-rays, the attenuation of the voltage pulse (and gain) as it propagates along the microstrip compensates. For most applications, however, this droop in gain is a drawback requiring careful calibration.

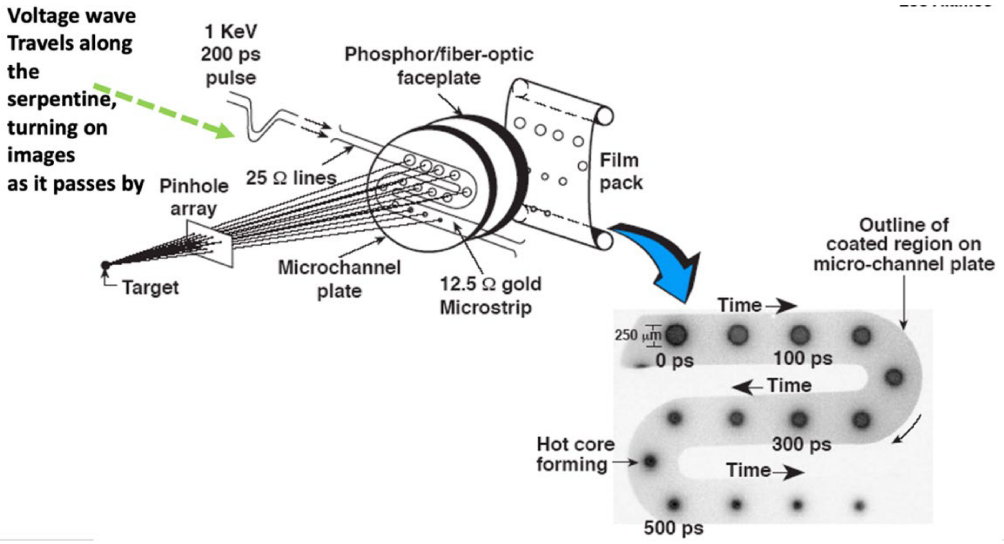

Figure 1. The genesis of the NDWG. The cartoon shows how the travelling voltage wave along a transmission line coated onto a MCP forming an x-ray movie of an implosion on OMEGA. The data is real.

Another notable outcome of LLNL/LLE collaboration was the demonstration of 30 psec gating by scaling the L/D micropore length/diameter ratio with the thickness of the MCP, taking advantage of the high shot rate on OMEGA for testing.[11, 12] Further reductions in gate time by going to an even thinner MCP are impractical due to fragility, x-ray straight-through, and lower gain, but are achieved by pulse dilation (Section 2.3.4).

A well-engineered version of gated MCP, the so-called MAX modules, was made to be fitted on chamber-mounted diagnostics on Nova.[10]

In the early nineties, LLNL developed the Gated X-ray pinhole cameras Detectors (GXD) to operate in the SIMs (Section 3.4) on Nova and potentially the TIMs at OMEGA. Initially the final recording of the gated MCPs was onto film. A major improvement was to couple a CCD to the output.[13] Some users needed a flexible gate pulse 100 psec to 500 psec and so LLNL worked with industry for a suitable voltage pulse generator.[14]

In a good example of interlab collaboration, LANL took over major responsibilities for the gated MCPs on Nova, OMEGA and initial NIF. LANL also built a dual MCP system for LLE to use on a Kirkpatrick Baez x-ray optic on OMEGA.[15]

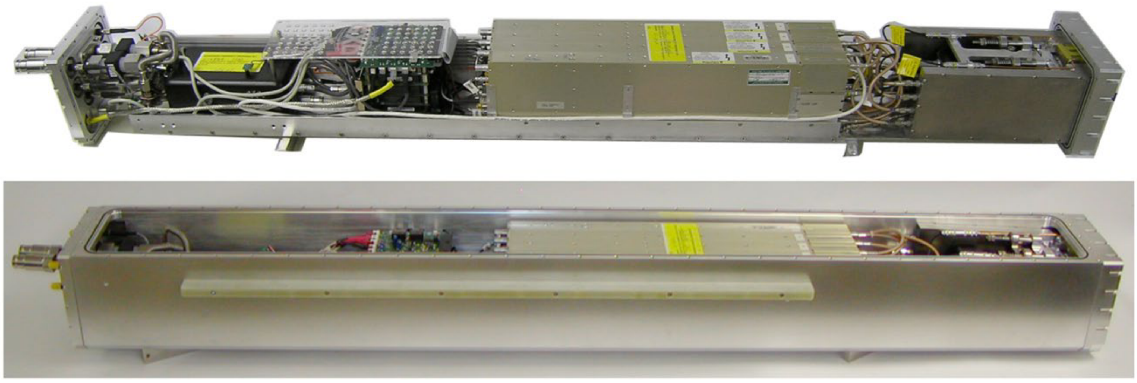

Figure 2. The gated x-ray detector pulled outside the air box (top) and within (bottom). Various types of imaging and spectrometer nosecones can be placed in front of the detector when the instrument is in the NIF vacuum chamber. These gated x-ray detectors are each designed to fit within an aluminum airbox and are fitted with an array of environmental housekeeping sensors. These instruments are significantly different from earlier generations of gated x-ray images due, in part, to an innovative impedance matching scheme, advanced phosphor screens, pulsed phosphor circuits, precision assembly fixturing, unique system monitoring, and complete remote computer control.

An innovation for the NIF was to field the GXD and its electronics in an "airbox" to protect it from the vicissitudes of chamber vacuums as well as system generated EMP. The airboxes were engineered to great effect to move around to any manipulator on NIF. Well-engineered versions of the GXD were constructed by LANL for early NIF.[16]

NIF now has eight air-box gated MCP detectors operable in any DIM location. There are four Gated X-ray detector (GXDs) with CCD readouts and four Hardened GXD (HGXD's) with film readout. Imagers or spectrometers are normally in front of the detector. LLE now has eight gated x-ray framing cameras. Four are called XRFC, which were assembled by LLNL: two have 30 psec gates and two have 100 psec gates. The LLNL–LLE developed technology was transferred to US industry and as a result OMEGA has four single frame cameras (SFC) built by Sydor Technologies Inc.[17] They provide 2D spatially time-resolved frames or 1D spectrally resolved images of target features. Their systems can be configured with fast or slow detection heads for frames ranging from 40 ps to 1000 ps in duration. OMEGA's GMXI gated camera came from LANL.

To improve ease of operation, an array of pinholes is used to make alignment easier and to also allow a time integrated detector, image plate to be placed around the gated detector as shown in Figure 3 and described by a LANL led paper.[18] Modern pinhole arrays have diamond looking signature pattern on the center to quantify mis-pointing of the snout.

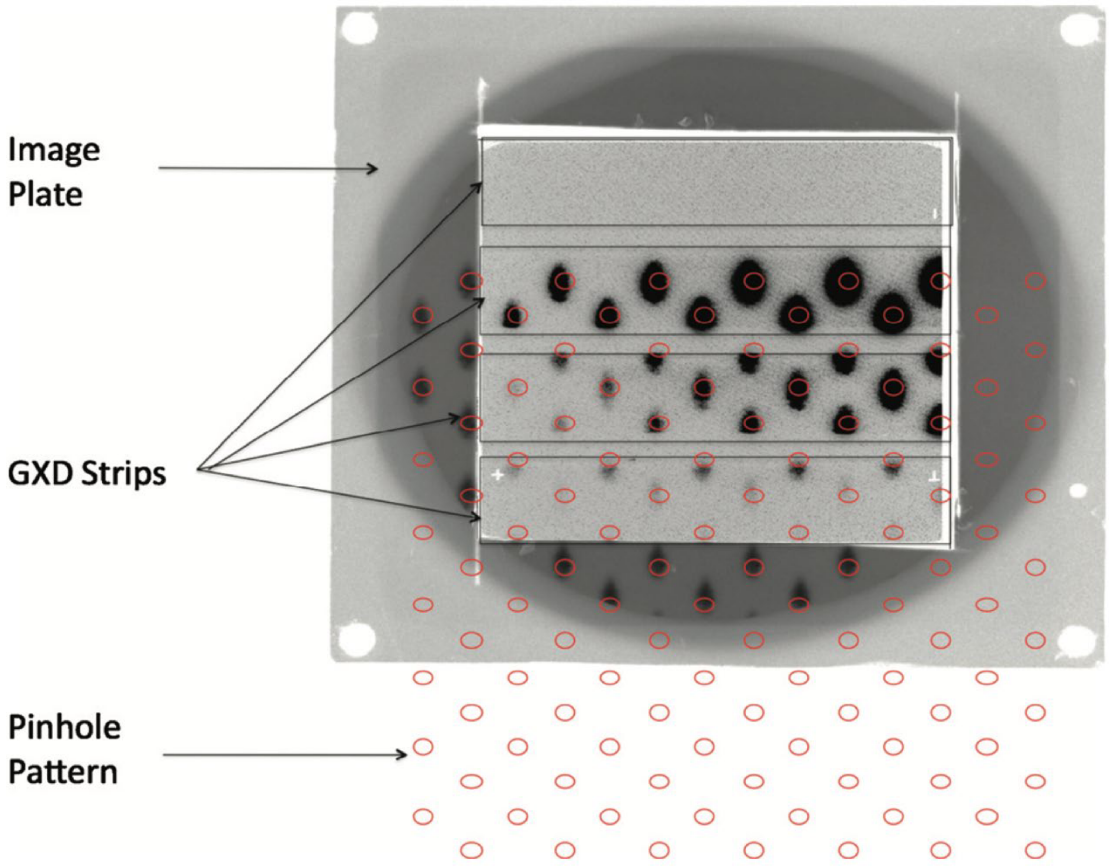

Figure 3. Image plate record surrounding the corresponding GXD image and with an overlay of the pin hole array.

The longer timescales on Z relaxed their need for ~ 100 psec gating, and several instruments with nsec gating of MCPs were in place on Z by the late nineties.[19] SNL accurately modelled the time response of MCP gain introducing the new technology of electrical microprobe.[20, 21]

Extensive use of MCP detectors on NIF unearthed nuances. Each conducting microstrip coated onto the MCP, together with the dielectric MCP and its rear-surface ground plane, acts as a transmission line: voltage is transmitted along the strip as a travelling electromagnetic wave. Because of the strong dependence of MCP gain on voltage, small variations in voltage along the microstrip can lead to substantial variations in gain. When more than one microstrip is used, the multiple propagating waves may interact, inducing currents and voltages on neighboring strips. Any induced signals also travel along the microstrip, and as a result, the effective pulse voltage and propagation velocity may be altered. LLNL collaborated with SNL which used slower gating of MCP cameras[21] to understand and develop mitigation of the effects of cross timing by careful relative strip timing.[22]

An even more subtle effect is that a MCP is slightly responsive to x-ray signals arriving before a gate pulse. Although gated MCPs had been used for decades increasingly sophisticated HED experiments revealed this kind of artefact. These x-rays liberate one or more electrons. While one might have expected any early electrons to dissipate by either leaving the MCP surface or being reabsorbed, it appears that some are trapped at the surface of the MCP. As a result, when the voltage pulse passes at a later time, those

trapped electrons are amplified, producing additional background signal. Mitigation can be by a small eraser D.C. field (Figure 4) applied to pull photo-electrons that are formed before a gate pulse is applied, away from the MCP.[23]

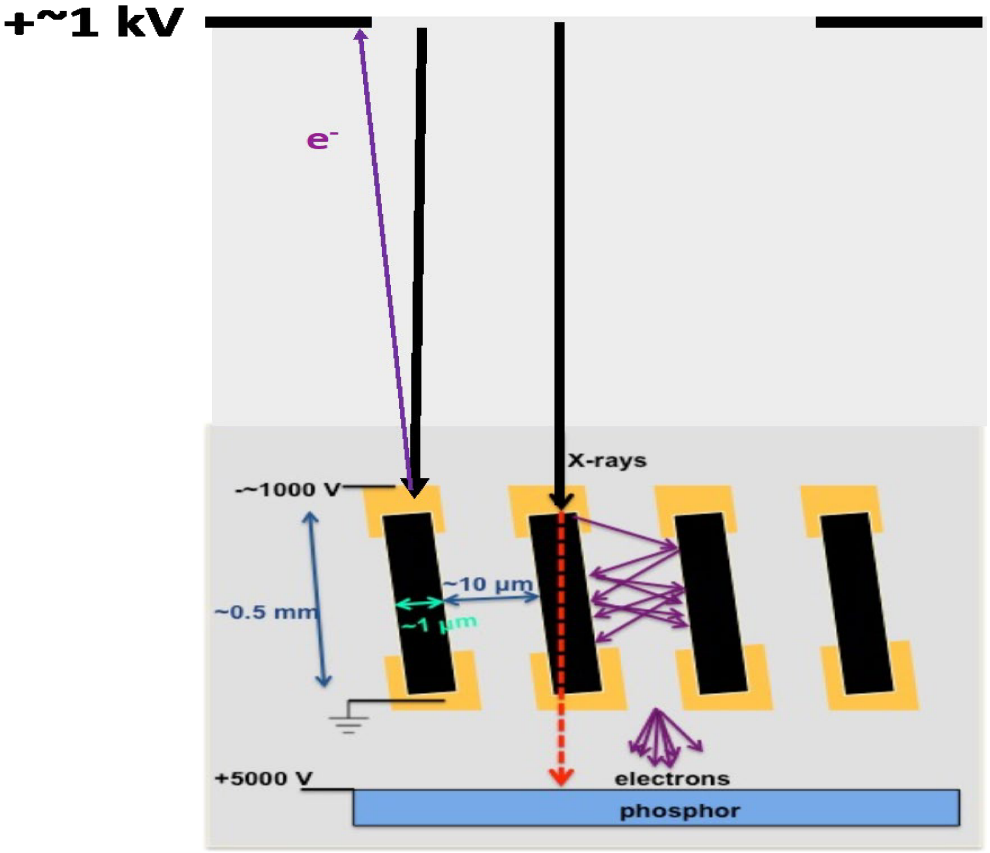

Figure 4. Schematic diagram of Early Radiation Artifact Suppression Electrode Rig (ERASER).[23]

There is significant attenuation of the MCP gain from a small drop in voltage and a large drop in gain as the voltage pulse propagate along the strip requiring a gain calibration against position along a strip. LLNL and CEA collaborated on complementary methods of calibration of the "droop" in MCP gain along the necessarily resistive microstrip.[24, 25]

Gated MCP imagers are widely used: one of many uses is to tune the symmetry of hohlraum drive. Importantly they have been used to falsify simulations of implosions and improve the physics model. For example, to match the measured implosion symmetry, models for heat transport[26, 27] and the cross-beam-energy-transfer[28] are added. The images also reveal critical aspects that were previously underestimated in modeling. For example, gated imaging has shown that the capsule support structure[29, 30] and the capsule fill tube[31, 32] have detrimental effects on implosions, that are underestimated by simulations. Similarly, imaging show the effects of under predicted mix.

In summary, gated MCP detectors are remarkably useful in HED applications. They do have limitations arising from relatively low saturation of gain, and low detective quantum efficiency but their use at almost all HED facilities is testament to their utility. Notably the present status is due to shared ideas and resources from LLNL, LLE, industry, SNL, CEA and LANL which has

taken about 30 years. Although the gated MCP instruments development started before the NDWG the multi lab, industry and international collaboration was a marvelously productive collaboration and set a model for the NDWG.

2.2 Neutron Spectroscopy

Nuclear diagnostics for inertial confinement fusion (ICF) plasmas are comprehensively reviewed by Frenje.[33] Behind Frenje's opus there is an interesting history that drove the nuclear diagnostics installed on the major HED facilities. In a burning plasma early simulations/theory predicted isotropic yield and areal density and a primary neutron spectral width ~ $T_{ion}^{½}$.[34] Brysk's paper suggests measuring T_{ion} from the spectral width of the primary neutrons: the conceptual simplicity of measuring T_{ion} with nToFs drove their installation on the early HED lasers as well in the NIF CDR.

Areal density can also be obtained from neutron spectroscopy. The areal density of DD implosions can be measured by secondary DT neutrons,[35] but only for imploded areal density less than 0.1 g/cm^2 and fusion of deuterium fuel. This means secondary neutron spectroscopy for areal density measurements was suitable for Nova, Z and OMEGA but not for NIF ignition scale implosions. Consequently, effort in the nineties concentrated on single-hit LaNSA arrays at Nova.[36, 37] The sensitive neutron spectrometer (SNS) was developed in the waning days of the Nova laser and conceptually similar to the LaNSA array. It was transferred to the OMEGA laser soon after Nova was shut down and operated continuously as the MEDUSA array on all of the neutron producing experiments OMEGA until it was decommissioned for the construction of the OMEGA EP laser beginning in 2006.

Measuring higher areal density is "formidable." The use of down-scattered neutrons for areal density was proposed by Azechi,[38] and is illustrated by Figure 5, but as Azechi says it is "a formidable task to measure the lower energy scattered neutrons in the presence of and importantly *after* a large numbers of un-scattered neutrons." Quantitatively it is hard because even a large areal density of, say, 1 gm/cm ^{2} of compressed DT only scatters ~20% of the 14 MeV primary neutrons and over a 11MeV neutron spectral width.

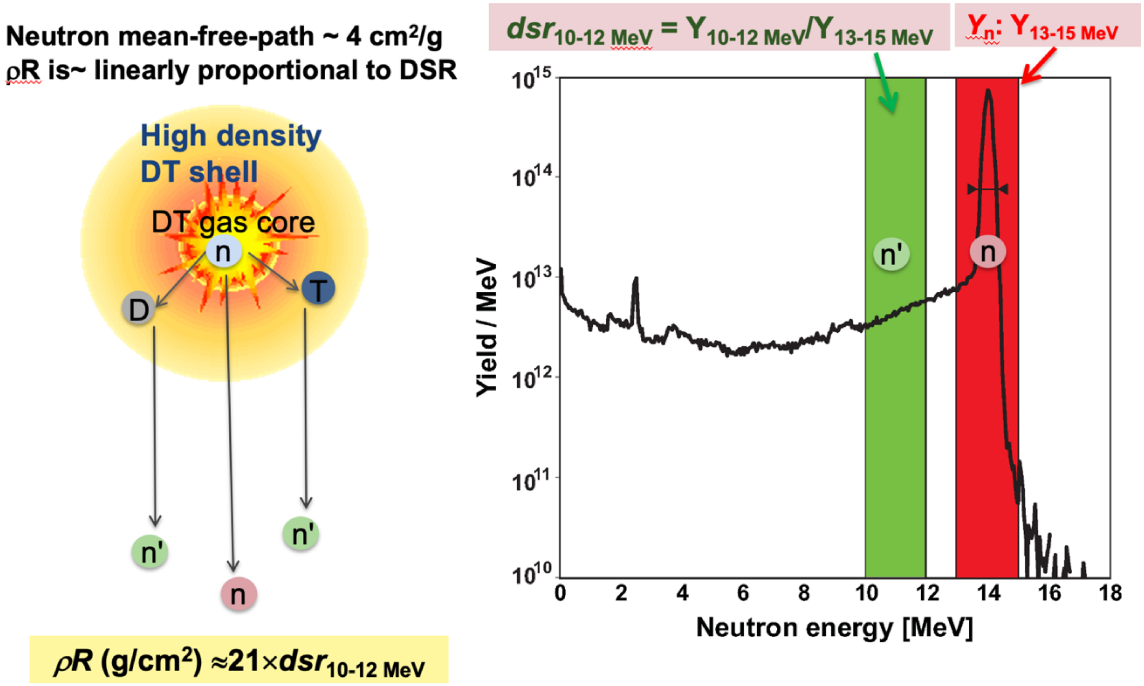

Figure 5. The physics of down-scattered neutrons. If a primary 14 MeV neutron scatters off surrounding deuterons (D) or tritons (T) it loses energy according to its scattering angle. The down-scatter ratio (DSR), defined on the right is a measure of the areal density of surrounding D &T.

The physics of using down-scattered neutrons to measure areal density of DT is shown in Figure 5. MIT scientist and LLE scientists started this "formidable task" on OMEGA and NIF using a magnetic recoil spectrometer (MRS) and one spectrally resolving nToF detailed in sections 2.2.2 & 2.2.1 respectively. NIF management scrutinized the reason for complementary measurement techniques. Popper's reasoning[2] about falsifiability eventually held sway because measuring an observable two different ways could falsify the measurements. Also two nToFs were sanctioned. NIF management asked why two nToFs were needed, but as the first years of NIF cryogenic implosions were disappointing the need for more diagnostics was becoming apparent. It is very interesting that initially the two nToFs systematically gave different results as shown in Figure 6 (the date code for the NIF shot number shown is yy/mm/dd) although MRS generally agreed with SpecA, which is the 20 m distance nToF in the neutron alcove. It was initially suspected that there was a difference in calibration and so the detectors were interchanged but to no avail, areal density was anisotropic. The assumption of areal density isotropy had been falsified.

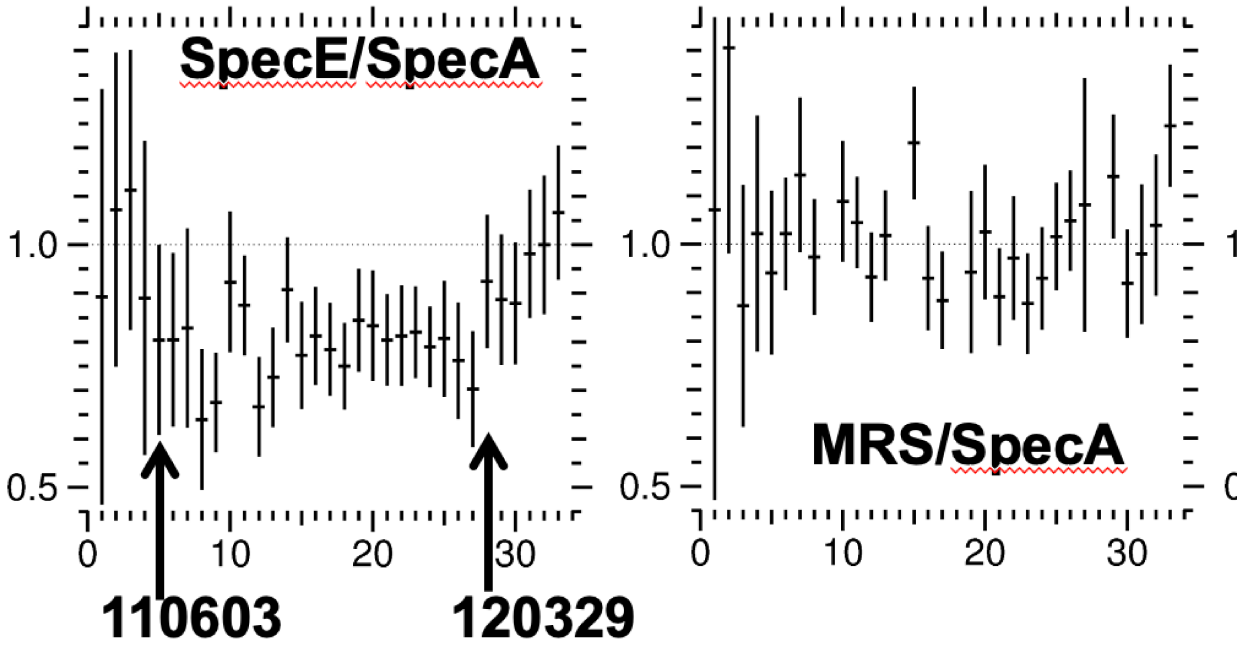

Figure 6. Ratios of the down-scattered ratios DSR from three diagnostics SpecE, SpecA and the MRS, plotted against NIF shot number from June 2011(110603) to March 2012 (120329). At the time it was thought, incorrectly, that the calibration of SpecE might have been systematically low.

Even unscattered yield was shown to be anisotropic. Initially yield on NIF was measured by one Zr and one Cu threshold Neutron Activation Detector (NAD). But an areal density anisotropy was measured by a diagnostic, flange NADs, measuring the un-scattered yield in 18 different directions[39] and later in 48 different directions RTNADS.[40] Falsification of the theory of symmetry led to two more generations of nToF diagnostics as shown on, an expanded scope that took well over a decade.

With the wisdom of hindsight, it is clear a poor implosion will have a lower areal density at the position of say the capsule fill-tube, causing a drift motion of the burning plasma and a consequent lower areal density in that direction. Such drift motion was first observed as shifts in neutron spectrum mean peak energy,[41] initiating an effort to understand the seeds for and effects of directional motion on NIF implosions.

There is as interesting story about T_{ion} as measured using Brysk's formula for spectral width. A LANL scientist[42] and LLNL theoreticians[43] realized that a variance of the drift velocity along the line of sight of a burning plasma adds to the Brysk neutron spectral broadening. Experimentalists[44] compared the spectral broadening of the DD to the DT neutrons verifying this theory. Moreover, in a series of beautiful experiments a deliberate drive asymmetry was imposed on a series of implosions showing that the Brysk derived T_{ion} varied with direction of observation.[45] So much for a scalar T_{ion} !

Again, with the wisdom of hindsight, the reliance on theory for complicated, unstable implosions was too optimistic but careful neutron spectroscopic measurements with input from LLE (and well-diagnosed DD and DT implosions on OMEGA), LANL, MIT as well as LLNL eventually improved our understanding. Central to the use of neutron

spectroscopy to advancing our understanding of implosions was the diagnostic collaborations between LLNL, LLE, MIT and LANL. The nToF story below also emphasizes this.

2.2.1 Neutron Time-of-Flight Diagnostic for OMEGA, NIF (and Z)

This is the story of the collaborations over two decades, producing three generations of nToFs for NIF as illustrated in Figure 7.

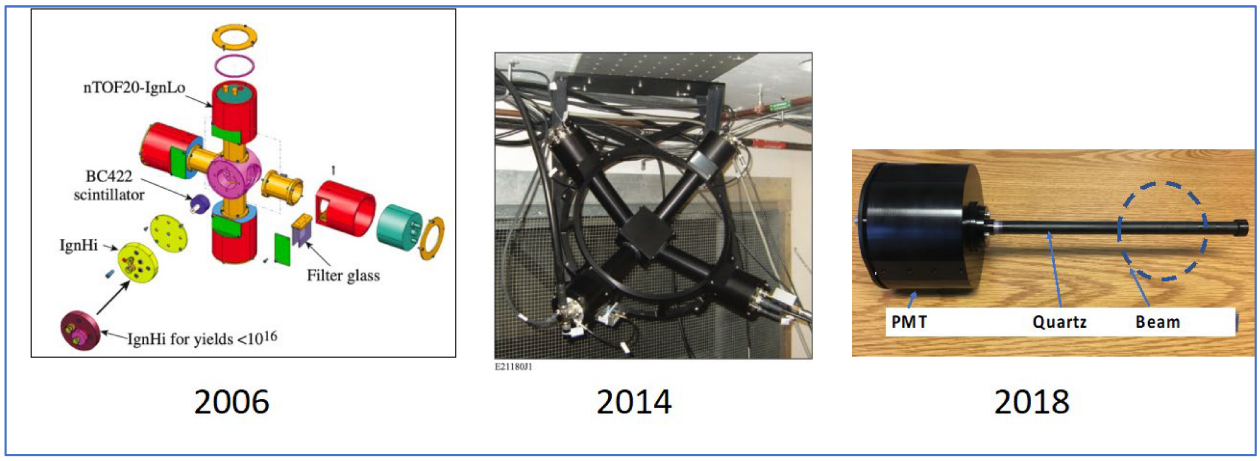

Figure 7. The three generations of neutron time-of-flight detectors (nToF) used on NIF.

For transitory HED experiments, nToF measurements are readily interpreted as a neutron spectrum as shown from a 1976 LLNL viewgraph (Figure 8). It is interesting that the detector building shown is far ~ 80m, from Argus one of the earliest implosion lasers, because of the slow detection (PMT and scopes) technology available in 1976. It was because of the simple yet incomplete argument in Figure 8 that nToFs were included in the NIF CDR.

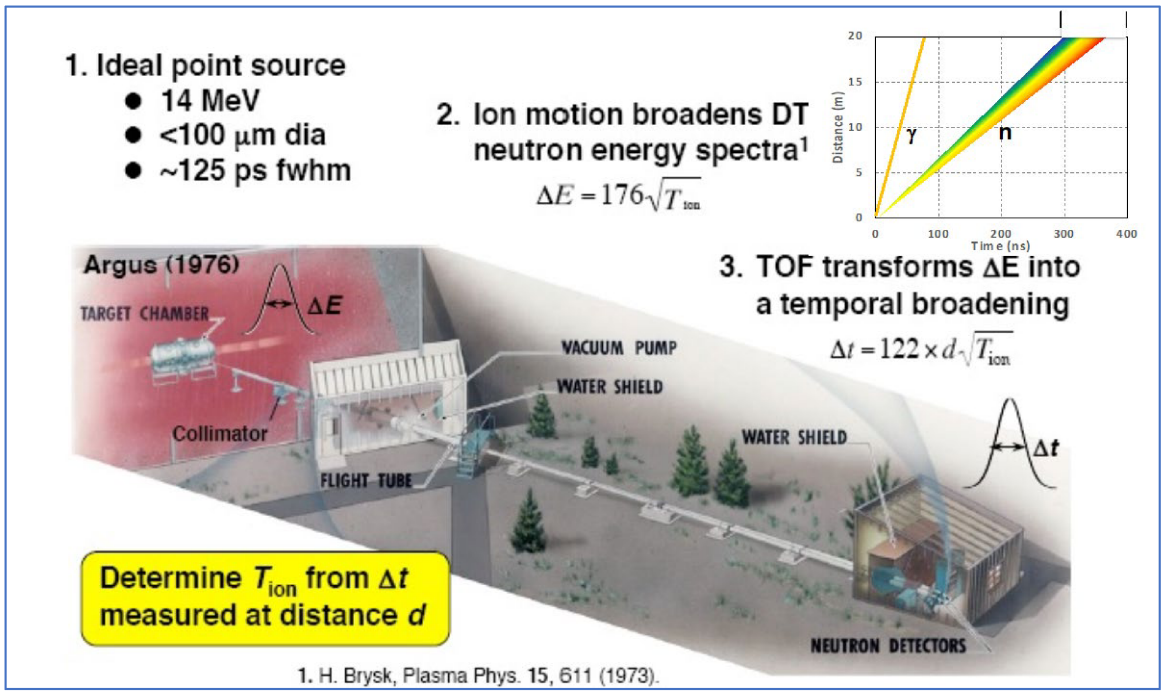

Figure 8. Cartoon from 1976 illustrating the simple yet incomplete physics argument for determining ion temperature from the broadening of neutron arrival times at a distant neutron detector. In 1976 the Argus laser in B381 at LLNL was producing neutrons, but slow detectors required a long flight path.

Nowadays, nToFs are vital to measure areal density. Azechi and Cable[38] had shown that areal density could be measured by down scattered ratio (DSR). Hatchett[46] (private communication) carefully defined DSR = Yield $_{12\text{-}10\ MeV}$/ Yield $_{15\text{-}13\ MeV}$ as shown in Figure 9. (Courtesy J Caggiano & D Wilson). Hatchett realized that 10 MeV stays above the TT neutrons and 12 MeV is below Brysk broadening.

However, it is a "formidable task," to quote Azechi, to make a tiny arrival rate measurement after a much larger signal, because of PMT saturation, scintillator slow decay, cables etc. Another formidable task is to make measurements over neutron yields from 10^{11} to 10^{18}. This is the amazing story of how the NDWG achieved this and much more. For the NIF CDR, this was thought to be too hard and tertiary neutrons were to be used.

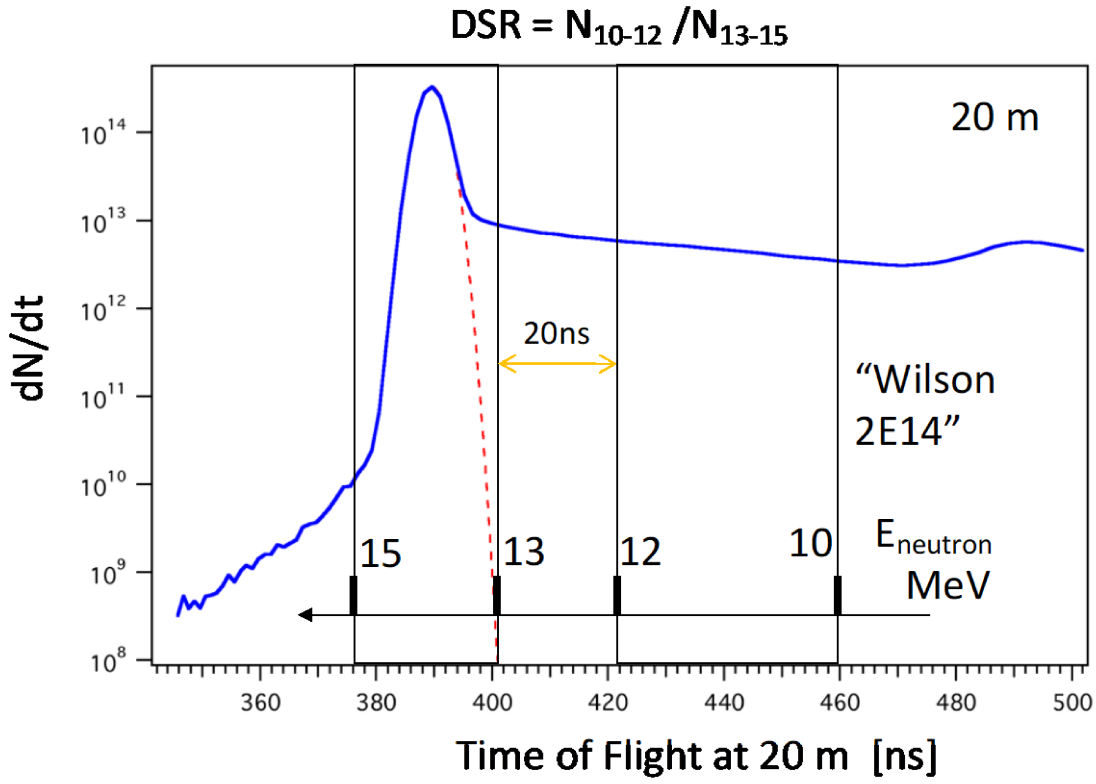

Figure 9. Calculated neutron spectrum versus arrival time at ~20m, showing the 15 to 13 MeV region and the 12 to 10 MeV region used to calculate the down scatter ratio (DSR) The TT edge is visible ~< 9 MeV, and the broadened 14 MeV primaries ~i

A standard nToF has a scintillator with neutron induced glow detected by a PMT outputting current to a "scope". This current mode type nToF detector was used on Nova with poor accuracy.[47] The expected higher yields and T_{ion} for NIF made one nToF part of the initial CDR planning on NIF but for T_{ion} not areal density. A much faster neutron detector than used for Nova had to be designed, tested, and calibrated. LLE staff led the nToF effort on NIF through the beginning of the NDWG.

LLE first worked on speeding up and increasing the dynamic range of the PMT. For DD neutrons they worked with UK industry and AWE to enable gating out the earlier and larger(100X) DT neutron signal (or for DT neutrons, the earlier gamma signals) This mitigated the important charge depletion of the PMTs.[48] This collaboration on next-generation PMTs was also central and key to the gamma spectroscopy work of the NDWG.

The PMT also needs to be linear. The onset of PMT nonlinearity for MCP PMT occurs as the 'reservoir' of charge at the end of each channel becomes depleted after about a nano Coulomb of extracted charge. Non-linearity develops into detector saturation. Non-linear effects in the photocathode have been observed by co-authors in other detectors but has not been examined or observed in this work. Studies of the saturation and speed of MCP PMTs were carried on for several years by the collaboration.[49] Speeds of ~100 psec FWHM but with ringing were achieved for 10 mm diameter photocathodes. A great

example of LLE collaboration with AWE and industry.

Another part of the formidable task was identifying a scintillator without a long decay, as the glow from slower down scattered 14 MeV neutrons would be contaminated by glow decaying from the much larger scintillation from the earlier, 14 MeV neutrons. Standard scintillators can be as fast as 4 nsec but with a much longer-lived residual decay. More work was done on this over the next 5 years by LLE and Lauck.[50] LLNL also found an alternative scintillator with less afterglow than standard scintillators.[51]

Both labs began to realize that a well-collimated line-of-sight minimized contributions from room re-scattering of neutrons was essential for making these measurements.[52]

OMEGA was routinely producing DT and DD neutron yields calibrated against activation or CR39 counting. As a result, LLE undertook responsibility for building, calibrating on OMEGA and then transporting to NIF the first 4.5 m distance nToFs (nToF4.5) on NIF.[53,54] The linearity of the nToFs was tested on OMEGA as shown in Figure 10b.

Rev. Sci. Instrum. **81**, 10D325 (2010)

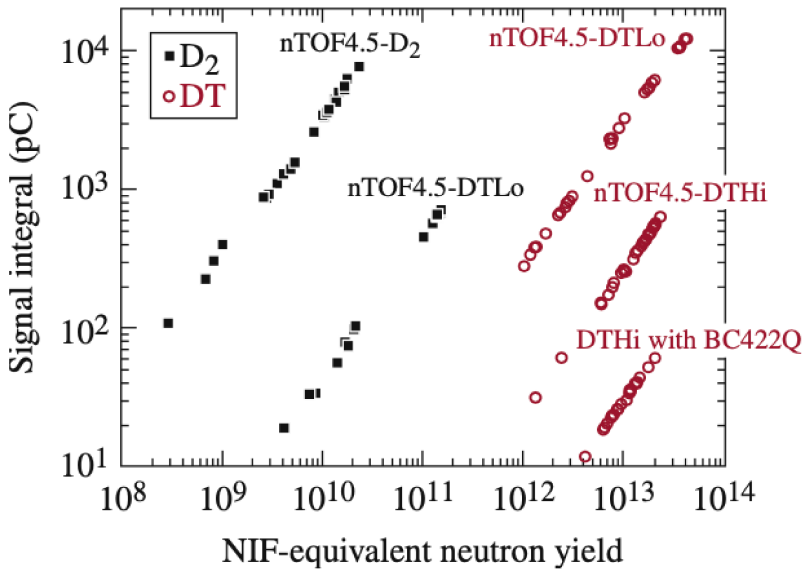

Figure 10. Summary of the nTOF4.5-K2, nTOF4.5-DTLo, and nTOF4.5-DTHi calibration on OMEGA.

A second-generation nToF detector for NIF was designed by LLNL and tested by LLE, incorporating features to reduce background signals from neutrons in the collimated beam scattered off the scintillator towards the four PMTs as shown in the Figure 8.[54] An important change shown in Figure 8 middle was to distance the PMT from the scintillator.

So after two generations of nTOF, with intense LLE- LLNL collaboration and using OMEGA as the best facility for the job of calibration, the nToFs were installed on NIF.

Even though we had made the nToFs faster, the response time of the detector was still about 4 nsec FWHM. This is about the same at 20m as the "Brysk" broadening at a $T_{ion} \sim$ 5 keV. Workable but not ideal for T_{ion} but not affecting yield nor DSR measurements. However, an important and arguably the most important physics that was coming out of the nToFs was a measurement of the drift velocity of burning plasma from the Doppler shift $dE/E_n = -2\, v_{drift} / v_n$. To measure drift velocities, four or five nToFs are needed as there are four free parameters in the shift, namely three directions plus the "Gamow" shift due to incident thermal energies of the triton and the deuteron. Also, for drift velocities ~ 10 km/sec, arrival times accuracies of ~ 50 psec are needed.

These drift velocity measurements falsified the expectation that the stagnating and burning plasma was "stationary". And it was re-discovered on both OMEGA and NIF and shared at a meeting of the NDWG.

And then in a stunning development a third-generation nToF was invented. Replacing the scintillator with a quartz Cherenkov, neutron to light transducer.[55] Neutrons can produce Cherenkov light in quartz by exciting a nucleus, which then beta decays. Unlike the atomic decay from a scintillator there is no long-lived glow: the speed of this neutron diagnostic is limited by the PMT, cabling and "scope". Although the use of quartz had been investigated decades earlier,[56] it was not until the availability of high purity quartz that the concept became viable. Notably a stimulus for LLNL to reengage this concept came from LLE via a national Diagnostic Workshop with the CEA. New or retread ideas arising from collaborations.

In the end, as illustrated in Figure 7 three generations of scientists produced three versions of the NIF nToFs. (LLE original, LLNL blackjack (middle) and quartz Cherenkov QCD) over a decade and a half. At each of the large 15 NDWG meetings and at about six nToF group meetings nToF progress was debated. There was significant input from LLE, LLNL, AWE and industry. Another marvelous story of collaborative research based on technology push. Moreover, the original motivation for one nToF measuring Tion was found to be false or incomplete, but that led to measuring areal density and large drift velocities which impact ignition. Because many nToFs give a direction, similar to a coarse picture, they suggest a direction for a fix to the drive asymmetry which causes a drift velocity. Advances in nToF have clearly discovered new implosion physics. The whimsical response to a NIF Director's question, "Why do we need two nToF's?" "Because we can't afford ten" is not quite right: NIF only has five nToFs at the moment.

2.2.2 Neutron Spectroscopy with Magnetic Recoil Spectrometer and Time Resolution

A complementary instrument to the nToF for neutron spectroscopy on OMEGA and NIF is the Magnetic Recoil Spectrometer (MRS),[57] first used on JET.[58] Neutron energy dispersion is achieved by knocking on deuterons from a nearby foil, and then magnetically analyzing them. MIT staff who implemented this technology on JET first installed an MRS on OMEGA[59] as at the time it seemed the only way to measure the low DSR on OMEGA. Installation of MRS on OMEGA was a critical learning experience for the NIF MRS. The detector is a plastic which when carefully etched can detect single deuterons. A critical nuance on the etching is the development of the coincidence counting.[60] Without it, MRS would not have worked at OMEGA.

The MRS on OMEGA first recorded DSR in 2008,[61] a major milestone. At the time, MRS was the only proven technique for measuring DSR and LLE and MIT took on responsibility for its design installation and operation on NIF. It recorded the first DSR data on NIF, as the nTOFs were at the time not capable of measuring down-scattered neutrons. The MRS worked beautifully on

the second shot and played a critical role in the development of the nTOFs.

The DSR proof of principle was done with the MRS on OMEGA by 2008 and a nearly identical spectrometer was installed on the NIF by 2011. With an MRS on each laser, it was possible to develop nTOFs on OMEGA and bring them to the NIF with the cross-calibration of the spectral sensitivity provided by the MRS.

It also provided critical guidance of the program as it provided robust data immediately. Complementary diagnostics with different weaknesses and strengths are incredibly important for HED science as measurements cannot be proven to be right but they can be falsified by a different instrument. MRS complement nToFs for DSR and "Tion " and complements NAD for yield, as, unlike nToF, MRS is an absolute-yield diagnostic. It is also incredibly important to use functioning diagnostics to validate diagnostics being implemented for similar measurements.[62] MRS also provided the first measurements of peak shifts, identifying them as signatures of drift velocity,[41] spurring the efforts to resolve these measurements in 3D using an upgraded high-precision quartz nTOF suite.

With higher yields on NIF, MRS provides better data including T_{ion} and peak shifts.[63] With adequate shielding, the MRS will continue to provide better data as we go along. [64] As yields get higher, it's critical to move the MRS behind the shield wall. Out there, the MRS performance will be an order of magnitude better in terms of S/N. Energy resolution will be better as well. MRS is still important for coverage, DSR asymmetry and 4PI DSR, especially when it is behind the shield wall for high yields and nTOFs are struggling.

This is another marvelous story of collaborations, bringing in new ideas and people and resource commitment by LLE and MIT to NIF diagnostics. And there is a great triple story on complementarity of measurements.

It is important but very difficult to time resolve the neutron spectrum from an implosion. Some concepts to use ultra-fast nToF are being developed but are a long way from implementation. Conceptually a time dependent spectrum can be obtained from MRS by a time resolving detector at the dispersion and focal plane of the magnetic spectrometer.[65, 66, 67, 68, 69] The trouble is a time skew at the focal plane that needs to be corrected for by the pulse dilation technique described in Section 2.3.4.[70] Smaller streak cameras can look at subsections of the focal plane and provide the same data as the PDDT, but at a worse quality.[71] Research continues.

2.3 The "SLOS/hCMOS" Work of the NDWG

The outstanding achievement of the NDWG is the imprecisely named work called single-line-of-sight (SLOS) hybridized complementary metal-oxide sensor (hCMOS) diagnostics/detectors. Figure 11 clarifies our terminology. There are two basic technologies (i) time-gated pixel Arrays at the Focal Plane (FPA) and (ii) diagnostic-signal Pulse Dilation (PD). On the right of Figure 11 are the diagnostics that use the two technologies, sometimes separately and sometimes together.

In this section we start with time gate focal plane arrays (FPAs) which use hCMOS technology. SNL has named these FPAs Furi, Icarus, and Daedalus (2.3.1). This nanosecond gating is fast enough for the many diagnostics shown on the top right of Figure 11. Details are in sections 2.3.1 to 2.3.3. Pulse dilation (PD) stretches diagnostic signals, allowing recording of 10 psec or less. The diagnostics that just use this technology alone are shown bottom right of Figure 11. And then in another tour de force the diagnostics that use both the FPAs and PD are shown in the middle on the right of Figure 11 2. This is all a marvelous collaboration between, SNL, LLNL, GA, LANL and CEA for HED diagnostic development: and every part of it is all well documented in the Review of Scientific Instruments.

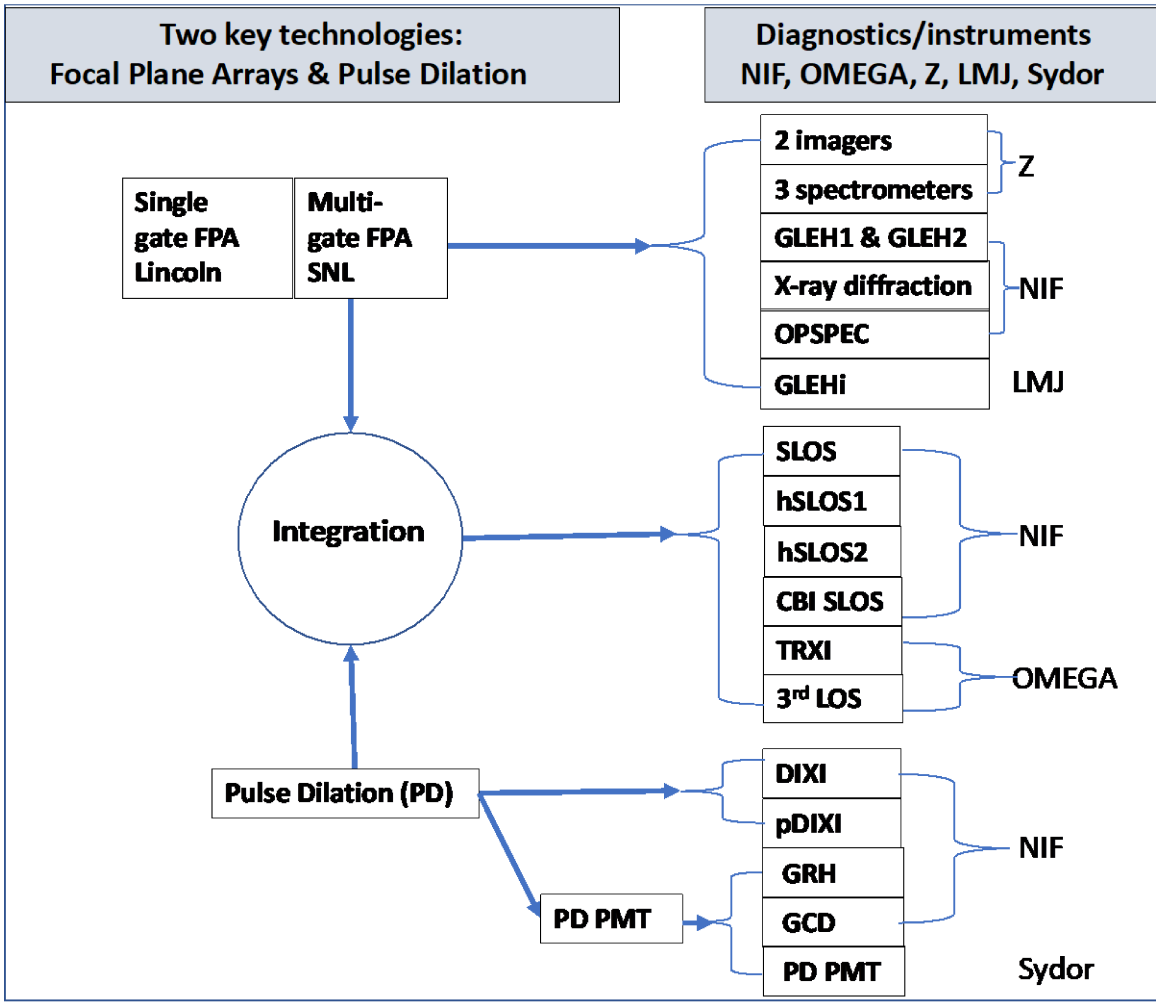

Figure 11. The two technologies—(left) time-gated focal-plane arrays and (right) pulse dilation—and the diagnostics that use either of the technologies alone (top and bottom right) or both technologies (middle right).

2.3.1 Multiple Time-Gated Hybridized CMOS Arrays

Many HED diagnostics need an array of gated light or x-ray detectors at their focal plane (FPA). About 2005, MIT–Lincoln Lab, LLNL, and LANL started work on gated FPAs. Gated MCP technology (section 2.1) had demonstrated the need for ~ 100 psec gating, guiding requirements for gating times of ~ 100psec, (PD had not been reinvented then). A 256 x 256, 250 psec, single-frame, read-out integrated circuit (ROIC) was built with limited success,[72,73,74] but resource limitation, and bump-bonding issues caused this effort to be abandoned.

At SNL on Z the time-gating requirement was more relaxed at ~ 2nsec,[75] and so an in-house foundry called MESA was used to develop a ~2 nsec-gated hybridized CMOS sensor array[76] as part of the NDWG. In contrast to the Lincoln Lab work, this was a multi-gate ROIC but with a propagating wave pixel switch. The FPA hybridized a silicon photodiode detector array, directly "bump" bonded to a CMOS ROIC. Several

generations of these so-called hybridized CMOS (hCMOS) were developed by SNL (see Table III).

FPA	Gate nsec	# frames	# pixels
Furi	2	2	448 x 1024
Hippogriff	2	2	448 x 1024
Icarus-2	~1.5	4	512 x 1024
Daedalus	1	3(6)	512 x 1024
dx microns	25		

Table III. Several generations of hybridized CMOS FPAs built at the MESA facility at SNL.

The drive electronics were eventually supplied by LLNL as was the calibration.[77] The second-generation FPA, Icarus-2, is the most utilized so far, with a total of fifty-two Icarus FPAs eventually delivered to Z, NIF, and OMEGA.[78] A third-generation FPA, Daedalus has been completed,(Q Looker ibid). Testing of Daedalus V2 has been through review and fabrication has started and it is planned to be used on the NIF gated opacity spectrometer OPSPEC.

The key issues of hCMOS arrays[76] are first the tradeoff between decreasing x-ray efficiency as hν increases, and longer photoelectron collection delay at the gated read out electronics,[76] and second the reduced dynamic range for harder x-rays when one photon produces thousands of electrons. Currently the photodiodes are Si with a hCMOS gate time 1–2 nsec—adequate for many applications (top right 11). High-energy photodiode array development has started with the design, fabrication, and testing of discrete pixelated arrays of GaAs photo detectors at SNL and design, fabrication, and testing of discrete Ge diodes at LLNL. A spinoff from the gated FPA work at SNL was a startup called Advanced hCMOS Systems Inc.

2.3.2 Gated Laser Entrance Hole Imager Application of hCMOS FPA on NIF and LMJ

The 1-2 nsec time gating of the SNL hCMOS FPAs is adequate for multi nsec phenomena such as measuring the morphology of the interior of hohlraums being irradiated by ~ 5 nsec, highly shaped laser pulses.[79]

This was first demonstrated successfully on NIF using a first-generation hCMOS sensor Furi behind an x-ray pinhole imager looking through a laser entrance hole (GLEH-1) to capture the plasma dynamic evolution from the hohlraum interior walls shown in Figure 12.[80]

An upgrade (GLEH-2) was implemented using two ICARUS hCMOS sensors which provide much improved spectral, temporal, and spatial response.[81]

In addition, an ICARUS hCMOS camera system was loaned to the CEA in 2019 for use on the Laser Mega Joule (LMJ) facility in Bordeaux, France, as part of the CEA/NNSA collaboration. It has been fitted to the LMJ DMX line of sight. This camera was implemented on LMJ as GLEHi in a similar setup as that of NIF GLEH to capture the hohlraum data and has provided valuable data to the CEA ICF physics study group.

These diagnostics are shown on the upper right of Figure 11: data is shown in Figure 12.

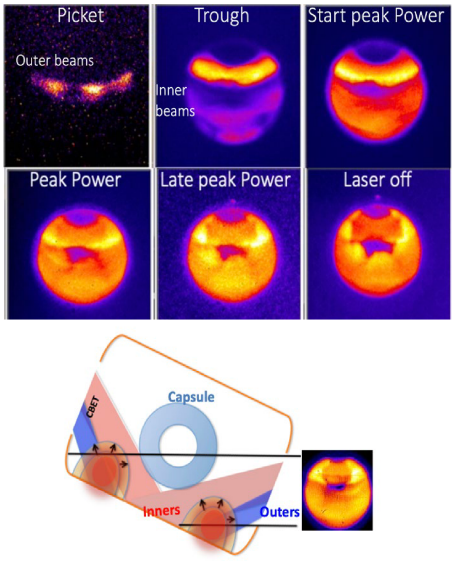

Figure 12. GLEH images on NIF throughout the picket, trough, and peak power of the laser. The geometry is shown in the lower cartoon and reference 81.

2.3.3 Time-Resolved X-Ray Diffraction and Opacity Diagnostics Using hCMOS FPAs on NIF

X-ray diffraction diagnostics for HED identify phases of compressed materials. The technique has been used on NIF and OMEGA, limited to using the TARget Diffraction In-Situ (TARDIS) diagnostic to obtain one or two snapshots per laser shot[82] X-ray diffraction is being developed for Z.[83]

Time-resolved x-ray diffraction using a gated hCMOS arrays provides a significant enhancement to the HED materials-diffraction program with the capability of making many diffraction measurements/shots with a multi-gate FPA such as Icarus. Recently a couple of four-frame hCMOS FPAs have been used to measure the transition in laser shocked lead from the hcp phase to the bcc phase at about 6 nsec, with higher signal to noise than achievable with TARDIS.

In addition, a time-gated spectrometer OPSPEC is being fabricated for NIF. This will use Daedalus, the next-generation SNL FPA, to reduce background emission recorded from a backlit test material in a NIF hohlraum.

2.3.4 Pulse- DIlation Technology: Application to Dilation X-Ray Imager (DIXI)

Although MCP detectors can record as fast as 30 psec, an alternative approach to faster time gating is to decouple the photoelectron production from the gain in the electron image. With a separated transmission photocathode, the resulting electron image can be manipulated by electromagnetic fields in a drift region before its arrival at an MCP or hCMOS for time gated gain. Importantly the brief electron image at the photocathode can be stretched or dilated in time by ramping down an accelerating field, by factors of tens allowing a relatively slow, say 200 psec MCP gate to be used as shown in the Figure 13.

Pulse dilation is not a new idea,[84,85] but was revised by Kentech personnel and tested using a short pulse U.V. laser by General Atomics, Kentech and LLNL- a result of NDWG meeting #2 see section 4.2.[86]

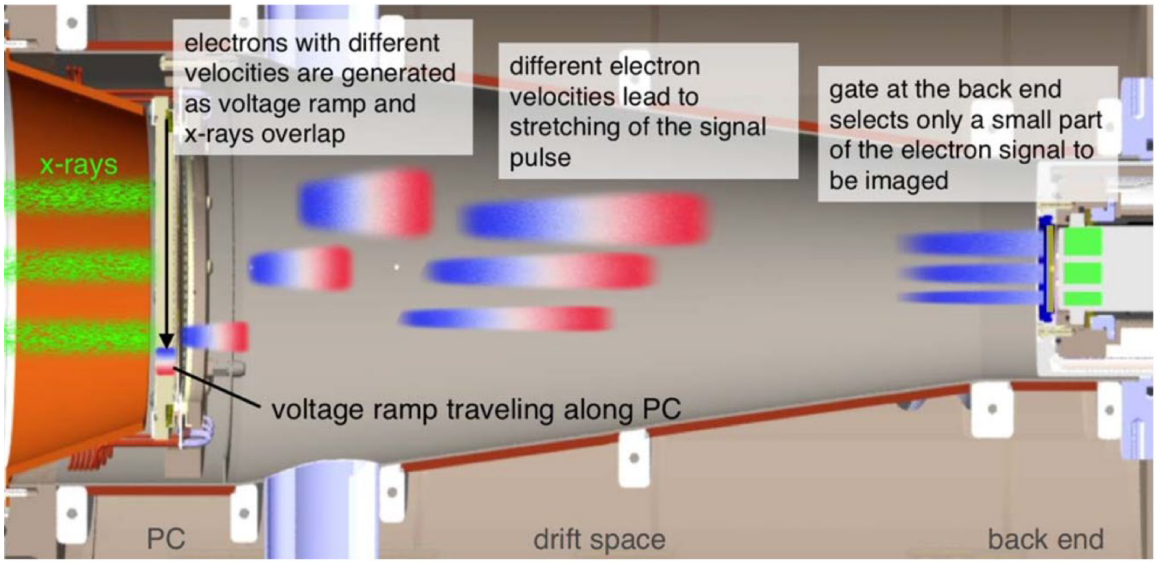

Figure 13. Cartoon showing how pulse dilation works for DIXI on NIF. A pinhole array forms many x-ray and photoelectron images. A travelling wave voltage on the photocathode accelerates electron images to different velocities. A drift tube dilates the photoelectron images by ~50 in time before a fraction of each image is recorded by a gated MCP. In contrast SLOS uses a multi-gate FPA for recording. (From Nagel_2014_RSI)

The PD concept was rapidly conceptualized by the NDWG and used in a diagnostic called the DIlation X-ray Imager (DIXI) for NIF.[87,88] DIXI records a time-sequence from many x-ray images. An array of pinholes casts multiple x-ray images onto a large, transmission photocathode which has a travelling voltage that is ramped down The electron images are transported to a 400 psec MCP single gate readout after the image temporal dilation resulting from the ramp, giving sub 10 psec gating at the photocathode. By using an array of pinholes an x-ray movie of an implosion results as the ramped pulse sweeps along an electrical microstrip(s). Results from the NIF pulse dilation x-ray camera (DIXI) were reported by Nagel et al.[89]

This rapid implementation of DIXI on NIF was helped by the use of test facilities at GA and brilliant re-tread of an idea from an industrial partner deeply involved in the HED program through HTPD and NDWG meetings.

2.3.5 Pulse Dilation Technology: Application to World's Fastest Photomultiplier

One stunning developments from PD that came from the NDWG meetings was the invention of the fastest (~20 psec) photomultiplier (PMT) in the world, the PD-PMT. It is currently used by LANL in the NDWG for gamma spectroscopy on the Gamma Cherenkov Detector (GCD).[90] and the Gamma Reaction History (GRH) diagnostic. This arose from an "aha" moment at the 16th NDWG meeting and is reported by A.K.L. Dymoke-Bradshaw et. al.[91] Importantly, the Pulse Dilation PMT instrument is now sold by a US vendor, Sydor Technologies, Inc.

2.3.6 Pulse Dilation and hCMOS Applied to a SLOS Detector

DIXI works by sweeping a time gate across many x-ray images formed by an array of many pinholes. The angular separation of the

pinholes is normally small, nevertheless each image is along a different line of sight. However, this concept does not easily work for more complex imaging systems, such as curved crystal imagers or Kirkpatrick-Baez (KB) microscopes, as there is not the space for many imaging systems, except as reported by Marshall.[92] For more complex imaging systems an x-ray "framing camera", recording many time-gated images along a single line of sight SLOS could replace DIXI.

The integration of the pulse-dilation technology with a multi-gated FPA for NIF and OMEGA diagnostics gave the world's fastest x-ray framing cameras used on NIF and OMEGA.[93,94,95]

Technical details and the many issues of the SLOS are covered elsewhere in this volume,[96, 97] but SLOS is the supreme example of the benefits of the collaboration within the NDWG: for the LLE instrument, (middle right Figure 11 GA was the integrator, SNL supplied the FPA(a.k.a. hCMOS), LLNL provided the readout electronics, and a vendor supplied the fast electronics. The NIF CBI instrument (middle right Figure 11 goes even one step further. The imager is a curved **C**rystal (**B**acklit) **I**mager which arose from a collaboration with between LLNL, GA, SNL and LLE (Section 2.4.2).

2.4 X-Ray Spectroscopy

Precision measurements of HED plasma conditions such as density and temperature of for example an implosion target at stagnation is of great importance. HED plasmas usually evolve rapidly, and so direct spectroscopic measurements with time resolution of these parameters can provide robust constraints on theory.

2.4.1 Collaborations in X-Ray Spectroscopy: Early Days

Four generations of x-ray spectrometers were designed, fabricated, calibrated, and fielded on NIF with an LLE lead. They were used to diagnose implosion hydrodynamics[98-100] hohlraum and coronal plasmas[101] x-ray source development for x-ray diffraction experiments and national security applications.[102, 103] All of the spectrometers utilized Bragg reflection and were positioned in the NIF target chamber using a DIM (section 3.4). Three of the spectrometers are time-integrated and combine a slit with a Bragg crystal to achieve one-dimensional spatial imaging in the direction perpendicular to the plane of dispersion. The time-integrated spectral images are recorded on calibrated image plates and a GXD/HGXD (Section 2.1). One of the spectrometers is coupled to an x-ray streak camera. Two used flat Bragg crystals, two used singly curved, elliptical Bragg crystals as shown in Table IV.

Genera-tion (year)	**Acro-nym**	**DIM-based detector s**	**Spectral range (keV)**	**dt, resolution spectrum, ps**	**dx X-ray spectru m (□m)**
1st (2009)	HSXRS	GXD, hGXI, IP	10.0-10.9, 11.7-12.8 keV (simultaneous)	≥ 100	10 or 100
2nd (2010)	SSI	GXD, hGXI, IP, CR39	9.75–11.2, 11.4-13.1 (simultaneous)	Time integrated	10 and 100
3rd (2012)	SSII	GXD, hGXI, IP, CR39	5.8-10.1, 6.4-11.2, 7.2-12.7, 9.3-16.5 (simultaneous)	Time integrated	30 or 100
4th (2014)	NXS	DISC, IP	1.9-2.4, 2.2-2.9, 2.6-3.7, 3.0-4.5, 3.6-6.0, 5.9-7.4, 6.7-8.9, 7.9-11.2, 9.0-13.7, 10.8-18.2 (one per NIF shot)	≥ 10 ps	Space integrat-ed

Table IV. The spectral range, time-resolution, and spatial resolution of the four generations of x-ray spectrometers designed, fabricated, calibrated, and fielded on the NIF by a LLE lead.

The first-generation instrument, called the hot-spot x-ray spectrometer (HSXRS), formed four temporally resolved spectral images covering the 10 to 10.9 keV photon energy range and four more covering the 11.7 to 12.8 keV range on a GXD. Slits provided 12x spatial magnification, showing doped ablator material being hydrodynamically mixed into the hot spot

The limited diagnostic lines-of-sight to the target motivated the second-generation spectrometer using flat Bragg crystals, called SSI (Super Snout I), which combined four time-integrated spectral channels covering the 9.75 to 13.1 keV range with gated and time-integrated, filtered x-ray imaging using pinhole arrays, and particle detectors. SSI increased the number of diagnostic lines-of-sight in a DIM from one to eight, increasing

the data collection on a single laser shot on NIF. Systematic hot-spot mix implosion experiments were performed with SSI using a Ge dopant in the ablator. An example of a Ge K-shell spectrum recorded with the SS I of a NIF symmetry capsule implosion can be found.[99]

A need for a broader spectral range and mm-scale x-ray sources motivated the third-generation spectrometer, called SSII, which combines time-integrated, elliptical Bragg crystal x-ray spectrometers for the 6 to 16 keV photon energy range, a GXD and time-integrated, filtered x-ray pinhole imager and particle detectors in a single snout to maximize the diagnostic access on the NIF. Hot-spot mix implosion experiments were performed with SSII using Ge and Cu dopants placed at different radial locations in the ablator to study the origin of hot-spot mix. An example of a Ge K-shell spectrum recorded with the SS II on a NIF DT cryogenic implosion can be found.[100] The wide spectral range in SSII was exploited to characterize laser-driven x-ray sources for x-ray diffraction source experiments and national security applications.

Time-resolved measurements of mm-scale x-ray sources in the 2.0 to 18 keV photon energy range motivated the fourth generation x-ray spectrometer, called the NIF X-ray Spectrometer (NXS), utilizing an x-ray streak camera and a time-integrated channel to provide an in-situ calibration of the streaked spectrum, with some work on OMEGA.[104] NXS has a spectral resolving power of ~100 and a temporal resolution ≥ 10 ps. The NXS does not cover the entire 2.0 to 18 keV range with a single snout, rather it divides the overall spectral range into ten spectral regions. Each spectral region is achieved using a dedicated snout housing a singly curved, elliptical Bragg crystal. One of the ten possible snouts is chosen for a NIF experiment to record the spectral range of interest.

As well as this LLE collaboration. X-ray spectroscopy experts from the Naval Research Laboratory (NRL) collaborated with LLNL to increase the fidelity of the spectral reconstruction of the gold M-band spectrum from the NIF Dante system. The NRL built, Virgil spectrometer uses the central line of sight of Dante-1. It uses a pair of cylindrically bent crystals covering 1.5-3.0 keV and 3.0-6.0 keV, providing time-integrated, high-resolution spectra over Au M-band emission (1.5-6 keV). It allows Dante unfold techniques to more accurately account for gold M-band emission.[105] Finally CEA provided a band selecting x-ray mirror for one channel of Dante.

This set of spectrometers shows a marvelous collaboration between LLE and LLNL and LLNL, CEA and NRL, taking advantage of the high shot rates on OMEGA and Nike at NRL for testing and calibrations.

2.4.2 High-Resolution X-Ray Spectroscopy: X-Ray Streak Cameras, hCMOS, and SLOS

High resolution x-ray spectroscopy is a powerful method to interpret the local plasma conditions.[106,107] High-efficiency spectrometers with a resolving power >>1000 beyond those described in section 2.4.1 and an x-ray streak camera are needed. Such high resolution spectrometers have now been built and fielded on each facility.

Figure 14 shows some surprising collaborations and inter-connections between different technology disciplines and institutions that have arisen from highlighting x-ray spectroscopy in the meetings of the NDWG.

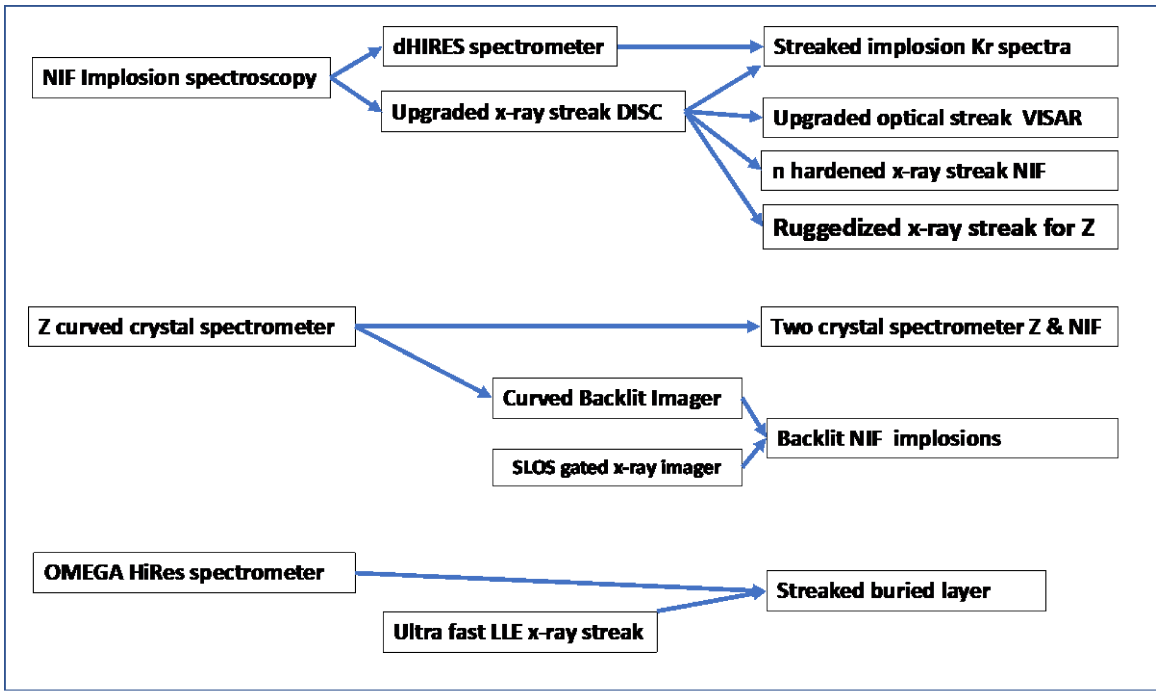

Figure 14. The requirements of high-resolution spectroscopy on the three HED facilities (left) and the NDWG resulted in many new diagnostic capabilities (right).

First, high resolution time-resolved spectroscopic diagnoses of NIF implosions drove a need for better x-ray streak cameras that was met by a NDWG-CEA collaboration on streak camera[108] and a connection with traditionally MFE experts in x-ray spectroscopy. (K. W. Hill, et. al., Rev. Sci. Instrum. 81, 10E322 (2010)). Second the utility of x-ray imaging by curved crystals had been recognized for about 20 years in HED. The NDWG brought together disparate expertise on this superb x-ray imaging capability and added to it detector development (SLOS, Section 2.3.6) for backlight imaging of NIF implosions, despite high levels of stagnation emission.

To spectroscopically diagnose implosion cores on NIF a high-Z dopant material is required such that its x-ray photons can propagate through the dense compressed shell without significant attenuation. To that end, a capsule with Kr-doped fuel was developed utilizing the 13–16 keV Kr K-emission lines from implosion cores.[100,109] A vital requirement of the design of the total instrument was that the NIF DIM mounted x-ray streak cameras needed a x-ray focusing design for high throughput and spectrometer dispersion perpendicular to the target chamber radius. This unusual configuration had been invented by an earlier generation of HED scientists[110] and was remembered at a NDWG meeting.

Using Hall's geometry[110], a three-channel, high-resolution, time-resolved x-ray spectrometer named dHIRES (DIM HIgh RESolution Spectrometer) using two conical crystals for time-resolved channels and one cylindrical crystal for a time-integrated channel was designed and fielded. A high spectral resolution enabled detailed line-shape measurements and a comparison to Stark broadening calculations. Because of the NDWG meetings, the design, fabrication, and calibration of the spectrometer utilized a group of scientists formerly experienced in MFE spectroscopy.[111]

The need to time-resolve the NIF implosion spectra (also OMEGA, LMJ and Z) drove an ongoing collaboration on improved streak-camera design. This was accomplished by engineering the streak camera inside the

protection of an airbox. This design will soon be fielded in the extremely harsh environment of Z. Separately, there was an effort on improved electron optics. Here LLE concentrated on ultra-high-speed detection.[112] NIF concentrated on improving the spatial resolution of their DIM Insertable Streak Cameras (DISC) to fully utilize the spectrometer dHIRES. As discussed by MacPhee,[108] the electron optics in streak cameras suffers from an optical aberration arising from the Petzval curvature of the focal plane of the electrons. A collaboration between industry and LLNL devised an aberration correction involving a grid that essentially flattened the field curvature at the detector plane doubling the spatial resolution. This breakthrough in electron optics is being applied to the manufacture by industry of an upgraded optical streak camera for NIF VISAR. The space charge saturation effects are being modelled by CEA partners in the NDWG. Another direct outcome of the NDWG.

NIF implosions using the dHIRES spectrometer in front of the upgraded DISC streak camera recorded data on a series of Kr-doped implosion shots, generating time-resolved (30ps) spectra of the Kr He_α and He_β lines, with E/dE ~ 1300. The Stark broadened data was analyzed to provide time evolution of both temperature and density.[113]

One advantage of running instruments in DIMs is that the $1/r^2$ drop in fluence is mitigated, at the expense of higher neutron fluxes which will "upset" the detectors. Recently we have taken a small step towards operating a time-resolving spectrometer at higher yield.[114] By radiation-hardening the streak tube control electronics, replacing the CCD with a hardened CMOS sensor and hardened electronics, shielding, attention to time of flight, and precision timing, we have collected useful streaked spectroscopy data on an ICF implosions with over 40× the operational neutron yield of the previous unhardened diagnostic.

The NDWG benefitted from the spherically bent crystal imaging work on Z, which included both x-ray radiography (i.e., backlighting) and self-emission imaging techniques.[115,116, 117] As a result of this work and NDWG discussions the Crystal Backlighter Imager (CBI) was built for the NIF.[118] The CBI produces a narrow-band, x-ray radiograph with several micron resolution that is imaged onto a SLOS. This complex instrument represents a tour de force diagnostic with outstanding spatial (7 micron), temporal (~20 psec) and spectral (~1 eV) resolution that limits the target self-emission allowing very bright implosion plasmas to be imaged, almost at peak stagnation.

The NDWG also discussed the use of bent crystals for self-emission imaging, which ultimately was made more appealing and easier to implement due to the previous success of the backlighter configurations at both Z and NIF. Benefits of the narrow-band nature of the Bragg reflection were first explored and used by both Harding et. al.[117] and Koch et. al.[119] Of particular interest to the NDWG was the two-crystal, differential-imaging technique developed by Harding et. al.[117] for magnetized liner inertial fusion (MagLIF) experiments on Z. This technique enables the visualization of wall mix by isolating spectral line emission from the background continuum emission. As a result of this work and further NDWG meetings a similar multi-crystal instrument is being built for the NIF.

Several gated FPA spectrometers and imagers have been used on Z:

i. Gated x-ray backlighting using a spherical crystal optic (now 4-frame compatible).
ii. Gated x-ray spectroscopy with 1-D imaging using a slit imaging optic and a convex crystal for opacity applications.
iii. Gated x-ray spectroscopy with 1-D imaging using a spherical crystal optic.
iv. Gated x-ray imaging using a pinhole optic.
v. Gated laser shadowgraphy

A high-resolving-power, x-ray spectrometer for OMEGA EP based on two diagnostic channels, each with a spherical Bragg crystal, was installed.[112] The instrument's capabilities have been demonstrated by resolving the Cu $K\alpha_{1,2}$ doublet on high-power shots.

2.5 VISAR (Velocity Interferometer System for Any Reflector)

The VISAR diagnostic is an interesting example of a diagnostic that was initially developed for equation-of-state experiments and not for ICF applications, yet later became a core ICF diagnostic on NIF as an innovative and critical use was developed. It is used to time the sequence of ablatively driven shocks in an ICF implosion. The VISAR diagnostic has continued to expand its application beyond what was initially conceived as new applications of the diagnostic have been developed. Table V lists some of the key advances in the use of VISAR on HED facilities.

VISAR Advances	Date
Velocity Interferometry System for Any Reflector (VISAR) developed[120]	1972
Line VISAR for diffuse reflecting surfaces, measurements of shock velocity in transparent materials[121]	1998
Application to ICF shock timing[122]	2001
Line VISAR on Omega and Application to Equation-of-state experiments and shock timing[123]	2004
Application to measurement of hohlraum temperature[124]	2006
Application to ICF shock timing inside an ICF Capsule[125]	2009
Use of target-mounted turning mirror to redirect VISAR to an orthogonal line-of-sight on a half hohlraum[126]	2010
2D VISAR system demonstrated on Omega[127]	2010
Use of turning mirror inside an ICF capsule for dual axis VISAR shock timing[128]	2014
Understanding of streak camera non-linearities[108]	2016
Effect of material structure on shock velocity non-uniformity measured on Omega[129]	2018

Table V. Major advancements of VISAR on HED facilities

The VISAR system concept was developed by Barker and Hollenbach[120] to broaden the application of laser interferometry to surfaces which are imperfect, e.g., moderately reflective or roughened. The application for VISAR initially was for measuring velocity of free surfaces, particularly in shock wave research. It was not planned as a core ICF diagnostic on Nova as the diagnostic was not mature and the applications had not yet been demonstrated.[130] A VISAR system was installed on Nova for Equation-of-state experiments. Instead of measurements from a free surface, which is the typical use of

VISAR, the Nova VISAR was designed to image in 1D, the shock propagation in transparent materials. When a shock passes through certain materials (i.e., deuterium, diamond, quartz), the material transforms into a metal and the optical reflectivity increases. Thus an incident laser from a VISAR can reflect off the shock, and the shock velocity measured.[121] This was the first use of VISAR in this manner. The success of this novel use of VISAR led to a proposal to use this to measure the shock timing in an ICF implosion on NIF.[43,131] The initial concept was to time the shocks in a planar sample attached to the side of the hohlraum; this evolved to measuring the shocks inside a capsule in perpendicular directions with the use of small turning mirrors. The successful use of VISAR on Nova resulted in the implementation of VISAR systems at other laser and Z-pinch facilities: Phebus, Vulcan, LULI, Z, and others. This same basic VISAR design is now a core diagnostic at HED facilities worldwide.

While NIF was under construction, a VISAR was installed on Omega[123] While similar in principle to the Nova VISAR, a number of improvements were made and tested. Due to the high shot rate on Omega, this allowed rapid testing of design concepts. These improvements were then implemented in the design of VISAR on NIF.[132]

Several new applications were developed on Omega using the VISAR. Measurements of shock velocity were used in Richtmyer-Meshkov growth experiments.[133] Since a non-constant shock velocity can result in Rayleigh-Taylor instability growth as well, precise and continuous measurements of the actual shock velocity enhance the accuracy of these hydrodynamic experiments. This was the first use of VISAR for hydrodynamic experiments on lasers. Another application was the use of VISAR to measure the hohlraum temperature.[124] Typically, there were two independent diagnostics used for the measurement of the temperature inside a hohlraum: The Dante, a set of soft x-ray filtered diodes, and a SOP (Streaked Optical Pyrometer) that measured the breakout of a shock from an aluminum wedge installed on the side of a hohlraum.[134] By placing a transparent material i.e., quartz on the side of the hohlraum, the shock velocity can be measured through the quartz and related to hohlraum temperature. There is a limit to the temperature that can be measured. Once it exceeds ~ 170 eV, the quartz loses its optical transparency due to ionization in the unshocked material and the VISAR signal disappears.

The NIF VISAR was installed along an equatorial line-of-sight and used on the NIF Early Light Experiments. Original plans were to also install an additional polar line-of-sight VISAR for half-hohlraum and direct-drive planar experiments. However, the use of a target mounted mirror to relay the equatorial VISAR to the polar axis removed the need for a separate Polar VISAR, the design which was even more complex than the equatorial VISAR due to the ~2x longer optical relay path length.[134] To make the target mounted turning mirror to operate successfully, the mirror had to be shielded from unconverted light and electrons from the target. An entrance cone for the VISAR extended beyond the unconverted light footprint on NIF. The turning mirror was chosen to be made from fused silica to reduce the absorption and heating from x-ray preheat and remain reflective. The x-ray loading limits and impact on reflectivity of various candidate mirror materials were tested on Omega. Once demonstrated, the concept of an enclosed VISAR turning mirror is now used routinely on NIF. This is an example of where a relatively inexpensive target modification can reduce the need for a costly new diagnostic as well as the use of other complementary facilities to make rapid design decisions. The use of a turning mirror was used inside an ICF capsule to acquire 2-axis shock timing data with a single VISAR to measure the effect of radiation asymmetry on shock timing.[128]

The accuracy of determining the shock velocity hinges on the accuracy of determining the fractional fringe shift in time recorded on an optical streak camera.[121, 135]

The dominant source of uncertainty is from the spatial nonuniformities present in streak cameras and limits the accuracy of the velocity determination to better than 1% at the center increasing to 3% at the edges. The spatial non-uniformity in a streak camera consists of spatial and temporal distortions, which can be calibrated out to some extent, and spatial resolution variations, which are more problematic.[136,] There has recently been a fundamental improvement in the understanding of the source of streak camera nonlinearities (section 2.4.2), which should lead to better accuracies in measurements using streak cameras, including VISAR.[108]

Electron optic aberrations in both x-ray and optical streak cameras are caused by Petzval field curvature and spherical aberrations, which result in reduced spatial resolution off axis. This can be corrected with electron optical components (mesh and cylinder) and demonstrated in an x-ray streak camera to have a near uniform spatial resolution across the camera. The improvement should be possible in optical streak cameras as well, and work is underway to incorporate this in optical streak cameras on NIF. This highlights how sometimes deeper understanding of detectors can impact overall performance in a diagnostic system.

The NDWG has planned a new high-Resolution 2D-VISAR system for NIF.[127] The concept was again first demonstrated on a small system, the Jupiter laser system at LLNL, then implemented on Omega to further test and develop. It is also being implemented on other HED facilities, e.g., Nike.[137] This diagnostic has been used to measure the effect of material grain size on the shock front perturbation as a seed for instability growth on ICF capsules[138], laser-imprint induced shock velocity non-uniformities,[139] and laser driven metal ejecta.[140] On NIF, the effect of grain size on the actual first shock in a NIF capsule can be measured, since Omega cannot reach the first shock pressure and duration a capsule will experience on NIF. It is expected that as scientists become more familiar with this diagnostic capability, new applications will be developed.

In summary, the development of the line VISAR capability to directly measure shock velocity in transparent materials has opened up many applications in ICF, and HED science that were not initially envisioned. Advances in fundamental streak camera understanding offer the potential of higher accuracy measurements. 2D VISAR is another new diagnostic capability in the early stages of development of applications. The evolution of this diagnostic progressed from a proof-of-principle on a small laser, to Omega for testing and improvements, and finally to NIF and other facilities. Thus the time scale from concept to capability and development of new applications is ~ 10+ years.

2.6 Wolter X-Ray Imager for Z and NIF

X-ray optics including the Wolter configurations are reviewed by Kozioziemski (B Kozioziemski "X-ray imaging on HED Facilities", ibid). A Wolter x-ray optic uses a full surface of revolution and so it provides orders of magnitude larger collecting solid angle than any other reflective x-ray optic.

The first use of a Wolter in HED was on Nova.[141] Time resolution was achieved using the first version of a production type module of a gated MCP detector. The optic was Ni coated optic and had a region that had good resolution but very bad scatter which complicated it use compared to the ease of use of imaging pinholes.

However, the success of NASA's Chandra x-ray telescope,[142] recent replica technologies development, and our need to image in spectral bands caused us to form a collaboration for x-ray microscope imaging on NIF and Z. The NDWG collaborated with NASA Marshall Space Flight Center for optic production and the Harvard Smithsonian for multi-layer mirror coating optimized for molybdenum characteristic x-ray lines. This group successfully delivered a multi-layer coated Wolter for use on Z.

Significantly better resolution and throughput compared to a pinhole system is discussed by Fein et al.[143] and recently improved the FWHM resolution to 8 microns of a Wolter for NIF.[144] In the course of this work some of the NIF expertise in optical polishing was useful to NASA in improving their polishing techniques. Again, a fruitful internal collaboration within the NDWG but also a mutually beneficial collaboration with NASA space flight x-ray telescope experts.

2.7 Neutron Imaging

Many HED and ICF diagnostics have their origins in the underground nuclear test program of the national laboratories. One of these was neutron imaging, where a pinhole creates an image of the neutron emitting region of a burning plasma. A proof-of-principle demonstration of neutron imaging was made on the Nova laser in the 1990s.

Starting in 2000, LANL began to develop new techniques, technology, and algorithms to make neutron imaging a standard diagnostic for ICF.[145] The project began by fielding a test bed at the Omega laser facility. Different methods of machining and fabricating complex pinhole arrays were tested, different types of scintillator material were used, and simple analysis algorithms tested. Most importantly, the demands of a reliable neutron imaging system (NIS) for the NIF were starting to be understood. Simultaneously, the CEA of France also tested alternative types of apertures and scintillators at Omega.

Many challenges needed to be overcome to achieve the desired 10-micron spatial resolution. The neutron pinhole has to be 20 cm in length in order to fully suppress the 14 MeV neutrons that do not pass through the open pinhole. Because NIS measurements were required to be made over a large range of neutron yields with good SNR, an array of pinholes, and eventually penumbra, are needed. In order to measure downscattered neutrons, those scattered by the cold dense DT fuel, a long line of sight is needed to separate the different components of the neutron spectrum by their arrival times. The long line of sight (28 m) was achieved by constructing a two-story addition to the NIF building. Penetrations through the bio-shield wall and external wall of the building had to be drilled ad collimators installed. This was another result of the collaboration between LANL and LLNL.

The neutron pinhole evolved from a single pinhole scribed in a 20-cm-long block of Au to an array of pinholes, now numbering 54 triangular pinholes and 16 penumbral apertures machined into 14 layers of Au, encased in a block of W, with 16 x-ray apertures in a foil mounted to the end of the block. This evolution occurred over 20 years and required the development of detailed molding of the pinhole imaging properties and improvements in micromachining techniques. Realization that high-resolution reconstructions of the burn region required exquisite characterization of each of the pinholes led to major improvements in characterizing each pinhole in the array and its location.

The relative shape of x-ray and neutron images was an ongoing question that led to the addition of x-ray apertures to the pinhole array, and innovative image plate detectors in the line of sight (CNXI) again arising from discussions at the NDWG meetings. This allowed collection of both time integrated x-ray and neutron images, on the same line of sight, proving that the sources varied significantly. Early experiments at NIF showed the need for more three-dimensional information on the implosion shape. This spurred the addition of a second line of sight to the original one. A polar NIS was chosen to break the symmetry of the hohlraum shape. Eventually a third line of sight was added to give three nearly orthogonal views of the implosion as shown in Figure 15.

The extensive building modifications and subsequent integration of the instrument into the facility its software controls required very close collaboration between the diagnostic scientists, engineering team, and NIF engineers and facility operations. For

example, the evolution of the alignment procedure for the NIS illustrates the close cooperation required. Recall that the pinholes are 20-cm long and less than 20-microns in extent. These pinholes must be placed along the axis of the NIS line of sight, not only in linear directions, but also in pitch and yaw. The original concept involved using an optical telescope placed in an opposed target chamber port. The results were less reproducible than desired. Later iterations of the pinhole array took this into account and enlarged the volume at best focus that is imaged onto the detector. When the polar NIS was added, an opposed port was not available. Using a newly developed laser positioning system, not only was the polar NIS able to be aligned, but more reproducible and faster alignment of the other two NISs was made possible.

The 2015 NDWG review, discussed previously, led to the new requirement of also measuring the gamma-ray image from an implosion. Copious numbers of gamma rays are produced when neutrons collide with carbon atoms in the capsule ablator. The gamma rays arrive at the NIS recording system much sooner than do the neutrons, so time gating the measurement can isolate the gamma image from the neutron images. The addition of this measurement required a redesign of the detector and pinhole arrays of the NIS. These changes were incorporated into the construction of the third line of sight instrument and are included in the refurbishment of the original line of sight.

Early data from the NIS showed the true shape of the burning region was similar to the x-ray emitting region.[146] The images also confirmed that the compressed core was larger than simulated, indicating that the adiabat of the fuel was significantly higher than designed. Other measurements showed that the jet of material from the fuel fill tube was cooling the plasma and that the hot-spot region could sometimes obtain unanticipated states such as a torus or as two separated burning regions. More recently, the addition of the gamma-ray imaging capability shows where the burning fuel shell, the cold fuel shell, and the ablator shells are, providing stringent constraints for simulation codes.

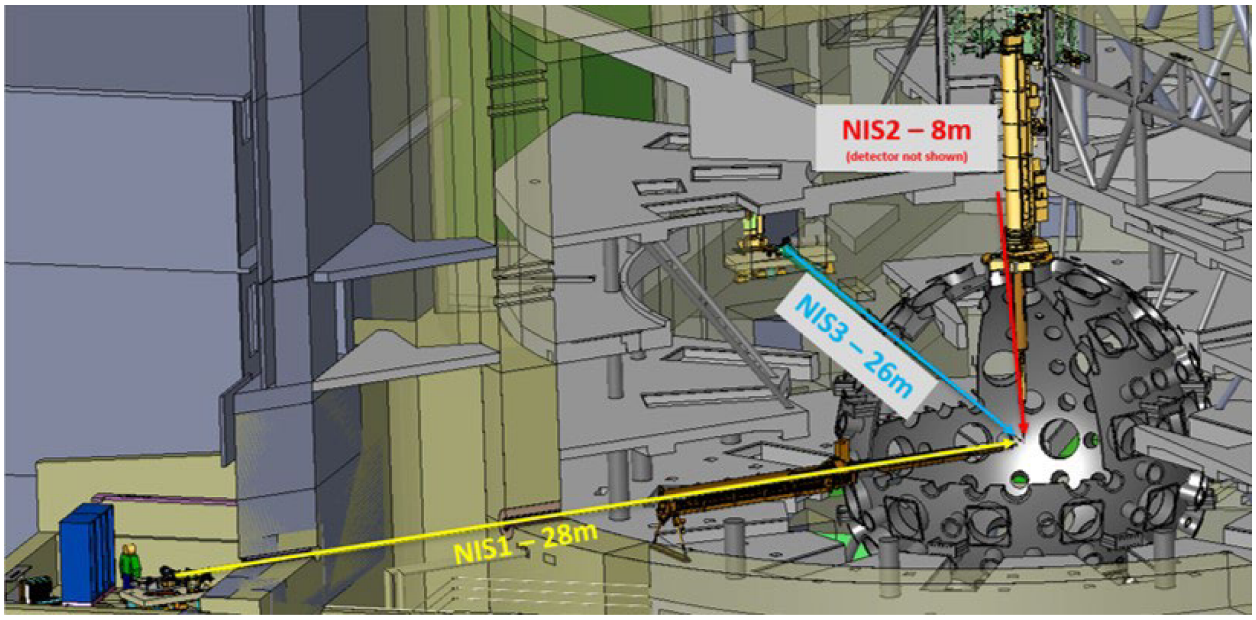

Figure 15. The locations and lengths of throw of the three neutron imaging lines of sight on NIF. NIS1 and NIS2 image the primary and down-scattered neutrons. NIS1 can also image gammas. NIS2 only images primary neutrons.

2.8 Ultraviolet Optical Thomson Scattering (UVTS)

Optical Thomson scattering (OTS) measures the spectrum of a probe laser scattered by a plasma to get time and space resolved measurements of nearly all of the plasma properties. It is the gold standard measurement used in tokomaks and at lower densities in ICF.

On NIF, Z, and OMEGA a high-density plasma produces high pressures to drive shocks or to inhibit hohlraum wall motion for all SSP programs. There are no direct measurements of the high-density plasmas needed to capture the complex dynamics inside a hohlraum. Fundamental hohlraum environment parameters will be uniquely measured, at high densities (n_e is calculated to be > 10^{21} e/cc in a NIF hohlraum) and this leads to the requirement for an ultraviolet Thomson scattering probe laser beam at the fifth harmonic, 5ω in order to avoid significant absorption and refraction. Background plasma emission and other sources of non-Thomson scattered light indicate that to exceed a signal-to-noise of unity the Thomson scattering probe laser must be 1-10J in 1ns at 210 nm, see Ross et al. [147]

There are also less challenging experimental configurations which can benefit from 3ω UVTS on the NIF and are benefitting from 4ω OTS on OMEGA.[148] OTS has been implemented on Nova, Trident, JLF and OMEGA although in less stressing conditions than an ignition hohlraum. UVTS on the NIF is therefore a transformative diagnostic because the uniquely short wavelength of the probe opens new windows in plasma density even after five decades of Thomson scattering from high-temperature plasmas.

For UVTS on the NIF an ultraviolet probe beam is generated by 5th harmonic conversion of a 1.06 μm glass laser beam. A separate 100J class laser beam line has been through the rigorous design review process and installed on the NIF including frequency conversion to 210 nm and delivery to target chamber center.

After discussion by the NDWG, work at LLE in FY16 measured conversion efficiencies

from 1.06 micron to 210 nm, albeit with smaller beams, of 10-20% The detector for the scattered light is a dual spectrometer multiplexing onto an ultraviolet sensitive streak camera. The detector was designed and built in FY16 [P Datte et al., (IFSA 2015) IOP Publishing]. The detector has been used to measure the background levels for NIF hohlraums and direct drive capsules. The detector has already been used for 3ω OTS on the NIF from relatively low-density plasma for planar laser plasma instability experiments.[149]

3. EARLY DAYS: COLLABORATIVE HED DIAGNOSTICS 1993–2008

This is a history of the collegially coordinated national diagnostic effort from the late 80s, through the NIF Conceptual Design Report (CDR) to an implementation of diagnostics for the first phase of NIF program ~2009.

3.1 The High-Temperature Plasma Diagnostic Conference and Proceedings of SPIE

The origin of the NDWG is the high-temperature plasma diagnostic (HTPD) conference formed because of the diagnostic commonality for hot HED and magnetically contained plasmas.

As shown in Table VI, the biannual HTPD series started in Knoxville in 1976 and has not missed a beat to the twenty-fourth HTPD in Rochester in 2022. Its longevity is testament to the utility of the conference. The community has voted with its feet, the conference has flourished: The committee is self-organizing: as members of the committee age and retire, new committee members are informally proposed and accepted and carry on the good work.

Number	Year	City	RSI Vol (Year)	HED papers
1	1976	Knoxville		
2	1978	Santa Fe, NM		
3	1980	Los Angeles, CA		
4	1982	Boston, MA		
5	1984	Tahoe City, NV	56 (1985)	25
6	1986	Hilton Head, SC	57(1986)	
7	1988	Napa, CA	59(1988)	
8	1990	Hyannis, MA	61(1990)	
9	1992	Santa Fe, NM	63 (1992)	
10	1994	Rochester, NY	66(1995)	
11	1996	Monterey, CA	68(1997)	
12	1998	Princeton, NJ	70 (1999)	
13	2000	Tucson, AZ	72(2001)	
14	2002	Madison, WI	74(2003)	
15	2004	San Diego, CA	75(2004)	
16	2006	Williamsburg, VA	77 (2006)	
17	2008	Albuquerque, NM	79 (2008)	67
18	2010	Wildwood, NJ	81(2010)	56
19	2012	Monterey, CA	83(2012)	61
20	2014	Atlanta, GA	85 (2014)	
21	2016	Madison, WI	87(2016)	76
22	2018	San Diego, CA	89 (2018)	
23	2020	Los Alamos, virtual		
24	2022	Rochester, NY		73

Table VI. The sequence, year and location and Review of Scientific Instruments volume where the HTPD conference papers are published and the number of High Energy Density diagnostic papers in that volume, where available.

A valuable feature of the HTPD is that the proceedings have been published in the Review of Scientific Instruments since the early 80s. A page limit makes the papers particularly readable. The proceedings are usually a special issue where scores of papers per volume archive the progress of diagnostics for HED plasmas.

High quality engineering is essential for diagnostics on large facilities. Starting 2012 a series of conferences "Target Diagnostics Physics and Engineering for Inertial Confinement Fusion" organized by SPIE, focused on Engineering of the HED diagnostics. About 20 papers/year from these meetings are published in each SPIE Proceedings from 2012 to 2018. As befits SPIE, an organization that initially called itself the Society of Photographic Instrumentation Engineers, before the above-mentioned conference there were, over the decades many high-speed imaging

conferences and proceedings that were relevant to HED Diagnostics. As for HTPD publishing in Review of Scientific. Instruments, a valuable feature of these SPIE conferences was publication in Proceedings of SPIE.

The HTPD and SPIE conferences generate a sense of community amongst diagnostic scientists and engineers, a backdrop for the NDWG.

3.2 Diagnostics for the NIF Conceptual Design Review (CDR).

The US inertial confinement fusion program evolved in the 80s and 90s: it is a long and fascinating story. By the late 80's and early 90's there were four major US HED facilities: the Nova laser at Livermore which also hosted experiments for LANL, the predecessor of the Z machine at SNL, the Omega laser at the University of Rochester and Phebus, a glass laser facility at NRL preceding their Nike laser. A kernel for the formation of the national diagnostic working group was forming.

LLNL had operated Nova since 1984 and in the early nineties had started to propose an ignition facility follow on to Nova.[150] In 1994 the Lawrence Livermore National Lab ICF program published a Conceptual Design Report.[151] We now know NIF came to pass and by the Lawson criterion[1] achieved ignition a quarter of a century after the CDR.

The team for the NIF CDR was based at Livermore but also had major contributions from LANL, SNL and LLE. Notably there was a national team in diagnostics for the NIF, based loosely on the high temperature plasma diagnostic community, which called itself the Joint Central Diagnostic Team (JCDT)—with apologies to the ITER joint central teams. The group was experienced in operating diagnostics on relatively large facilities.[47] The JCDT had met several times to discuss the diagnostics required for ignition and formulated the diagnostic section of the CDR document, which was also presented at the 1994 HTPD in Rochester.[152]

The functional requirements of the NIF[153] were driven by the implosion/ignition mission of NIF. In the CDR phase I HED diagnostics were needed to verify achievement of these requirements. They were NIF versions of previous Nova diagnostics as are shown in Table VII Much later as described in Section 4.3, the use of HED facilities for non-implosion HED missions evolved together with additional diagnostics.

Diagnostic	Acronym	Lab	Nova Equivalent
Laser validation-pointing, focusing, and synchronization			
Static x-ray imager (ruggedized)	SXI	LLNL	
Streak x-ray cameras	SSC	LLNL	SSC
Twelve-inch manipulator	TIM	LLNL	SIM
Hohlraum temperature tuning and shock timing			
Soft x-ray power diagnostic	SXSS	SNL/LLNL	SOP
Shock breakout systems	SOP	LLNL/SNL	SOP
Filter flourescer	FFLEX	LLNL	FFLEX
Hohlraum symmetry tuning			
Gated x-ray imaging system	GXI	LANL/SNL	GXI
Target yield	YN	SNL	Yield
Neutron time of flight	NTOF	LANL	
Neutron imaging	NI	LLNL	NPAM
Soft x-ray imager	SXRI	SNL	GSXRFC

Table VII. NIF CDR anticipated collaborations between LLL, LANL and SNL on diagnostics nurtured by the HTPD and the SPIE Conferences.

At this time, some Phase II diagnostics were envisaged, a large neutron scintillator array (like LANSA on Nova) and neutron penumbral imaging.

3.3 Post-CDR NIF Diagnostic Activities

Two years later in 1996, there was another invited talk on NIF diagnostics at the HTPD meeting in Monterey where another diagnostic leader, this time from SNL, reported the current planning status for NIF diagnostics.[154] Besides the three labs, there were coauthors from LLE and MIT. Institutional responsibility had been assigned for each diagnostic; see Table VIII.

Measurement	Diagnostic	Acronym	Lab
Laser characterization diagnostics			
Beam spot size, position, and smoothing	Static x-ray imaging system	SXI	LLNL
Beam synchronization	Streak x-ray camera system	SSC	LLNL
Energy reflected from laser plasma	Optical backscattering system	FABS	LANL/LLNL
Hohlraum characterization diagnostics			
Time history of hohlraum radiation temperature	Soft x-ray power spectral	SXSS	SNL/LANL/LLNL
Time-dependent size of hohlraum diagnostic hole	Soft x-ray imaging system	SXRI	SNL
Spatial symmetry of hohlraum radiation drive			
Hohlraum radiation temperature	Passive shock breakout system	SOP	LLNL
Hohlraum radiation temperature	Active shock breakout system	ASBO	SNL/LLNL
Spatial symmetry of hohlraum radiation drive	Time-resolved x-ray imaging	TRXI	LANL/LLNL/LLE
Absolute, high-energy x-ray spectra	Filter fluorescer diagnostic	FFLEX	LLNL
Capsule Characterization Diagnostics			
Capsule neutron yield	Total neutron yield system	YN	SNL/LANL
Fuel ion temperature	Neutron time-of-flight system	NTOF	LANL
Bang time and fuel burn history	Reaction history system	RHS	LLNL/LANL
Capsule imploded core image	Neutron imaging system	NI	LLNL
Fuel areal density	Tertiary neutrons or protons	TN or TP	LLNL/LLE/MIT
Time-resolved fuel ion temperature	n-p recoil technique	TRIT	LANL/SNL

Table VIII. Agreed diagnostic responsibilities for NIF between labs as of 1997.

Unsurprisingly there were several areas where eventual implementation of the diagnostics differed from the planning as discussed by Leeper:

- The soft x-ray spectral diagnostic was finally the Dante system, not a transmission grating system.
- Tertiary neutron diagnosis was not used for areal density. Downscattered neutrons were eventually used (Section 2.2.1).
- Although Cu activation is used for yield measurements the main nuclear activation effort is with Zr.
- The soft x-ray imaging system was in the end simplified to a pinhole camera imaging system

- A workhorse diagnostic on NIF is VISAR (Section 2.5) but it was absent from plans in the mid-90s, as its utility only became apparent in the late 90s.

Four years later at HTPD 2000, a leader from LANL summarized for the community the state of preparation of the NIF neutron diagnostics.[155] This time there were 45 authors from nine institutions: newcomer institutions were CEA, New York State University Geneseo and General Atomics.

A notable inclusion in Murphy's paper that came to be, was the gamma Cherenkov detector variously called the GCD or in a folded version the gamma reaction history (GRH) detector.

3.4 Diagnostic Vacuum Insertors and Manipulators

The size of the Nova and the NIF target chambers and the concomitant pump down times drove the planning of how diagnostics were attached to the target chambers and aligned to targets. Although some diagnostics can be attached to the outside of the chamber, some need to be closer and need to be removed before unloading of a data recording media or refurbishment after a shot without venting the target chamber.

One advantage of laser facilities is that the laser beams can be repointed, thus allowing for flexible target geometries. The diagnostics lines-of-sight need to also be flexible to take advantage of the different target geometries. By using vacuum load lock manipulators arranged around the target chamber, the same diagnostic can rapidly load along different lines-of-sight. This provides an enormous flexibility in diagnosing experiments and is much more cost effective than building complex diagnostics along each of the possible lines-of-sight. It also allowed the sharing of instrument engineering and even instruments among facilities with similar manipulators. Instruments built for the Nova laser were fielded on Omega, for example.

On Nova an initial learning experience with four-inch manipulators led to the design of many six-inch diameter vacuum load lock manipulators called SIMs, illustrated in the cartoon in Figure 16. Diagnostics could be loaded onto a cart from the load lock, which was then evacuated, allowing the gate valve to be opened, the cart and manipulator to be inserted allowing adjustment of the alignment of the diagnostic via the gimbals shown around a large bellows. The bellows allows a small angular but relatively large positional motion of a diagnostic on the end of the long SIM. Similarly, NIF planned DIMs (Diagnostic Insertion Manipulators), OMEGA built TIMs (Ten Inch) and LMJ planned SIDs.

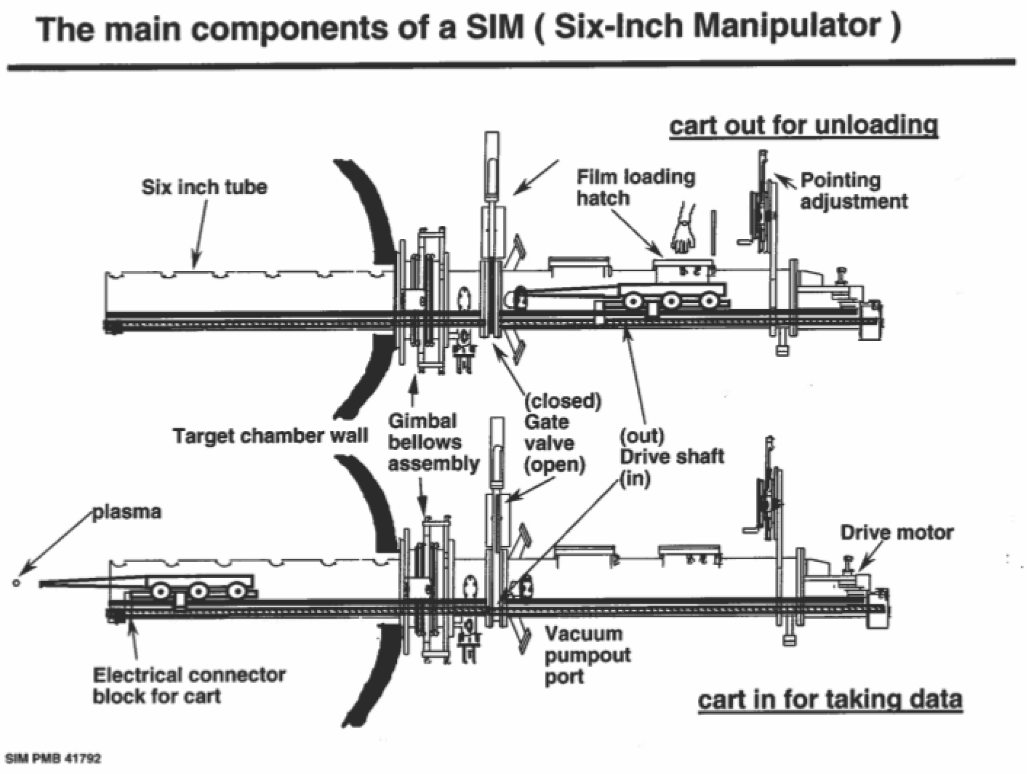

Attribute	SIM -Nova	TIM (OMEGA)	SID (LMJ)	DIM (NIF)
Chamber diam.	4.4	3.25	10	10
Diagnost. length m	1.7	1.5	5.5	3
Diagnost. diam. M	0.11	.18 x.23	0.2	0.3
Diagnost. Mass lb	23	45	20	195
Positioning x/y, z micron	$50^{-5}0$	30,10	10,100	25,250
Port size m	0.2	.6 x .45	0.5	0.48
Diagnostic loading	end/top	top	Top	end became side

Figure 16. Main characteristics of three US and one French (LMJ) diagnostic inserters/manipulators.

This was planned 25 years ago and as of the 2021 NIF has three DIMS, OMEGA has seven TIMS and LMJ has six SIDs. A good example of a diagnostic that was designed to operate in the Omega TIM is described by Oertel.[156]

4. THE NIF DIAGNOSTIC WORKING GROUP, 2009–2014

4.1 Diagnostic Status at start of NIF Operations: A Need to Evolve

When NIF started operating with all 192 beams in 2008 there were only eight diagnostics in operation, those used on an eight-beam version of NIF called NEL. Although there was another dozen diagnostics conceptually planned, it was realized that a more detailed and realistic plan needed to be formulated for the NIF diagnostics. Also, these initial planned set of diagnostics were success oriented for 1018 neutron yield and chosen to make a few key measurements on the performance of the hohlraums and implosions, based on prior experience from Nova and OMEGA. Measurement accuracy requirements were created based on success philosophy. As it turned out there was a lot of unknown science. As we now know there can be large implosion anisotropies from fill tubes, support tents, capsule pits, and implosion drift velocities and hohlraum wall motion, but at the time these factors did not figure in describing the diagnostic accuracy requirements.

The plan needed to evolve due to diagnostics improvements and a need for failure diagnostics. As a result, starting in 2009, a set of workshops was initiated that led to a far more formalized apportioning of responsibility for NIF diagnostics. This set of meetings gradually transformed itself into meetings of the National Diagnostic Working Group (NDWG) creating a living National Diagnostic Plan (NDP) for the three major US facilities.

4.2 National Diagnostic Meetings, 2009–2014

In this quinquennium NIF diagnostics went from a handful of operational with collegial inter-lab responsibilities, to 65 operational diagnostics with significant responsibility in the national program. The method of accomplishment used the factors laid out in the table at the end of section 1: first and foremost, detailed, transparent collaboration accomplished at nine large general workshops. These large meetings with 60–117 participants are listed in Table IX There were also many more, smaller workshops focused on specific diagnostics.

Workshop #	Date	Attendees
1	Feb 09	60
2	Jul 09	72
3	Jan 10	88
4	May 10	92
5	Jan 11	NA
6	May 11	~110
7	May 12	NA
8	May 13	~80
9	Sep 14	117

Table IX. Sequence, dates, and number of attendees at the first nine plenary diagnostic meetings at LLNL.

The initial goals of the meetings were to develop NIF ignition diagnostics and plan scope, schedule, budget, and risk. The goals evolved and by the eighth workshop, NNSA had said that the NIF diagnostics working group had been so successful that its charter should be expanded to include the other large HED facilities: the NIF Diagnostic Workshop group morphed into a broader National Diagnostic Working Group (NDWG). The final workshop in this period focused on discussions of a new generation of diagnostics to more fully exploit NIF, OMEGA and Z, and to examine the failure modes in the attempts so far to achieve ignition. The Senate Energy and Water Appropriation Subcommittee

> …directed NNSA to better coordinate diagnostic development across the national labs and universities for use at the major inertial confinement fusion facilities-NIF, Omega and to make sure that

critical diagnostics are in place to take needed scientific measurement.

A national management group had identified 18 possible major new diagnostics and calibration facilities to be considered for the plan with associated multi-institutional teams, as discussed in Section 4.5.

The method of accomplishment at the workshops was to have large (60–110 participants) plenary sessions interspersed with many targeted smaller (~25) group meetings. A management group suggested a set of questions pertinent to the small groups to answer. An example of the questions posed to the small groups in shown in Table X.

High Speed Photo Diode/PMT	Is the pulse dilation PMT working ? Are there incremental improvements of PMT and PD
3D X-ray Implosion Imagining	Where next for each of the three facilities?
Optical diagnostic for neL and B Probing	With the deep u.v. optical probes available can we use phase shifts/Faraday rotation to measure B ?
Calibration of Image Plates	Should we regularize the calibration and readout procedures for NIF OMEGA and Z?

Where Next for nToFs on NIF, Z & OMEGA?	Do the new Cherenkov detectors change the way we field the next nToFs on the three facilities?
Coded Aperture Imaging: X-rays and neutrons	Given progress with circular apertures on NIF is there any benefit to other coded aperture schemes ?
VISAR Next Step on NIF, OMEGA, and Z	Where next, both incremental and sudden for VISAR on NIF, OMEGA, and Z
Hardened Focal Plan Arrays(FPA)	National plan for the best schemes, such as dump and read, to harden our FPAs?

Table X. Examples of directed questions posed to small parallel groups on successive days of a plenary NDWG meeting. A summary of the small group discussions was reported out to the plenary session at the end of the large workshop and a subsequent report was made to the NIF Director and NNSA.

Participation at the large workshop started with 60 scientists and engineers from LLNL, LANL, SNL, State University of New York (SUNY), MIT and LLE and grew to 117 by the ninth workshop in 2014 (see Tables IX and XI). Importantly new participants with their own ideas and resources had been added.

Inst.	Attendees	Inst.	Attendees	Inst.	Attendees
LLNL	55	Industry (US, UK)	8	MIT	3
SNL	11	LLE	8	PPL	2
LANL	10	CEA, AWE, IC	7	NNSA	1
NSTec	9	LBL	3	NRL	1
				U of N	1

Table XI. Typical attendee number and institutions at NDWG meetings

Besides the large group meetings which had plenary and parallel small-group breakout sessions, other small, targeted workshops were held during the year. For example, the fourth large workshop in 2010 was preceded during the year by eight mini workshops on high-yield x-ray imaging, nToF PMT electrical recording, mix modelling, scanning/etching for MRS, wedge range filters, nuclear activation, nToF scintillators, and south-pole bang time (SPBT).

Many new ideas arose during the workshops. For example, SPBT and SPIDER (Streaked Polar Instrumentation for Diagnosing Energetic Radiation) came directly from the workshops. A better measure of when stagnation of an implosion occurs was needed. At the second workshop, we realized there was a lot of access space below (south pole) and above the NIF hohlraums, which have a vertical axis. A group at the workshop suggested a fixed position crystal spectrometer bang time diagnostic located below (south) the hohlraum as shown in Figure 17. LLE took responsibility and this SPBT diagnostic was run for about a decade.[157]

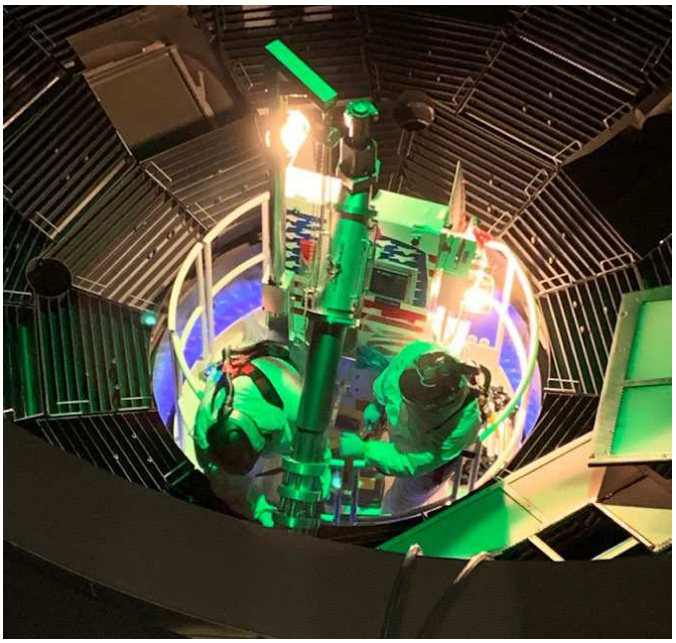

Figure 17. The south-pole bang-time diagnostic being removed from the NIF target chamber for decommissioning August 2022.

Likewise, the need for a higher speed fixed x-ray detector, SPIDER, was satisfied by an SNL mounting an x-ray streak camera on a port close (7 degrees) to the north pole.[158]

As expected after robust discussions, some proposals were not pursued. The need to time-resolve gamma emission in a complementary manner to GRH had been recognized. A Gamma-to-electron magnetic spectrometer (GEMS) had been conceived. Knocked on Compton electrons would be magnetically energy analyzed. As this was explored consensus on inadequate temporal performance coupled with a low level of technological development caused this concept to be abandoned.

4.3 Overview of Non-Ignition HED-Based Diagnostics

While the largest laser and pulse power facilities were initially built to pursue inertial confinement fusion, the high energy density (HED) conditions achievable coupled with the broad suite of diagnostics developed led to strong interest in developing applications and diagnostics for HED experiments. The set of ICF diagnostics were used for these HED experiments, and new diagnostics were developed whose main purpose initially were to support these HED experiments. Many of these HED diagnostics also found important applications to ICF as well (i.e., 1D, 2D VISAR). The NDWG develops diagnostics that have broad application to both ICF and HED applications.

The HED applications can be broadly grouped into four categories with associated diagnostics:

- Radiation transport and opacity
- Material properties at high pressure
- Hydrodynamics and radiation-hydrodynamics
- Ignition applications and burn

Each category benefits from a group of diagnostics which are often shared between them. Radiation transport and opacity experiments use calibrated broad band time-resolved and imaging spectrometers. High pressure material experiments utilize phase structure and kinetics diagnostics such as time resolved diffraction diagnostics, 1D and 2D VISAR for equation-of-state and temperature diagnostics such as optical pyrometer and EXAFS spectrometers. High photon energy radiography is used for higher-Z measurements to infer strength via Rayleigh-Taylor growth. Hydrodynamics and radiation-hydrodynamics measurements use high-resolution x-ray imaging diagnostics to measure instability growth and mix. Burn diagnostics use radiochemical diagnostics to measure isotopes from nuclear reactions and decay products. Table XII lists diagnostics that have been developed in these areas along with citations of their first publications.

Category	HED Diagnostic	Date
Radiation transport and opacity	Long-duration point radiography[159]	2008
	Soft x-ray imaging spectrometer[160, 161]	2012
	Second Dante on NIF[162]	2014
Material properties	1D VISAR[123]; turning mirror[126]	2004
	EXAFS spectroscopy to CID[163]	2005
	2D VISAR system demonstrated on Omega[127]	2010
	Powder X-Ray Diffraction Image Plate (PXRDIP)[164]	2012
	TARDIS (x-ray sample diffraction)[86]	2013
	Time-resolved diffraction detector[165]	2018
	Multi-optic EXAFS spectrometer[166]	2021
Hydrodynamics and Radiation Hydrodynamics	250ps x-ray CMOS detector[74]	2012
Ignition applications and burn	Grating Actuated Transient Optical Recorder (GATOR)[167]	2012
	Gaseous collection radiochemistry[168]	2012
	Solid Collection radiochemistry[169]	2012

Table XII. HED non-implosion diagnostics developed on NNSA HED facilities.

Radiation transport diagnostics include the set of diagnostics developed on Nova, Omega and NIF to measure subsonic and supersonic radiation driven Marshak waves in low density materials and their interactions with materials.[170]

A 6 nsec point backlighter was developed to radiograph material evolution[159] and detected with an x-ray streak camera in a DIM along a polar axis.[171]

A second Dante was developed in collaboration with AWE and installed on NIF to measure the radiation transported thru material perturbations. As such, the second Dante was placed on the opposite hemisphere on NIF from the existing DANTE. It was also placed closer to the target chamber center to measure lower temperatures than the existing Dante. The 64° angle from the polar axis is greater than the 36° original DANTE angle and was chosen due to practical constraints.[172] To corroborate the drive on the half-hohlraum driven by laser beams from the lower hemisphere of NIF, an enclosed VISAR turning mirror was used to redirect the equatorial VISAR to the polar axis.[126] A transmission grating imaging spectrometer front end to an x-ray streak camera was developed to measure the burn-through of a Marshak wave.[160] A similar diagnostic was developed and used on Omega experiments.[170] Most of these diagnostics are now used by all programs on NIF. X-ray streak cameras and other instruments are routinely run in the polar DIM. This second DANTE is used by other programs, including ICF to measure the x-ray flux on the upper hemisphere on NIF. The enclosed VISAR turning mirror technique is routinely used by many experiments. Opacity experiments use specialized calibrated spectrometers, either variable spaced gratings coupled to an x-ray framing camera or crystal spectrometers coupled to film or an image plate. Work is ongoing to replace the film/image plate with a CMOS detector.

Capabilities that HED facilities provide are the ability to compress materials quasi-isentropically to high pressure (tens of MBars) and shock compress materials to extremely high pressure (~GBar). Material property experiments use 1D line VISAR and 2D VISAR systems for equation-of-state measurements. VISAR diagnostics are covered in more detail elsewhere in this article. Temperature measurements are made by an optical pyrometer diagnostic system as part of the 1D VISAR system and with spectrometers using the EXAFS technique.[173] The EXAFS measurement technique is routinely used on synchrotrons to measure temperature in materials; it is being actively developed on laser driven high pressure experiments as well. The first demonstration at Omega used an implosion to create a continuum source of x-rays and a flat crystal spectrometer to measure the x-ray absorption for Ti and Fe K-edges.[174,163]

The design on NIF moves to increasingly higher Z materials, requiring higher photon energy x-ray sources generated by laser illumination onto foils and measurements at the K and L-edges of elements. The spectrometer design uses a toroidal crystal that has high collection efficiency and minimizes the effect of source size broadening on the spectral resolution. Different crystals are used to match the K and L edges of particular materials.[166] These are particularly challenging measurements due to the need for high spectral resolution and collection efficiency, which places very high demands on the crystal surface and uniformity. Another important measurement in materials at high pressure is the structure and phase. The material structure can be measured by using diffracting x-rays from the compressed material. Typically the detector is film or an image plate. The time resolution comes from the impulse of x-rays created; typically one data point at compression is collected on a single experiment. The diagnostic detector is usually integrated with the target holder, which is a unique feature among the diagnostics. Because of the close proximity of the target with the detector, debris and background signal mitigation are issues that must be mitigated. To increase the data from a single experiment and also be able to study the kinetics of phase transitions, work is ongoing to replace the detector from film or image plate to an active gated CMOS detector.[165] Because the active detector is 10x closer to the target than any other diagnostic, much work is required to mitigate debris and background signal. The approach is promising, and data has been acquired on a prototype instrument.

Hydrodynamic and radiation-hydrodynamic experiments measure the instability growth in planar and convergent geometry. Typically they use x-ray radiography as the primary measurement. Key attributes of the measurement are high spatial resolution and temporal gating to reduce motion blurring. The typical configuration uses an area x-ray source of a few keV and a pinhole onto a gated microchannel plate detector.[175,176] This provides about 10–20 μm spatial resolution at the target and 100 psec of temporal resolution. However, as the opacity of the experiment increases due to the larger target sizes, higher density materials and/or higher compression, higher photon energy is required. This in turn requires point backlighters to create the necessary fluence of higher photon energy x-rays and a single-line-of sight gated detector. Earlier attempts were made to create a fast CMOS direct x-ray detector for this purpose. A 512 x 512 segmented detector was designed by MIT Lincoln Labs, the CMOS fabricated at Taiwan Semiconductor Manufacturing Company (TSMC), and a detector constructed and tested at LLNL.[74]

The temporal gate width was measured to be 250 ps. The work was discontinued due to the high costs to iterate on the design and fabrication of prototype CMOS chips and the year long lead time at a commercial foundry. The current work on CMOS detectors takes advantage of the existing CMOS fabrication facility at Sandia National Laboratories which is more suited to R&D as well as the invention of the time dilation front end which

eliminated the need for short gate times. Work is also currently underway to improve the spatial resolution for hydrodynamics experiments to ~ 3-5μm using collection optics such as a curved crystal[118] or zone plates[177] and to reduce temporal blurring by using a shorter pulse x-ray source.

Two classes of diagnostics were developed to study burning plasmas. Radiochemistry is a measurement technique that was developed to study reactions in a burning plasma.[178]

By selectively doping portions of a capsule, the resultant nuclear reaction products can provide information on mix, reaction chains and branching ratios that are not possible elsewhere due to the high n fluences from a burning DT plasma. Hardware to collect the reaction products, gaseous[168] and solids,[169] and rapid analysis of the decays have been developed and installed. Selective capsule doping has been a challenge to develop and has limited the application of these diagnostics. Another diagnostic was developed to provide an x-ray image in the presence of high yield. It utilizes x-ray absorption induced index of refraction changes in a semiconductor, which has a response time of ~ 30 fs.[179] A binary grating on the surface of the semiconductor encodes the x-ray image onto the semiconductor. An interference pattern results, which can be encoded onto an incident laser beam, transported a distance away and the image optically reconstructed. The technique has been demonstrated in the laboratory recording two static frames. While promising, it still requires demonstration on an implosion at a smaller scale before being considered as a viable diagnostic.

Since most HED experiments are used to compare with simulations, careful instrumental calibrations are required. There has been a long standing collaboration with the Livermore Operations run currently by the Nevada National Security Site (NNSS) organization in this area.[136]

In summary, a number of diagnostics have been developed for non-implosion HED applications. Some have been broadly applicable to many other areas as people have discovered new applications for these diagnostics, such as VISAR, second DANTE, polar DIM. Most of the other diagnostics have highly specialized applications and have also been used for discovery science in the same physics area. The NDWG has played a major role in the development of these broad use diagnostics and also the most important specialized diagnostics.

4.4 Commissioning the Set of NIF Diagnostics Installed by 2014

By 2014 a first set of 65, mainly implosion, diagnostics was operational on NIF.[180] The implosion diagnostic suite for NIF had to be commissioned and calibrated. Ideally, measurements would be made with a neutron source with characteristics close to a burning plasma and the many observables would be validated or at least cross checked against each other. Initially direct-drive gas-filled capsule implosions were used.[181] in a collaboration between LLNL, LANL, LLE and GA. However the limitations of using NIF for direct drive implosions in terms of implosion drift velocity became apparent, and so indirectly driven capsules in near vacuum hohlraums began to be used.[182] By using relatively low implosion convergences good agreement with simulations was obtained thus providing a well characterized sources of x-rays, gamma rays and nuclear particles to ensure all diagnostics were performing well.

4.4.1 Directly Driven Capsules: "Exploding Pushers"

Thin glass shells filled with DD, DHe^3 or DT gas mixtures were used to provide sources of neutrons, protons and x-rays using on the NIF utilizing polar direct drive geometry[183] In this design the thin glass outer wall of the capsule wall is heated by keV electrons produced by the laser illumination. This causes the wall to "explode" into the interior gas driving a strong shock, which heats the gas rapidly to high temperatures (~10keV) in

a low convergence implosion, which produces a short burst of fusion neutrons and/ or protons with negligible areal density at stagnation[184] These implosions provided a good source of nuclear particles without the complication of scattered neutrons and allowed cross calibration of neutron time of flight diagnostics against absolute techniques such nuclear activation.

The 1.5–2.1mm diameter, 4-10um thick glass shells were fabricated at General Atomics These "Hoppe" shells were then filled with DT, DD or DHe^3 gas mixtures at LLE and used for calibration experiments on both OMEGA and NIF. This is another example of the strong national collaboration that pooled expertise and resources at multiple institutions to develop these diagnostics. Interestingly the experimental design for the NIF polar direct drive geometry was put together by a summer high school intern at LLE; this work was published in 2008[183] Figure 18 shows how the DT neutron yield varied as function of NIF laser energy. These low mass targets produced yields in the range of 10^{13} to 7 10^{14}, areal densities < 20 mg/cc and ion temperatures around 10keV, which were ideal for commissioning NIF's nuclear diagnostics.

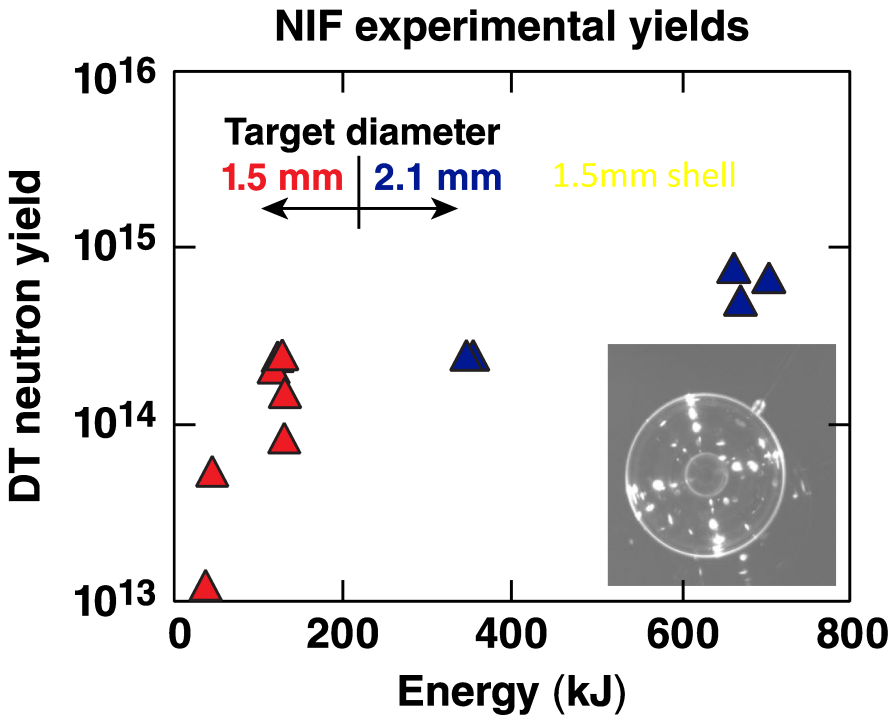

Figure 18. DT neutron yield from NIF direct drive capsules.

Initial predictions of the DT neutron yields produced by these targets proved to be optimistic, as the actual yield was about a factor of 2-3 lower than the estimates based on 2D simulations and OMEGA polar direct drive experiments from 2009. Later work suggested that the neutron yield predicted from the stagnating plasma was not accurately captured in the simulations and cross beam energy transfer (CBET) between NIF beams was also not accounted for in the early simulations. Later work has shown that including CBET is important to fully understand the performance of these implosions[181] More recent exploding pusher experiments that used larger capsules and higher laser power/ energy have increased the DT neutron yield to > 10^{16}. In summary the direct drive exploding pushers have proved to be very useful for initial commissioning and calibration of nuclear diagnostics on NIF but there were some limitations in the bulk velocity of the neutron emitting hotspot on directly driven exploding pushers, which were too high (on average > 100 km/s) to commission the un-scattered neutron diagnostics FNADS/RTNADS. A new platform utilizing indirectly driven single shock implosions was used to fill this gap.

X-ray instrument timing is routinely verified by direct illumination of gold spheres.[185]

4.4.2 Indirectly Driven Single-Shock Implosions

A new commissioning platform that provided DT neutron yields in range of 5 10^{14}, with negligible stagnation DT fuel areal density (<20mg/cm-2) and minimal hotspot bulk velocity (< 50km/s) was developed using near vacuum hohlraum and a thin (120um) plastic capsule driven by a simple one-shock pulse shape[182] When driven by low power 325 TW, total energy of 933 kJ in a 4.5ns laser pulse, this experiment resulted in a low convergence (5x) implosion with measured stagnation parameters (e.g., DD/DT neutron yield, Ion temperature, fuel areal density, time of peak x-ray emission and fwhm of both x-ray and neutron emitting hotspot)

which agreed with 1D HYDRA simulations within experimental errors as shown in Table XIII.[182]

Observable	N130312	unc.	N130503	unc.	Hydra post shot
DD n yield 10^{-12}	5.1	0.2			4.3
DT n yield 10^{-14}			5.12	0.09	5
DD T_{ion} (keV)	3.5	0.2			3.5
DT T_{ion} (keV)			4.6	0.2	4.6
Bang time ns	4.8	0.1	4.8	0.1	4.7
Radius μm	197	6	197	6	200
T_{rad} (eV)	293	5	293	5	290
Fuel ρr mg/cm^2	16	2	16	2	15.5
Total ρr mg/cm^2	52	8	52	8	44

Table XIII. Summary of the performance of the DD implosion (N131203) and the DT implosion (N130503) with uncertainties(unc) compared to the corresponding integrated HYDRA simulations.

This platform has become a workhorse experiment that is used to provide a reproducible and well-behaved quiescent source to both commission new diagnostics and recalibrate existing diagnostics following component changes and upgrades. In addition, the 1D behavior and good agreement with HYDRA simulations helped to spur new interest in low gas filled hohlraums as an experimental platform using high density carbon (HDC) ablators.[186, 187] Developments of these platforms in turn led to the Near ignition result on the NIF.[1]

4.4.3 List of Diagnostics Operational by ~ 2014

Tables XIV to XVII describe the NIF diagnostics operational by about 2014.

Acronym	Name	Who
FABS31 FABS36	Full Aperture Backscatter Station	LLNL
NBI23.5 NBI31 NBI36	Near Backscatter Imager	LLNL
Dante1 Dante2	Broadband, time-resolved x-ray spectrometer	LLNL
FFLEX FFLEX TR	Filter Fluorescer (time-resolved)	LLNL/AWE
SXI-L SXI-U	Static X-ray Imager, Lower, Upper	LLNL
EHXI	Equatorial Hard X-ray Imager	LLNL
EMP	Electromagnetic Power	LLNL

Table XIV. Diagnostics of laser absorption and hohlraum condition.

Acronym	Na	Who
SOP	Streaked Optical Pyrometer	LLNL
VISAR	Velocity Int. System for Any Reflector	LLNL/LLE
DISC (3*)	DIM Insertable (x-ray) Streak Camera	LLNL/LLE
GXD (2*)	Time-Gated X-ray Detector	LLNL/LANL
hGXI (2*)	Hardened (gated) X-Ray Imager	LLNL/LLE
NToF4BT	Neutron Time-of-Flight bang time at 4 m	LLE/LLNL
pToF	Proton (particle) Time-of-Flight Detector	MIT/LLNL/LLE
SPBT	South Pole Bang Time	LLE/LLNL
SPIDER	Streak. Polar Instrument for Detecting Energetic Radiation	SNL/LLNL
GRH	Time resolved Gamma Reaction History	LANL/LLNL

* Number in parentheses is the number of units.

Table XV. Target response/implosion diagnostics.

Acronym	Name	Who
NAD—Cu	Neutron Activation Detector using Cu	SNL
Well NAD	Well-mounted Neutron Activation Detector, Zr	LLNL
NAD—Snout ARIANE	Neutron Activation Detector in Active Readout Neutron Environment GXD	LLNL LLNL
DIXI	Dilation Imager for X-rays at Ignition	GA/LLNL
NIS	Neutron Imaging System	LANL/LLNL
NITOF	Neutron Imaging Time-of-Flight	LANL
IgnHi	Neutron Time-of-Flight	LLE/LLNL
NTOF4 (3*)	Neutron Time of flight 4m	LLE/LLNL

Table XVII Diagnostics of the hot spot.

Acronym	Name	Who
CR	Compton Radiography	LLNL
MRS	Magnetic Recoil Spectrometer	MIT/LLE/LLNL
FlNAD(17)	Neutron Activation Detector (flange mounted)	LLNL
SPEC-A, SPEC-E	Neutron Time-of-Flight- Spectrometer	LLNL/LLE
RAGS	Radiochemical Analysis of Gaseous Samples	LLNL
SRC (many)	Solid Radiochemical Collection Diagnostic	LLNL/LANL
WRF (many)	Wedged Range Filter	MIT/LLNL

Table XVII. Diagnostics of areal density.

4.5 The National Diagnostic Plan (NDP): 2015

With input from the broad diagnostic program described in section 4.2, a National Diagnostic Plan (NDP) was developed in 2014 by a diagnostic management group of scientists and engineers. A very important increase in the scope work was to include diagnostics for all HED Stockpile Stewardship experiments and not just ignition related diagnostics.

The NDP is a long document that is revised annually. The 2015 version was published by NNSA.[188] Since 2015 the NDP has evolved: the 2021 version is discussed in section 6 and accessible in full online.[189]

Here is a summary of the 2015 NDP: Recognizing the need for enhanced coordination to develop advanced ICF diagnostics, the ICF/HED community formed the national diagnostic working

group (NDWG) of technical experts to formulate and execute a national diagnostic plan (NDP). Seventeen institutions participate in the NDP including LLNL, LANL, SNL, GA, NRL, MIT and other organizations such as PPPL and industry. International involvement from AWE and Commissariat Energie Atomique (CEA) also contributes to the depth and breadth of the NDP.

The NDWG identified eight transformational diagnostics in the NDP. These will provide unprecedented information on the implosion physics in fusion relevant regimes, determine the plasma conditions created by both laser and pulse power drivers, and enable dynamic measurements of a range of relevant conditions on the properties of materials utilized in nuclear weapons.

4.6 Expert Review of the NDP 2015

In 2014, NNSA contracted a group of subject matter experts to review the work and the plans of the NDWG described in this paper to prepare for its own internal planning and also to prepare a report requested by the Senate. In January 2015 a seven-person external group of diagnostic experts and a Federal Official reviewed the National Diagnostic Plan. The full report is available and excerpted below.

> Overall the comments from the individual reviewers were highly positive on the feasibility, practicability and transformative nature of each of the eight diagnostics proposed. Each was considered highly worthy of continued development with the potential to improve experimental measurements vital to and tied to key mission requirements, and reviewers were favorably impressed at the breadth of discussions across the community that had revitalized this area by bringing to bear several new capabilities in development elsewhere. The efforts highlight the value of the Federally Funded Research and Development Center construct.

Some reviewers expressed concern at the outset that the proposed list only contained “winners” and that therefore some other diagnostics worthy of consideration were excluded prematurely. These concerns were allayed when “also rans” were discussed and it became clear that these were proposals where technical risk was very much higher or the scope and reach was much smaller, in both cases, therefore, more suitable for a smaller development effort within the discretion and budget of a specific facility.

A second common concern is that no overall sense of priorities among the proposals was presented to guide development in the event that there is a shortfall in available resources. Two key technologies did rise to the forefront as seminal developments that had a cross-cutting impact, the pulse-dilation technology being developed at General Atomics, and already employed as a first step in the LLNL DIXI detector, and the fast gated CMOS framing camera technology which is an unanticipated spin-off from years of investment in fabrication capabilities at the MESA facility at SNL.

There was some concern that even tighter integration was needed between the diagnostics development effort and the experimental and design communities to ensure that diagnostic capabilities continue to meet needs and expectations as progress is made on all fronts.

Overall, however, the considered review of each reviewer was that each of the eight proposed diagnostics was transformative, had

a reasonable probability of success, would have substantial payoff to the mission requirements and should proceed if resources can be made available

5. NDWG MEETINGS 2015–2021

Following the 2015 review of the NDP, NNSA agreed to a charter for the NDWG and its relationship to the NNSA HED plan. In summary large meetings of the NDWG were held annually, except 2020, to review the NDP and provide recommendations to a NDP Management review group to increment or decrement the NDP. A summary of the large meetings of the NDWG is shown in Table XVIII, together with dates and locations.

#	Section	When	Where	# attendees
10	5.1	Oct-15	LANL	133
11	5.2	Nov-16	LLNL	115
12	5.3	Dec-17	GA	~110
13	5.4	Dec-18	LLE	127
14	5.5	Dec-19	LLNL	~120
15	5.6	Dec-21	LANL,virtual	NA

Table XVIIII. Summary of large meetings of the NDWG.

With input from these large NDWG meetings, the management group readjusts the NDP including the expected diagnostic schedule and makes recommendation to the managers of the facilities and NNSA for changes to the diagnostics at the facilities.

5.1 The Tenth National Diagnostic Working Group Meeting

The tenth group meeting was held 10/6–8/15 and to symbolize the national character of the meeting it was hosted by LANL, with a record number of attendees. As this was the first broad meeting after the January 2015 review, the National Diagnostic Plan was presented. Two of the plenaries were about diagnostics for underground testing and for the proposed MARIE facility. In addition, there were seven plenaries and ten small group discussions summarized in a plenary. Each of the ten parallel sessions had four or five mini-discussion topics. A notable technical breakthrough was the realization that the pulse dilation technology used for x-ray imaging (Section 2.3.5) could be used to manufacture a 10 psec PMT allowing the gamma Cherenkov detectors (GCD and GRH) to have a much faster response time. This PMT came to fruition by the 15th NDWG meeting in 2021.

5.2 The Eleventh National Diagnostic Working Group Meeting

The eleventh NDWG meeting was held at LLNL, November 29–30, 2016 with 115 participants. Four of the eight transformational diagnostics had detailed engineering plans which were presented in plenary sessions, namely optical Thomson Scattering, hCMOS, neutron imaging and high-resolution x-ray spectrometry. Most of the work of the meeting was done in a set of eleven breakout groups during three parallel sessions. These were set up with directed scientific discussions to address specific questions posed by the NDWG management group and needed to update the National Diagnostic Plan and recommend important areas of collaboration and investment to the NNSA and Laboratory leaderships. The eleven breakout sessions were: Precision nToF, Mix and T_e, Pulse Dilation, Image Analysis, Hard X-Ray Detectors, MRS (time), XDV, Phase Change, n /gamma

imaging, synthetic data, and reflective x-ray imaging. The detailed breakout reports are available.

5.3 The Twelfth NDWG Meeting

The twelfth NDWG meeting was held at General Atomics, 12/5–12/7, 2017, with ten plenary sessions and eight small group discussions in parallel sessions. The NDWG meeting was followed by a joint diagnostic meeting with CEA. Highlights of the plenary sessions were:

i. A description of the wide range of diagnostics used in the material group (Section 4.3) work for diffraction, strength, EOS, and EXAFS with the point that diagnostic development will have a significant aid to understanding high Z material aging. It is of note that tthe multi-frame x-ray diffraction diagnostic using the multi time gated hCMOS arrays (section 2.3.1) came to fruition in 2022.

ii. Exciting results from neutron imaging reconstruction.

iii. Reports out from small workshops during the year on stagnation, nToF and spectroscopy

iv. A summary of progress on the recommendations of the previous (11th) NDWG reports out.

There were eight small-group discussions of the following topical questions:

i. High Speed Photo Diode/PMT. Is the time dilation PMT concept viable?

ii. 3D X-ray Implosion Imaging – Where next for NIF, OMEGA, & Z? In light of experience and requirements of spatial, temporal & spectral resolution and throughput where next for each of the three facilities.

iii. Optical probing for n_e x L and B. With the deep u.v. optical probes available can we use phase shifts and Faraday rotation to measure B.

iv. Calibration of Image Plates. Should we regularize the calibration and readout procedures for NIF, OMEGA and Z?

v. Where Next for nToFs on NIF, Z & OMEGA? Do the new Cherenkov quartz detectors change the way we field the next nToFs on the three facilities?

vi. Coded Aperture Imaging: X-rays and neutrons. Given progress with penumbral x-ray imaging on NIF, is there any benefit to other coded aperture schemes for NIF OMEGA and Z

vii. VISAR Next Step Line and 2D on NIF, OMEGA, and Z. In light of many years use on OMEGA and NIF, where next, for VISAR on NIF, OMEGA, and Z

viii. Hardened Focal Plan Arrays (FPA). Should we develop a national plan for the best schemes such as dump and read, to harden our FPAs against neutrons and EMP?

There was a plenary report out of these small group discussions.

5.4 The Thirteenth National Diagnostics Working Group Meeting

Held 12/5–12/6, 2018, at the Laboratory for Laser Energetics, the thirteenth NDWG included eight breakout sessions with action items with responsible individuals There were plenary summaries: the previous NDWG at GA, a VISAR workshop, a nToF workshop. There was a visit to a nearby industrial partner Sydor Technologies Inc.

Of note were

i. A discussion the hard x- ray transmission and structured photo-cathode detection issues,

ii. Hard X-ray Hybrid CMOS opportunities and development plans of hCMOS readout electronics, GaAs, and Ge photodiodes).

iii. Assessment of the Dual Slot (DS) Streak Tube.

iv. A discussion of a major upgrade to the VISAR/SOP system at LLNL.

Of note were two longer term overview talks:

i. Diagnostic needs of HED experiments.

ii. What is next for transformative diagnostics? The original team decided on the eight transformational diagnostics in 2014. Progress has been good on most of the transformative diagnostics but to flourish the group must continually enforce down selection and addition of new ideas.

The small group discussions were: Existing calibration capabilities for x rays, Bayesian analysis-imaging, machine learning, Bragg crystals (fabrication, calibration), Fresnel zone plate imaging, neutron imaging on OMEGA, hotspot diagnostics, time resolved diffraction path forward, diagnostic development for EXAFS, MRSt path forward, optical, and nuclear calibration facilities. As usual the meeting finished with a plenary on reports from the ten small-group sessions.

5.5 The Fourteenth National Diagnostics Working Group Meeting

The fourteenth meeting was held 12/10–12/11, 2019, at LLNL.

Plenary talks covered time-dependent x-ray diffraction, MRSt update, next-generation streak cameras, summary of optical Thomson scattering, x-ray crystal imaging, data fusion, next-generation NIF VISAR, diagnostic needs for Z & NIF, Wolter x-ray microscope and Z line VISAR There were six small-group sessions on topics: high- resolution x-ray imaging, passive detectors, hotspot drift velocity, 15 keV photon detection, Burn widths, and magnetic field diagnostics. As usual the meeting finished with a plenary on reports out from the ten small group sessions.

5.6 The Fifteenth National Diagnostic Working Group Meeting

This meeting was held virtually and hosted by LANL in December 2021, delayed from 2000.

6. THE NATIONAL DIAGNOSTIC PLAN (NDP) FOR HED SCIENCE, SEPTEMBER 2021

The NDP is updated annually as described earlier in this paper. Section 4.5 is a summary of the NDP written in 2015. The latest (2021) version of the NDP is a 44-page document accessible online.[189]

This section is a summary of the latest version of the NDP.

The national diagnostics development effort is divided into three groups:

- Transformational diagnostics: diagnostics requiring a major national effort with the potential to transform experimental capability for the most critical science needs across the complex.
- Broad diagnostics: diagnostic efforts and techniques requiring significant national efforts which will enable new or more precise measurements across the complex.
- Local diagnostics: important diagnostics that implement known technology for a local need and are identified by facility management responding to the needs of the local user community.

The NDWG has identified ten transformational diagnostics, shown in Table XIX, that will provide unprecedented information from experiments in support of the SSP at NIF, Z and OMEGA. Table XIX shows how the missions of the SSP experiments including materials, complex hydrodynamics, radiation flow and effects and thermo-nuclear burn and boost will produce new observables, which need to be measured using a variety of the largely new diagnostic technologies used in the ten transformational diagnostics. The data provided by these diagnostics will validate and improve the physics contained within the SSP's simulations and both uncover and

quantify important phenomena that lie beyond our present understanding.

Transformative diagnostic	Collaborating Institutions	New capability
Single LOS imaging (SLOS or DIXI-SLOS)	SNL, GA, LLNL, LLE	Multi-dimensional shape and spectra with unprecedented time and space resolution for fusion, Pu strength, and radiation effects sources
Ultraviolet Thomson Scattering (UVTS)	LLE, LLNL, LANL, NRL	Localized plasma conditions and turbulence in hohlraums and Laser Direct Drive ablation plasma. Additional uses include plasma conditions at low density for rad flow studies and many discovery science applications.
3D n/gamma imaging (NIS)	LANL, LLNL	3D shape & size of both burning and cold compressed fuel, as well as remaining carbon ablator
Gamma spectroscopy (GCD)	LANL, AWE, GA, LLNL, SNL, NNSS	Fusion burn history allowing inferred pressure with increased precision and measured truncation of burn from degradation mechanisms such as mix and loss of confinement.
Time resolved neutron spectrum (MRS-time)	MIT, LLNL, GA, LLE	Time evolution of the fusion burn temperature and areal density
Hard x-ray imaging (Wolter)	SNL, LLNL, NASA, Harvard	High energy source distribution and space-resolved plasma conditions in the hot plasma. Also enables high spatial and temporal resolution for radiography to infer material strength.
Time resolved diffraction (XRDt)	SNL, LLNL, LLE	Time evolution of material structure (including weapon materials) and compression at high pressure. Also enables more efficient facility use through multiple measurements on a single shot.
High Resolution Velocimeter (HRV)	LLNL, LLE, SNL	Higher accuracy (< 1%) time evolution of material EOS at high pressure. Also enables more efficient facility use through multiple high-fidelity measurements on a single shot.
>15 keV X-ray detection (DHEX)	LLNL, LLE, SNL	Multiple-frame time resolved detection of high energy (>15 keV) x-rays with high detection efficiency.
hCMOS	SNL, LLNL	Multi-frame, burst mode imaging sensor capable of capturing images on the nanosecond timescale.

Table XIX. The ten transformational diagnostics og the NDP with institutional involvement, and capability.

Mission	New Observable	Technique	Acronym
Materials	Strength vs time of compressed Pu	>4 images/costly target	SLOS, hCMOS
	Phase change of compressed Pu – rates	Time resolved x-ray diffraction	XRDt
	EOS of compressed Pu	High resolution velocimeter	HRV
Hydro and Properties	3D Structure at ~50 keV	X-ray bands imager +SLOS	Wolter, hMCOS
	High energy x-ray images of structure	Detection of high-energy x-rays	DHEX
	T_e of Marshak wave	Deep U.V. Thomson scattering	UVTS
Outputs and Survivability	Hard spectrum vs space & time	X-ray bands imager +SLOS	Wolter, hCMOS
TN Burn and Pursuit of High Yield	Time history of burn	Ultra-fast Cerenkov detector	GCD
	3D T_e and density vs time	Dilation tube +SLOS +Wolter	SLOS, hCMOS
	3D burn, 3D mix vs time	3D neutron/ imaging	NIS
	T_{ion} and areal density vs time	Neutron spectrum vs time	MRS-time
All	Hohlraum density & T vs space & time	Deep U.V. Thomson scattering	UVTS

Table XX. How the missions of the SSP will be enhanced by new observables measured by the ten transformational diagnostics being developed under the guidance of the NDWG.

In addition to these transformational diagnostics there are

- a set of broad diagnostics coordinated across the ICF sites,
- a large number of local diagnostics associated with the three large facilities: NIF, Z and OMEGA.

7. CONCLUSION

The National Diagnostic Working Group has been highly successful in coordinating and implementing the HED diagnostics on NIF, OMEGA and Z. It is the work of well over 100 scientists and engineers over more than a decade. This paper summarizes the achievements of the NDWG. The paper analyzes the reasons for its success.

First and foremost are the collaborations of the NDWG. As well as the NNSA Labs, participants include universities, European institutions, and importantly, industry. Collaborations attract external experts. Examples of the benefits of involving experts from industry as well as other institution are referenced in Table XXI. Industry also benefits by spinoffs marketable products, as seen in Table XX. Collaborations also lead to the use of non-home facilities for testing and calibrations. The high shot rate of OMEGA has been particularly useful as discussed in sections 2.1 and 2.2.2. And a final benefit of collaboration is the agreed diagnostic responsibility and usually some financial responsibility at other institution.

A second factor is the accommodations of change of scope of diagnostics. As theories and ideas are falsified or improved, more diagnostics are needed with a concomitant scope and schedule change. Examples are referenced in table XXI. Likewise, as better experiments are developed a need for improved accuracy arises as referenced in table nn. Schedule expansion leading to many generations of diagnostic, such as three generations of nToFs and four generations at least of spectrometers. Staff benefit greatly from publications. The HTPD and SPIE conferences and the associated publications has been a forcing factor in motivating copious diagnostic papers over the years.

A third factor is the methods of accomplishment of the NDWG. A moderately large (to cover personnel

changes) management group is responsible for keeping a national diagnostic schedule updated. As the schedule is often paced by resources, the members of this group have significant budget responsibility at their home institutions and respect from NNSA. The members of the group get information about diagnostic from the large annual NDWG meetings, see Table XVIII. These large meetings alone cannot engender detailed discussion and so typically several parallel small group discussions with discussion topics set by the management meeting occur. Importantly, the small groups report out at the plenary session and thus the management group at the end of the meetings. A hybrid meeting process leads to many scientists and engineers feeling ownership of the NDP. Clearly this method works.

The entire ICF and NNSA community supported the development of very difficult, expensive instruments that took a long-time to germinate and develop. The success of the NDWG is a credit to the whole community.

Factor	Attribute	Examples		Section
		Institution	**Diagnostic**	
Collaborations	Attract external experts	Industry	Gated MCP	2.1
		Industry	Pulse Dilation	2.3.4
		Industry	Gated PMT	2.2.1
		Industry	Electron optics	2.4.2
		MIT	MRS	2.2.2
		PPPL	DHIRES	2.4.2
		NRL	Virgil	2.4.1
		CEA	Dante mirror	2.4.1
	Spinoffs	Photek/Sydor	PD PMT	2.3.5
		Sydor	XRFC	2.1
		SNL	Advanced hCMOS Systems	2.3.1
		NASA Marshall	X-ray optics polishing	2.6
	Best facility for the job	OMEGA	nToF calibration	2.2.1
		OMEGA	NXS calibration	2.4.1
		Nike	Virgil calibration	2.4.1
		OMEGA	OMEGA Gated MCP, Serpentine	2.1
		NNSS Liv. Office	Calibration	4.3
	Agreed diagnostic responsibility	LLNL	nToF calibration OMEGA	2.2.1
		LLNL	XRFC for OMEGA	2.1
		SNL	hCMOS	2.3.1
		LANL	NIS, GRH and GCD	2.7
		LLNL	Wolter for Z	2.6
Scope expansion in time	Falsifiability/ accuracy – new/ upgraded diagnostics	Reason	Diagnostic	
		Falsifiability: anisotropy	Many nTOFs, many NADS	2.2.1
		Falsifiability: burn drift velocity	Faster nToFs	2.2.1
		Falsifiability: fill tube, mix	X-ray gating	2.1
		Accuracy	VISAR	2.5
		Accuracy	Spectrometers, streak cameras	2.4.2
	Copious publications	Review of Scientific Instruments		3.1
		Proceedings of the SPIE		3.1
Methods of accomplishment	NDWG management group with engineers	Updated National Diagnostic Plan (NDP) with schedules		4.5,5
		Resource recommendations to facilities/NNSA		4.2,6
	Targeted NDWG parallel sessions	New ideas from broad community		4.2, 5.1-5.6
	Large NDWG Plenary Meeting	Review updated NDP		4.2
		Review output parallel session Updated NDP		5.1-5.6
		Changes in programs		

Table XXI. The success factors of the NDWG, some attributes of the success factors with examples discussed in this paper.

ACKNOWLEDGEMENTS

The NDWG is a collegial association of greater than 100 scientists and engineers who have all contributed to the work of the NDWG. One hundred and seventeen, or less of us, are shown here from the ninth meeting, 9/2014 (Section 4.2).

AUTHOR DECLARATIONS

The authors have no conflicts of interest to disclose.

AUTHOR CONTRIBUTIONS

J. D. Kilkenny: Conceptualization (equal); lead author. S. Batha: Conceptualization (equal): Section 2.6. W. W. Hsing: sections 2.4, 4.3. G. A. Rochau: Conceptualization (equal); Section 2.1. T. C. Sangster: Conceptualization (equal); Section 2.2. P. M. Bell: Section 2.1. H. Chen: Section 2.3.7. J. A. Frenje: Section 2.2. M. Gatu-Johnson: Section 2.2.2. V. Yu Glebov: section 2.2.1. A. J. Mackinnon: Section 4.4. S. P. Regan: Section 2.3.7 J. S. Ross: Section 2.7.

APPENDIX. DIAGNOSTIC ACRONYMS

Acronym	Meaning
ARIANE	Active Readout in a Neutron Environment
CBI	X-ray Crystal Backlit Imager
CDR	Conceptual Design Review
CNXI	Combined Neutron and X-ray Imager
Dante	Broad-band, time-resolved x-ray spectrometer
dHIRES	DIM HIgh RESolution Spectrometer)
DIM	Diagnostic Insertion Manipulator
DISC	DIM Insertable (x-ray) Streak Camera
DIXI	Dilation X-ray Imager
DSR	Down Scatter Ratio
EMP	Electromagnetic Power
EHXI	Equatorial Hard X-ray Imager
ERASER	Early Radiation Artifact Suppression Electrode Rig gated MCP
EXAFS	Extended X-ray Absorption Fine Strucre
FABS	Full Aperture Backscatter Station
FFLEX	Filter Flourescer
Flange-NADS	Flange Neutron Activation Diagnostic
GCD	Gamma Cherenkov Detector
FPA	Focal Plane Array of detectors, usually hCMOS
GLEH	Gated Laser Entrance Hole x-ray pinhole imager
GRH	Gamma Reaction History
GXD	Time-Gated X-ray Detector
hCMOS	Hybridized complementary metal-oxide sensor
hDISC	Hardened DIM Insertable (x-ray) Streak Camera
HSXRS	Hot-spot x-ray spectrometer (
HTPD	High Temperature Plasma Diagnostic conference
GXI	Time-Resolved X-ray Imagers
HED	High Energy Density
hGXI	Hardened (gated) X-ray Imager
KB	Kirkpatrick Baez x-ray microscope
hSLOS	Hardened SLOS
LaNSA	Large Area Neutron Scintillator Array on Nova
L/D	Length to diameter of pores in an MCP
LEH	Laser Entrance Hole
LOS	Line Of Sight

MCP	MicroChannelPlate
MRS	Magnetic Recoil Spectrometer
MRSt	time resolved Magnetic Recoil Spectrometer
NAD Well-Zr	Neutron Activation Detector in a well using zirconium
NAD–Cu	Neutron Activation Detector using copper
NAD—Snout	Neutron Activation Detector DIM mounted snout
NBI	Near Backscatter Imager
NIS	Neutron Imaging System
NDWG	National Diagnostic Working Group
NDP	National Diagnostic Plan
NIS	Neutron Imaging System
NITOF	Neutron Imaging Time of Flight
NSTec	National Securities Technology
NTOF20 SPEC-A	Neutron Time-of-flight Spectrally Resolving Detector in the Alcove
NTOF20 SPEC-E	Neutron Time-of-flight Spectrally Resolving Detector on the Equator
NTOF20IgHi	Neutron Time of Flight at 20 m for Ignition
NToF4	Neutron Time of Flight at 4 m (NToF4)
NTOF4BT	Neutron time of flight bang-time at 4 m
NXS	NIF x-ray spectrometer
OTS	Optical Thomson Scattering
OPSPEC	Opacity x-ray Spectrometer–time gated
PD	Pulse Dilation of the time history of a signal for detection by a slow detector
PMT	Photo Multiplier
pToF	Proton (particle) Time-of-flight detector (pToF):
pDIXI	Polar Dilation X-ray Imager
RadChem	Radio Chemistry
RAGS	Radiochemical Analysis of Gaseous Samples diagnostic
RIC	Radiation Induced Conductivity
ROIC	Read out integrated circuit
RTNADS	Real Time Neutron Activation Detectors
SID	System for Insertable Diagnostics
SIM	Six-inch manipulators
SFX	Sydor x-ray Framing Camera
SLOS	Single Line of Sight x-ray imager usually with pulse dilation (PD)
SOP	Streaked Optical Pyrometer
SPBT	South Pole Bang Time
SPIE	Formerly Society of Photographic Instrumentation Engineers
SPIDER	Streaked Polar Instrumentation for Detection of Energetic Radiation

SRC	Solid Radiochemical Collection diagnostic
SSC	Streaked Slit Camera
SSI / SSII	Super snouts I /II. Multi-wavelength x-ray Spectrometer
SXI	Static X-ray Imager
SXRI	Soft X-ray Imager
SXSS	Soft X-ray Streak Spectrometer
TARDIS	Target Diffraction In-Situ
TIM	Ten-inch manipulators
TRXI	Time Resolved X-ray Imager (OMEGA)
VISAR	Velocity Interferometer System for Any Reflector
WRF	Wedged Range Filters
XRFC	X-Ray Framing Camera

References

[1]I. D. I. Collaboration, Phys. Rev. Lett. **129,** (2022).
[2]K. Popper, *The Logic of Scientific Discovery* (Hutchinson, 1974).
[3]G. Power and P. Bell, *Proceedings of 32nd Annual International Technical Symposium on Optical and Optoelectronic Applied Science and Engineering,* San Diego, CA, 1989, (SPIE).
[4]M. J. Eckart, R. L. Hanks, J. D. Kilkenny, R. Pasha, J. D. Wiedwald and J. D. Hares, Rev. Sci. Instrum. **57,** 2046 (1986).
[5]G. Power, "Gain Variation with Gold Coating Thickness in Pulsed MicroChannel Plate Striplines", Lawrence Livermore National Laboratory Report UCID-21321, 1988 Unpublished.
[6]J. D. Kilkenny, P. Bell, R. Hanks, G. Power, R. E. Turner and J. Wiedwald, Rev. Sci. Instrum. **59,** 1793 (1988).
[7]D. Bradley, J. Delettrez, P. Jaanimagi, F. Marshall, C. Verdon, J. Kilkenny and P. Bell, *Proceedings of 32nd Annual International Technical Symposium on Optical and Optoelectronic Applied Science and Engineering,* San Diego, CA, 1989, (SPIE).
[8]P. Bell, J. Kilkenny, G. Power, R. Bonner and D. Bradley, *Proceedings of 33rd Annual Technical Symposium,* San Diego, California, 1989, (SPIE).
[9]D. K. Bradley, P. M. Bell, J. D. Kilkenny, R. Hanks, O. Landen, P. A. Jaanimagi, P. W. Mckenty and C. P. Verdon, Rev. Sci. Instrum. **63,** 4813 (1992).
[10]J. Wiedwald, Hanks, R., Tietbohl, G., Bishop, D., Power, G., Kelly, F., Bell, P., *Proceedings of Ultrahigh Speed and High Speed Photography, Photonics, and Videography '89,* 1989, (SPIE).
[11]O. L. Landen, *Proceedings of Ultrahigh- and High-Speed Photography, Videography, and Photonics '94,* 1994, (Proc SPIE).
[12]D. K. Bradley, P. M. Bell, O. L. Landen, J. D. Kilkenny and J. Oertel, Rev. Sci. Instrum. **66,** 716 (1995).
[13]L. M. Logory, D. R. Farley, A. D. Conder, E. A. Belli, P. M. Bell and P. L. Miller, Rev. Sci. Instrum. **69,** 4054 (1998).
[14]K. S. Budil, T. S. Perry, P. M. Bell, J. D. Hares, P. L. Miller, T. A. Peyser, R. Wallace, H. Louis and D. E. Smith, Rev. Sci. Instrum. **67,** 485 (1996).
[15]J. A. Oertal, T. Archuleta; C. G. Peterson; F. J. Marshall, *Proceedings of 22nd International Congress on High-Speed Photography and Photonics,* 1997, (SPIE).
[16]J. A. Oertel, R. Aragonez, T. Archuleta, C. Barnes, L. Casper, V. Fatherley, T. Heinrichs, R. King, D. Landers, F. Lopez, P. Sanchez, G. Sandoval, L. Schrank, P. Walsh, P. Bell, M. Brown, R. Costa, J. Holder, S. Montelongo and N. Pederson, Rev. Sci. Instrum. **77,** 10e308 (2006).
[17]S. Technologies.
[18]G. A. Kyrala, S. Dixit, S. Glenzer, D. Kalantar, D. Bradley, N. Izumi, N. Meezan, O. L. Landen, D. Callahan, S. V. Weber, J. P. Holder, S. Glenn, M. J. Edwards, P. Bell, J. Kimbrough, J. Koch, R. Prasad, L. Suter, J. L. Kline and J. Kilkenny, Rev. Sci. Instrum. **81,** 10e316 (2010).
[19]T. Nash, M. Derzon, R. Leeper, D. Jobe, M. Hurst and J. Seamen, Rev. Sci. Instrum. **70,** 302 (1999).
[20]C. A. Kruschwitz, M. Wu and G. A. Rochau, Rev. Sci. Instrum. **82,** 023102 (2011).

[21]G. A. Rochau, M. Wu, C. Kruschwitz, N. Joseph, K. Moy, J. Bailey, M. Krane, R. Thomas, D. Nielsen and A. Tibbitts, Rev. Sci. Instrum. **79,** 10e902 (2008).
[22]L. R. Benedetti, P. M. Bell, D. K. Bradley, C. G. Brown, S. M. Glenn, R. Heeter, J. P. Holder, N. Izumi, S. F. Khan, G. Lacaille, N. Simanovskaia, V. A. Smalyuk and R. Thomas, Rev. Sci. Instrum. **83,** 10e135 (2012).
[23]L. R. Benedetti, J. P. Holder, M. Perkins, C. G. Brown, C. S. Anderson, F. V. Allen, R. B. Petre, D. Hargrove, S. M. Glenn, N. Simanovskaia, D. K. Bradley and P. Bell, Rev. Sci. Instrum. **87,** 23511 (2016).
[24]C. Trosseille, D. Aubert, L. Auger, S. Bazzoli, T. Beck, P. Brunel, M. Burillo, C. Chollet, J. Gazave, S. Jasmin, P. Maruenda, I. Moreau, G. Oudot, J. Raimbourg, G. Soullie, P. Stemmler and C. Zuber, Rev. Sci. Instrum. **85,** 11d620 (2014).
[25]L. R. Benedetti, C. Trosseille, J. P. Holder, K. Piston, D. Hargrove, D. K. Bradley, P. Bell, J. Raimbourg, M. Prat, L. A. Pickworth and S. F. Khan, Rev. Sci. Instrum. **87,** 11d622 (2016).
[26]N. B. Meezan, D. T. Woods, N. Izumi, H. Chen, H. A. Scott, M. B. Schneider, D. A. Liedahl, O. S. Jones, G. B. Zimmerman, J. D. Moody, O. L. Landen and W. W. Hsing, Phys. Plasmas **27,** 102704 (2020).
[27]O. S. Jones, L. J. Suter, H. A. Scott, M. A. Barrios, W. A. Farmer, S. B. Hansen, D. A. Liedahl, C. W. Mauche, A. S. Moore, M. D. Rosen, J. D. Salmonson, D. J. Strozzi, C. A. Thomas and D. P. Turnbull, Phys. Plasmas **24,** 056312 (2017).
[28]D. A. Callahan, O. A. Hurricane, J. E. Ralph, C. A. Thomas, K. L. Baker, L. R. Benedetti, L. F. B. Hopkins, D. T. Casey, T. Chapman, C. E. Czajka, E. L. Dewald, L. Divol, T. Doppner, D. E. Hinkel, M. Hohenberger, L. C. Jarrott, S. F. Khan, A. L. Kritcher, O. L. Landen, S. LePape, S. A. MacLaren, L. P. Masse, N. B. Meezan, A. E. Pak, J. D. Salmonson, D. T. Woods, N. Izumi, T. Ma, D. A. Mariscal, S. R. Nagel, J. L. Kline, G. A. Kyrala, E. N. Loomis, S. A. Yi, A. B. Zylstra and S. H. Batha, Phys. Plasmas **25,** 056305 (2018).
[29]R. Tommasini, J. E. Field, B. A. Hammel, O. L. Landen, S. W. Haan, C. Aracne-Ruddle, L. R. Benedetti, D. K. Bradley, D. A. Callahan, E. L. Dewald, T. Doeppner, M. J. Edwards, O. A. Hurricane, N. Izumi, O. A. Jones, T. Ma, N. B. Meezan, S. R. Nagel, J. R. Rygg, K. S. Segraves, M. Stadermann, R. J. Strauser and R. P. J. Town, Phys. Plasmas **22,** 056315 (2015).
[30]S. R. Nagel, S. W. Haan, J. R. Rygg, M. Barrios, L. R. Benedetti, D. K. Bradley, J. E. Field, B. A. Hammel, N. Izumi, O. S. Jones, S. F. Khan, T. Ma, A. E. Pak, R. Tommasini and R. P. J. Town, Phys. Plasmas **22,** 022704 (2015).
[31]A. Pak, L. Divol, C. R. Weber, L. F. B. Hopkins, D. S. Clark, E. L. Dewald, D. N. Fittinghoff, V. Geppert-Kleinrath, M. Hohenberger, S. Le Pape, T. Ma, A. G. MacPhee, D. A. Mariscal, E. Marley, A. S. Moore, L. A. Pickworth, P. L. Volegov, C. Wilde, O. A. Hurricane and P. K. Patel, Phys. Rev. Lett. **124,** 145001 (2020).
[32]A. G. MacPhee, V. A. Smalyuk, O. L. Landen, C. R. Weber, H. F. Robey, E. L. Alfonso, J. Biener, T. Bunn, J. W. Crippen, M. Farrell, S. Felker, J. E. Field, W. W. Hsing, C. Kong, J. Milovich, A. Moore, A. Nikroo, N. Rice, M. Stadermann and C. Wild, Phys. Plasmas **25,** 054505 (2018).
[33]J. A. Frenje, Plasma Phys. Contr. F **62,** 023001 (2020).
[34]H. Brysk, Plasma Phys. Contr. F **15,** 611 (1973).
[35]M. D. Cable and S. P. Hatchett, J. Appl. Phys. **62,** 2233 (1987).

[36]M. D. Cable, S. P. Hatchett and M. B. Nelson, Rev. Sci. Instrum. **63,** 4823 (1992).
[37]R. G. Watt, R. E. Chrien, K. A. Klare, T. J. Murphy, D. C. Wilson and S. Haan, Rev. Sci. Instrum. **72,** 846 (2001).
[38]H. Azechi, M. D. Cable and R. O. Stapf, Laser Part. Beams **9,** 119 (1991).
[39]D. L. Bleuel, C. B. Yeamans, L. A. Bernstein, R. M. Bionta, J. A. Caggiano, D. T. Casey, G. W. Cooper, O. B. Drury, J. A. Frenje, C. A. Hagmann, R. Hatarik, J. P. Knauer, M. G. Johnson, K. M. Knittel, R. J. Leeper, J. M. McNaney, M. Moran, C. L. Ruiz and D. H. G. Schneider, Rev. Sci. Instrum. **83,** 10d313 (2012).
[40]R. M. Bionta, G. P. Grim, K. D. Hahn, E. P. Hartouni, E. A. Henry, H. Y. Khater, A. S. Moore and D. J. Schlossberg, Rev. Sci. Instrum. **92,** 043527 (2021).
[41]M. G. Johnson, D. T. Casey, J. A. Frenje, C. K. Li, F. H. Seguin, R. D. Petrasso, R. Ashabranner, R. Bionta, S. LePape, M. McKernan, A. Mackinnon, J. D. Kilkenny, J. Knauer and T. C. Sangster, Phys. Plasmas **20,** 042707 (2013).
[42]T. J. Murphy, Phys. Plasmas **21,** 072701 (2014).
[43]D. H. Munro, J. E. Field, R. Hatarik, J. L. Peterson, E. P. Hartouni, B. K. Spears and J. D. Kilkenny, Phys. Plasmas **24,** 056301 (2017).
[44]M. G. Johnson, J. P. Knauer, C. J. Cerjan, M. J. Eckart, G. P. Grim, E. P. Hartouni, R. Hatarik, J. D. Kilkenny, D. H. Munro, D. B. Sayre, B. K. Spears, R. M. Bionta, E. J. Bond, J. A. Caggiano, D. Callahan, D. T. Casey, T. Doppner, J. A. Frenje, V. Y. Glebov, O. Hurricane, A. Kritcher, S. LePape, T. Ma, A. Mackinnon, N. Meezan, P. Patel, R. D. Petrasso, J. E. Ralph, P. T. Springer and C. B. Yeamans, Phys. Rev. E **94,** 021202 (2016).
[45]D. J. Schlossberg, G. P. Grim, D. T. Casey, A. S. Moore, R. Nora, B. Bachmann, L. R. Benedetti, R. M. Bionta, M. J. Eckart, J. E. Field, D. N. Fittinghoff, M. G. Johnson, V. Geppert-Kleinrath, E. P. Hartouni, R. Hatarik, W. W. Hsing, L. C. Jarrott, S. F. Khan, J. D. Kilkenny, O. L. Landen, B. J. MacGowan, A. J. Mackinnon, K. D. Meaney, D. H. Munro, S. R. Nagel, A. Pak, P. K. Patel, B. K. Spears, P. L. Volegov and C. V. Young, Phys. Rev. Lett. **127,** 125001 (2021).
[46]S. P. Hatchett (private communication).
[47]J. D. Kilkenny, Rev. Sci. Instrum. **63,** 4688 (1992).
[48]J. S. Milnes, C. J. Horsfield, M. S. Rubery, V. Y. Glebov and H. W. Herrmann, Rev. Sci. Instrum. **83,** 10d301 (2012).
[49]J. S. Milnes, C. J. Horsfield, T. M. Conneely and J. Howorth, Rev. Sci. Instrum. **85,** 11e601 (2014).
[50]R. Lauck, M. Brandis, B. Bromberger, V. Dangendorf, M. B. Goldberg, I. Mor, K. Tittelmeier and D. Vartsky, Ieee T. Nucl. Sci. **56,** 989 (2009).
[51]R. Hatarik, L. A. Bernstein, J. A. Caggiano, M. L. Carman, D. H. G. Schneider, N. P. Zaitseva and M. Wiedeking, Rev. Sci. Instrum. **83,** 10d911 (2012).
[52]V. Y. Glebov, C. J. Forrest, K. L. Marshall, M. Romanofsky, T. C. Sangster, M. J. Shoup and C. Stoeckl, Rev. Sci. Instrum. **85,** 11e102 (2014).
[53]V. Y. Glebov, T. C. Sangster, C. Stoeckl, J. P. Knauer, W. Theobald, K. L. Marshall, M. J. Shoup, T. Buczek, M. Cruz, T. Duffy, M. Romanofsky, M. Fox, A. Pruyne, M. J. Moran, R. A. Lerche, J. McNaney, J. D. Kilkenny, M. J. Eckart, D. Schneider, D. Munro, W. Stoeffl, R. Zacharias, J. J. Haslam, T. Clancy, M. Yeoman, D. Warwas, C. J. Horsfield, J. L. Bourgade, O. Landoas, L. Disdier, G. A. Chandler and R. J. Leeper, Rev. Sci. Instrum. **81,** 10d325 (2010).

[54]V. Y. Glebov, C. Forrest, J. P. Knauer, A. Pruyne, M. Romanofsky, T. C. Sangster, M. J. Shoup, C. Stoeckl, J. A. Caggiano, M. L. Carman, T. J. Clancy, R. Hatarik, J. McNaney and N. P. Zaitseva, Rev. Sci. Instrum. **83,** 10d309 (2012).
[55]A. S. Moore, D. J. Schlossberg, E. P. Hartouni, D. Sayre, M. J. Eckart, R. Hatarik, F. Barbosa, J. Root, C. Waltz, B. Beeman, M. S. Rubery and G. P. Grim, Rev. Sci. Instrum. **89,** 10i120 (2018).
[56]'See' Document No. UCRL-7032 (J. E. Doyle and W. C. Dickenson, The Cherenkov response of lucite and quartz to gamma and fast neutron radiation, 1962).
[57]D. T. Casey, J. A. Frenje, M. G. Johnson, F. H. Seguin, C. K. Li, R. D. Petrasso, V. Y. Glebov, J. Katz, J. Magoon, D. D. Meyerhofer, T. C. Sangster, M. Shoup, J. Ulreich, R. C. Ashabranner, R. M. Bionta, A. C. Carpenter, B. Felker, H. Y. Khater, S. LePape, A. MacKinnon, M. A. McKernan, M. Moran, J. R. Rygg, M. F. Yeoman, R. Zacharias, R. J. Leeper, K. Fletcher, M. Farrell, D. Jasion, J. Kilkenny and R. Paguio, Rev. Sci. Instrum. **84,** 043506 (2013).
[58]E. A. Sunden, H. Sjostrand, S. Conroy, G. Ericsson, M. G. Johnson, L. Giacomelli, C. Hellesen, A. Hjalmarsson, E. Ronchi, M. Weiszflog, J. Kallne, G. Gorini, M. Tardocchi, A. Combo, N. Cruz, A. Batista, R. Pereira, R. Fortuna, J. Sousa and S. Popovichev, Nucl. Instrum. Meth. A **610,** 682 (2009).
[59]J. A. Frenje, D. T. Casey, C. K. Li, J. R. Rygg, F. H. Seguin, R. D. Petrasso, V. Yu Glebov, D. D. Meyerhofer, T. C. Sangster, S. Hatchett, S. Haan, C. Cerjan, O. Landen, M. Moran, P. Song, D. C. Wilson and R. J. Leeper, Rev. Sci. Instrum. **79,** 10e502 (2008).
[60]D. T. Casey, J. A. Frenje, F. H. Seguin, C. K. Li, M. J. Rosenberg, H. Rinderknecht, M. J. E. Manuel, M. G. Johnson, J. C. Schaeffer, R. Frankel, N. Sinenian, R. A. Childs, R. D. Petrasso, V. Y. Glebov, T. C. Sangster, M. Burke and S. Roberts, Rev. Sci. Instrum. **82,** 073502 (2011).
[61]J. A. Frenje, D. T. Casey, C. K. Li, F. H. Seguin, R. D. Petrasso, V. Y. Glebov, P. B. Radha, T. C. Sangster, D. D. Meyerhofer, S. P. Hatchett, S. W. Haan, C. J. Cerjan, O. L. Landen, K. A. Fletcher and R. J. Leeper, Phys. Plasmas **17,** 056311 (2010).
[62]M. G. Johnson, J. A. Frenje, D. T. Casey, C. K. Li, F. H. Seguin, R. Petrasso, R. Ashabranner, R. M. Bionta, D. L. Bleuel, E. J. Bond, J. A. Caggiano, A. Carpenter, C. J. Cerjan, T. J. Clancy, T. Doeppner, M. J. Eckart, M. J. Edwards, S. Friedrich, S. H. Glenzer, S. W. Haan, E. P. Hartouni, R. Hatarik, S. P. Hatchett, O. S. Jones, G. Kyrala, S. Le Pape, R. A. Lerche, O. L. Landen, T. Ma, A. J. MacKinnon, M. A. McKernan, M. J. Moran, E. Moses, D. H. Munro, J. McNaney, H. S. Park, J. Ralph, B. Remington, J. R. Rygg, S. M. Sepke, V. Smalyuk, B. Spears, P. T. Springer, C. B. Yeamans, M. Farrell, D. Jasion, J. D. Kilkenny, A. Nikroo, R. Paguio, J. P. Knauer, V. Y. Glebov, T. C. Sangster, R. Betti, C. Stoeckl, J. Magoon, M. J. Shoup, G. P. Grim, J. Kline, G. L. Morgan, T. J. Murphy, R. J. Leeper, C. L. Ruiz, G. W. Cooper and A. J. Nelson, Rev. Sci. Instrum. **83,** 10d308 (2012).
[63]M. G. Johnson, J. A. Frenje, R. M. Bionta, D. T. Casey, M. J. Eckart, M. P. Farrell, G. P. Grim, E. P. Hartouni, R. Hatarik, M. Hoppe, J. D. Kilkenny, C. K. Li, R. D. Petrasso, H. G. Reynolds, D. B. Sayre, M. E. Schoff, F. H. Seguin, K. Skulina and C. B. Yeamans, Rev. Sci. Instrum. **87,** 11d816 (2016).
[64]M. G. Johnson, T. M. Johnson, B. J. Lahmann, F. H. Seguin, B. Sperry, N. Bhandarkar, R. M. Bionta, E. Casco, D. T. Casey, A. J. Mackinnon, N. Masters, A. Moore, A. Nikroo,

M. Hoppe, R. Mohammed, W. Sweet, C. Freeman, V. Picciotto, J. Roumell and J. A. Frenje, Rev. Sci. Instrum. **93,** 083513 (2022).
[65]J. A. Frenje, T. J. Hilsabeck, C. W. Wink, P. Bell, R. Bionta, C. Cerjan, M. G. Johnson, J. D. Kilkenny, C. K. Li, F. H. Seguin and R. D. Petrasso, Rev. Sci. Instrum. **87,** 11d806 (2016).
[66]C. E. Parker, J. A. Frenje, M. G. Johnson, D. J. Schlossberg, H. G. Reynolds, L. B. Hopkins, R. Bionta, D. T. Casey, S. J. Felker, T. J. Hilsabeck, J. D. Kilkenny, C. K. Li, A. J. Mackinnon, H. Robey, M. E. Schoff, F. H. Seguin, C. W. Wink and R. D. Petrasso, Rev. Sci. Instrum. **89,** 113508 (2018).
[67]C. E. Parker, J. A. Frenje, O. H. W. Siegmund, C. J. Forrest, V. Y. Glebov, J. D. Kendrick, C. W. Wink, M. G. Johnson, T. J. Hilsabeck, S. T. Ivancic, J. Katz, J. D. Kilkenny, B. Lahmann, C. K. Li, F. H. Seguin, C. M. Sorce, C. Trosseille and R. D. Petrasso, Rev. Sci. Instrum. **90,** 103306 (2019).
[68]J. H. Kunimune, J. A. Frenje, G. P. A. Berg, C. A. Trosseille, R. C. Nora, C. S. Waltz, A. S. Moore, J. D. Kilkenny and A. J. Mackinnon, Rev. Sci. Instrum. **92,** 033514 (2021).
[69]G. P. A. Berg, J. A. Frenje, J. H. Kunimune, C. A. Trosseille, M. Couder, J. D. Kilkenny, A. J. Mackinnon, A. S. Moore, C. S. Waltz and M. C. Wiescher, Rev. Sci. Instrum. **93,** 033505 (2022).
[70]T. J. Hilsabeck, J. A. Frenje, J. D. Hares and C. W. Wink, Rev. Sci. Instrum. **87,** 11d807 (2016).
[71]J. H. Kunimune, M. G. Johnson, A. S. Moore, C. A. Trosseille, T. M. Johnson, G. P. A. Berg, A. J. Mackinnon, J. D. Kilkenny and J. A. Frenje, Rev. Sci. Instrum. **93,** 083511 (2022).
[72]R. Berger, D. D. Rathman, B. M. Tyrrell, E. J. Kohler, M. K. Rose, R. A. Murphy, T. S. Perry, H. F. Robey, F. A. Weber, D. M. Craig, A. M. Soares, S. P. Vernon and R. K. Reich, Ieee J. Solid-St. Circ. **43,** 1940 (2008).
[73]R. K. Reich, D. D. Rathman, D. M. O'Mara, D. J. Young, A. H. Loomis, E. J. Kohler, R. M. Osgood, R. A. Murphy, M. Rose, R. Berger, S. A. Watson, M. D. Ulibarri, T. Perry and B. B. Kosicki, Rev. Sci. Instrum. **74,** 2027 (2003).
[74]A. T. Teruya, S. P. Vernon, J. D. Moody, W. W. Hsing, C. G. Brown, M. Griffin, A. S. Mead and V. Tran, *Proceedings of SPIE Optical Engineering + Applications,* San Diego, CA, 2012, (OCt 15, 2012).
[75]L. Claus, T. England, L. Fang, G. Robertson, M. Sanchez, D. Trotter, A. Carpenter, M. Dayton, P. Patel and J. L. Porter, *Proceedings of SPIE Optical Engineering + Applications,* San Diego, California, 2017, (SPIE).
[76]Q. Looker, A. P. Colombo and J. L. Porter, Rev. Sci. Instrum. **92,** 053504 (2021).
[77]L. R. Benedetti, N. E. Palmer, E. R. Hurd, C. E. Durand, A. C. Carpenter, M. S. Dayton, B. Golick, J. P. Holder, C. Trosseille, K. Werellapatha and M. G. Gorman, Rev. Sci. Instrum. **92,** 044708 (2021).
[78]Q. Looker, A. P. Colombo, M. Kimmel and J. L. Porter, Rev. Sci. Instrum. **91,** 043502 (2020).
[79]H. Chen, D. T. Woods, O. S. Jones, L. R. Benedetti, E. L. Dewald, N. Izumi, S. A. MacLaren, N. B. Meezan, J. D. Moody, N. E. Palmer, M. B. Schneider and M. Vandenboomgaerde, Phys. Plasmas **27,** 022702 (2020).
[80]H. Chen, N. Palmer, M. Dayton, A. Carpenter, M. B. Schneider, P. M. Bell, D. K. Bradley, L. D. Claus, L. Fang, T. Hilsabeck, M. Hohenberger, O. S. Jones, J. D.

Kilkenny, M. W. Kimmel, G. Robertson, G. Rochau, M. O. Sanchez, J. W. Stahoviak, D. C. Trotter and J. L. Porter, Rev. Sci. Instrum. **87,** 11e203 (2016).
[81]H. Chen, B. Golick, N. Palmer, A. Carpenter, L. D. Claus, M. Dayton, J. Dean, C. Durand, B. Funsten, R. B. Petre, C. M. Hardy, J. Hill, J. Holder, E. Hurd, N. Izumi, J. Kehl, S. Khan, C. Macaraeg, M. O. Sanchez, T. Sarginson, M. B. Schneider and C. Trosseille, Rev. Sci. Instrum. **92,** 033506 (2021).
[82]J. R. Rygg, R. F. Smith, A. E. Lazicki, D. G. Braun, D. E. Fratanduono, R. G. Kraus, J. M. McNaney, D. C. Swift, C. E. Wehrenberg, F. Coppari, M. F. Ahmed, M. A. Barrios, K. J. M. Blobaum, G. W. Collins, A. L. Cook, P. Di Nicola, E. G. Dzenitis, S. Gonzales, B. F. Heidl, M. Hohenberger, A. House, N. Izumi, D. H. Kalantar, S. F. Khan, T. R. Kohut, C. Kumar, N. D. Masters, D. N. Polsin, S. P. Regan, C. A. Smith, R. M. Vignes, M. A. Wall, J. Ward, J. S. Wark, T. L. Zobrist, A. Arsenlis and J. H. Eggert, Rev. Sci. Instrum. **91,** 043902 (2020).
[83]T. Ao, D. V. Morgan, B. S. Stoltzfus, K. N. Austin, J. Usher, E. Breden, L. M. Pacheco, S. Dean, J. L. Brown, S. Duwal, H. Fan, P. Kalita, M. D. Knudson, M. A. Rodriguez and J. M. D. Lane, Rev. Sci. Instrum. **93,** 053909 (2022).
[84]R. D. Prosser, J. Phys. E Sci. Instrum. **9,** 57 (1976).
[85]J. D. Mcgee, J. Beesley and A. D. Berg, J. Sci. Instrum. **43,** 153 (1966).
[86]M. F. Ahmed, A. House, R. F. Smith, J. Ayers, Z. S. Lamb and D. W. Swift, *Proceedings of Proc Spie,* San Diego, California, 2013, (SPIE).
[87]S. R. Nagel, T. J. Hilsabeck, P. M. Bell, D. K. Bradley, M. J. Ayers, M. A. Barrios, B. Felker, R. F. Smith, G. W. Collins, O. S. Jones, J. D. Kilkenny, T. Chung, K. Piston, K. S. Raman, B. Sammuli, J. D. Hares and A. K. L. Dymoke-Bradshaw, Rev. Sci. Instrum. **83,** 10e116 (2012).
[88]S. R. Nagel, T. J. Hilsabeck, P. M. Bell, D. K. Bradley, M. J. Ayers, K. Piston, B. Felker, J. D. Kilkenny, T. Chung, B. Sammuli, J. D. Hares and A. K. L. Dymoke-Bradshaw, Rev. Sci. Instrum. **85,** 11e504 (2014).
[89]S. R. Nagel, L. R. Benedetti, D. K. Bradley, T. J. Hilsabeck, N. Izumi, S. Khan, G. A. Kyrala, T. Ma and A. Pak, Rev. Sci. Instrum. **87,** 11e311 (2016).
[90]H. Geppert-Kleinrath, Y. Kim, K. D. Meaney, H. W. Herrmann, N. M. Hoffman, A. Kritcher, J. A. Carrera and S. Gales, High Energy Dens. Phys. **37,** 100862 (2020).
[91]A. K. L. Dymoke-Bradshaw, J. D. Hares, J. Milnes, H. W. Herrmann, C. J. Horsfield, S. G. Gales, A. Leatherland, T. Hilsabeck and J. D. Kilkenny, Rev. Sci. Instrum. **89,** 10i137 (2018).
[92]F. J. Marshall, R. E. Bahr, V. N. Goncharov, V. Y. Glebov, B. Peng, S. P. Regan, T. C. Sangster and C. Stoeckl, Rev. Sci. Instrum. **88,** 093702 (2017).
[93]K. Engelhorn, T. J. Hilsabeck, J. Kilkenny, D. Morris, T. M. Chung, A. Dymoke-Bradshaw, J. D. Hares, P. Bell, D. Bradley, A. C. Carpenter, M. Dayton, S. R. Nagel, L. Claus, J. Porter, G. Rochau, M. Sanchez, S. Ivancic, C. Sorce and W. Theobald, Rev. Sci. Instrum. **89,** 10g123 (2018).
[94]S. R. Nagel, A. C. Carpenter, J. Park, M. S. Dayton, P. M. Bell, D. K. Bradley, B. T. Funsten, B. W. Hatch, S. Heerey, J. M. Hill, J. P. Holder, E. R. Hurd, C. C. Macaraeg, P. B. Patel, R. B. Petre, K. Piston, C. A. Trosseille, K. Engelhorn, T. J. Hilsabeck, T. M. Chung, A. K. L. Dymoke-Bradshaw, J. D. Hares, L. D. Claus, T. D. England, B. B. Mitchell, J. L. Porter, G. Robertson and M. O. Sanchez, Rev. Sci. Instrum. **89,** 10g125 (2018).

[95]W. Theobald, C. Sorce, M. Bedzyk, S. T. Ivancic, F. J. Marshall, C. Stoeckl, R. C. Shah, M. Lawrie, S. P. Regan, T. C. Sangster, E. M. Campbell, T. J. Hilsabeck, K. Englehorn, J. D. Kilkenny, D. Morris, T. M. Chung, J. D. Hares, A. K. L. Dymoke-Bradshaw, P. Bell, J. Celeste, A. C. Carpenter, M. Dayton, D. K. Bradley, M. C. Jackson, L. Pickworth, S. R. Nagel, G. Rochau, J. Porter, M. Sanchez, L. Claus, G. Robertson and Q. Looker, Rev. Sci. Instrum. **89,** 10g117 (2018).
[96]C. Trosseille, C. E. Durand, E. R. Hurd, M. S. Dayton, K. Engelhorn, G. N. Hall, J. P. Holder, O. L. Landen, A. C. Carpenter and S. R. Nagel, Rev. Sci. Instr. **93,** 023505 (2022).
[97]C. Trosseille, A. M. Garafalo, M. S. Dayton, C. E. Durand, B. T. Funsten, T. J. Hilsabeck, E. Imhoff, S. B. Morioka, K. W. Piston, A. E. Raymond, A. C. Welton, L. Claus, M. Sanchez, J. D. Hares, T. M. Chung, A. C. Carpenter and S. R. Nagel, Rev. Sci. Instr. **93,** 083516 (2022).
[98]S. P. Regan, R. Epstein, B. A. Hammel, L. J. Suter, J. Ralph, H. Scott, M. A. Barrios, D. K. Bradley, D. A. Callahan, C. Cerjan, G. W. Collins, S. N. Dixit, T. Doeppner, M. J. Edwards, D. R. Farley, S. Glenn, S. H. Glenzer, I. E. Golovkin, S. W. Haan, A. Hamza, D. G. Hicks, N. Izumi, J. D. Kilkenny, J. L. Kline, G. A. Kyrala, O. L. Landen, T. Ma, J. J. MacFarlane, R. C. Mancini, R. L. McCrory, N. B. Meezan, D. D. Meyerhofer, A. Nikroo, K. J. Peterson, T. C. Sangster, P. Springer and R. P. J. Town, Phys. Plasmas **19,** 056307 (2012).
[99]S. P. Regan, R. Epstein, B. A. Hammel, L. J. Suter, H. A. Scott, M. A. Barrios, D. K. Bradley, D. A. Callahan, C. Cerjan, G. W. Collins, S. N. Dixit, T. Doppner, M. J. Edwards, D. R. Farley, K. B. Fournier, S. Glenn, S. H. Glenzer, I. E. Golovkin, S. W. Haan, A. Hamza, D. G. Hicks, N. Izumi, O. S. Jones, J. D. Kilkenny, J. L. Kline, G. A. Kyrala, O. L. Landen, T. Ma, J. J. MacFarlane, A. J. MacKinnon, R. C. Mancini, R. L. McCrory, N. B. Meezan, D. D. Meyerhofer, A. Nikroo, H. S. Park, J. Ralph, B. A. Remington, T. C. Sangster, V. A. Smalyuk, P. T. Springer and R. P. J. Town, Phys. Rev. Lett. **111,** 045001 (2013).
[100]T. Ma, H. Chen, P. K. Patel, M. B. Schneider, M. A. Barrios, D. T. Casey, H. K. Chung, B. A. Hammel, L. F. B. Hopkins, L. C. Jarrott, S. F. Khan, B. Lahmann, R. Nora, M. J. Rosenberg, A. Pak, S. P. Regan, H. A. Scott, H. Sio, B. K. Spears and C. R. Weber, Rev. Sci. Instrum. **87,** 11e327 (2016).
[101]M. A. Barrios, D. A. Liedahl, M. B. Schneider, O. Jones, G. V. Brown, S. P. Regan, K. B. Fournier, A. S. Moore, J. S. Ross, O. Landen, R. L. Kauffman, A. Nikroo, J. Kroll, J. Jaquez, H. Huang, S. B. Hansen, D. A. Callahan, D. E. Hinkel, D. Bradley and J. D. Moody, Phys. Plasmas **23,** 056307 (2016).
[102]K. B. Fournier, M. J. May, J. D. Colvin, M. A. Barrios, J. R. Patterson and S. P. Regan, Phys. Rev. E **88,** 033104 (2013).
[103]M. A. Barrios, S. P. Regan, K. B. Fournier, R. Epstein, R. Smith, A. Lazicki, R. Rygg, D. E. Fratanduono, J. Eggert, H. S. Park, C. Huntington, D. K. Bradley, O. L. Landen and G. W. Collins, Rev. Sci. Instrum. **85,** 11d502 (2014).
[104]F. Perez, G. E. Kemp, S. P. Regan, M. A. Barrios, J. Pino, H. Scott, S. Ayers, H. Chen, J. Emig, J. D. Colvin, M. Bedzyk, M. J. Shoup, A. Agliata, B. Yaakobi, F. J. Marshall, R. A. Hamilton, J. Jaquez, M. Farrell, A. Nikroo and K. B. Fournier, Rev. Sci. Instrum. **85,** 11d613 (2014).

[105]M. J. May, J. Weaver, K. Widmann, G. E. Kemp, D. Thorn, J. D. Colvin, M. B. Schneider, A. Moore and B. E. Blue, Rev. Sci. Instrum. **87,** 11e330 (2016).
[106]J. D. Kilkenny, R. W. Lee, M. H. Key and J. G. Lunney, Phys. Rev. A **22,** 2746 (1980).
[107]C. J. Keane, B. A. Hammel, D. R. Kania, J. D. Kilkenny, R. W. Lee, A. L. Osterheld, L. J. Suter, R. C. Mancini, C. F. Hooper and N. D. Delamater, Phys. Fluids B - Plas. Phys. **5,** 3328 (1993).
[108]A. G. MacPhee, A. K. L. Dymoke-Bradshaw, J. D. Hares, J. Hassett, B. W. Hatch, A. L. Meadowcroft, P. M. Bell, D. K. Bradley, P. S. Datte, O. L. Landen, N. E. Palmer, K. W. Piston, V. V. Rekow, T. J. Hilsabeck and J. D. Kilkenny, Rev. Sci. Instrum. **87,** 11e202 (2016).
[109]H. Chen, T. Ma, R. Nora, M. A. Barrios, H. A. Scott, M. B. Schneider, L. B. Hopkins, D. T. Casey, B. A. Hammel, L. C. Jarrott, O. L. Landen, P. K. Patel, M. J. Rosenberg and B. K. Spears, Phys. Plasmas **24,** 072715 (2017).
[110]T. A. Hall, J. Phys. E Sci. Instrum. **17,** 110 (1984).
[111]K. W. Hill, M. Bitter, L. Delgado-Aparicio, D. Johnson, R. Feder, P. Beiersdorfer, J. Dunn, K. Morris, E. Wang, M. Reinke, Y. Podpaly, J. E. Rice, R. Barnsley, M. O'Mullane and S. G. Lee, Rev. Sci. Instr. **81,** 10e322 (2010).
[112]P. M. Nilson, F. Ehrne, C. Mileham, D. Mastrosimone, R. K. Jungquist, C. Taylor, C. R. Stillman, S. T. Ivancic, R. Boni, J. Hassett, D. J. Lonobile, R. W. Kidder, M. J. Shoup, A. A. Solodov, C. Stoeckl, W. Theobald, D. H. Froula, K. W. Hill, L. Gao, M. Bitter, P. Efthimion and D. D. Meyerhofer, Rev. Sci. Instrum. **87,** 11d504 (2016).
[113]L. Gao, B. F. Kraus, K. W. Hill, M. B. Schneider, A. Christopherson, B. Bachmann, M. Bitter, P. Efthimion, N. Pablant, R. Betti, C. Thomas, D. Thorn, A. G. MacPhee, S. Khan, R. Kauffman, D. Liedahl, H. Chen, D. Bradley, J. Kilkenny, B. Lahmann, E. Stambulchik and Y. Maron, Phys. Rev. Lett. **128,** 185002 (2022).
[114]A. G. MacPhee, P. M. Bell, D. Boyle, A. C. Carpenter, L. Claus, M. Dayton, J. Dean, A. K. L. Dymoke-Bradshaw, C. Durand, B. Funsten, A. Garafalo, B. P. Golick, J. D. Hares, J. Hill, J. M. Kehl, S. F. Khan, J. D. Kilkenny, M. J. MacDonald, D. Maheshwari, I. J. Mccubbin, S. R. Nagel, P. R. Nyholm, N. E. Palmer, R. B. Petre, M. Sanchez, M. B. Schneider, M. O. Schoelmerich, S. Stoupin and A. Welton, Rev. Sci. Instrum. **93,** 083519 (2022).
[115]M. S. Schollmeier, M. Geissel, J. E. Shores, I. C. Smith and J. L. Porter, Appl. Optics **54,** 5147 (2015).
[116]K. R. Carpenter, R. C. Mancini, E. C. Harding, A. J. Harvey-Thompson, M. Geissel, M. R. Weis, S. B. Hansen, K. J. Peterson and G. A. Rochau, Phys. Plasmas **27,** 052704 (2020).
[117]E. C. Harding, (2022, in publication).
[118]G. N. Hall, C. M. Krauland, M. S. Schollmeier, G. E. Kemp, J. G. Buscho, R. Hibbard, N. Thompson, E. R. Casco, M. J. Ayers, S. L. Ayers, N. B. Meezan, L. F. B. Hopkins, R. Nora, B. A. Hammel, L. Masse, J. E. Field, D. K. Bradley, P. Bell, O. L. Landen, J. D. Kilkenny, D. Mariscal, J. Park, T. J. McCarville, R. Lowe-Webb, D. Kalantar, T. Kohut and K. Piston, Rev. Sci. Instrum. **90,** 013702 (2019).
[119]J. A. Koch, J. E. Field, J. D. Kilkenny, E. Harding, G. A. Rochaud, A. M. Covington, E. C. Dutra, R. R. Freeman, G. N. Hall, M. J. Haugh and J. A. King, High Energy Dens. Phys. **23,** 184 (2017).

[120]L. M. Barker and R. E. Hollenbach, J. Appl. Phys. **43,** 4669 (1972).
[121]P. M. Celliers, G. W. Collins, L. B. Da Silva, D. M. Gold and R. Cauble, Appl. Phys. Lett. **73,** 1320 (1998).
[122]D. H. Munro, P. M. Celliers, G. W. Collins, D. M. Gold, L. B. Da Silva, S. W. Haan, R. C. Cauble, B. A. Hammel and W. W. Hsing, Phys. Plasmas **8,** 2245 (2001).
[123]P. M. Celliers, D. K. Bradley, G. W. Collins, D. G. Hicks, T. R. Boehly and W. J. Armstrong, Rev. Sci. Instrum. **75,** 4916 (2004).
[124]R. E. Olson, D. K. Bradley, G. A. Rochau, G. W. Collins, R. J. Leeper and L. J. Suter, Rev. Sci. Instrum. **77,** 10e523 (2006).
[125]T. R. Boehly, D. Munro, P. M. Celliers, R. E. Olson, D. G. Hicks, V. N. Goncharov, G. W. Collins, H. F. Robey, S. X. Hu, J. A. Morozas, T. C. Sangster, O. L. Landen and D. D. Meyerhofer, Phys. Plasmas **16,** 056302 (2009).
[126]S. A. MacLaren, H.-S. Park, P. M. Celliers, A. R. Cooper, M. E. Foord, M. B. Schneider, R. M. Seugling, R. J. Wallace, P. E. Young, T. R. Boehly and A. S. Moore, "Characterization of a halfraum x-ray drive using VISAR at the National Ignition Facility", American Physical Society Report 2011 Unpublished.
[127]P. M. Celliers, D. J. Erskine, C. M. Sorce, D. G. Braun, O. L. Landen and G. W. Collins, Rev. Sci. Instrum. **81,** (2010).
[128]J. D. Moody, H. F. Robey, P. M. Celliers, D. H. Munro, D. A. Barker, K. L. Baker, T. Doppner, N. L. Hash, L. B. Hopkins, K. LaFortune, O. L. Landen, S. LePape, B. J. MacGowan, J. E. Ralph, J. S. Ross, C. Widmayer, A. Nikroo, E. Giraldez and T. Boehly, Phys. Plasmas **21,** 092702 (2014).
[129]A. G. e. a. Macphee, **93,** (2022).
[130]E. M. Campbell, J. T. Hunt, E. S. Bliss, D. R. Speck and R. P. Drake, Rev. Sci. Instrum. **57,** 2101 (1986).
[131]H. F. Robey, T. R. Boehly, R. E. Olson, A. Nikroo, P. M. Celliers, O. L. Landen and D. D. Meyerhofer, Phys. Plasmas **17,** 012703 (2010).
[132]R. M. Malone, J. R. Bower, D. K. Bradley, G. A. Capelle, J. R. Celeste, P. M. Celliers, G. W. Collins, M. J. Eckart, J. H. Eggert, B. C. Frogget, R. L. Guyton, D. G. Hicks, M. I. Kaufman, B. J. MacGowan, S. Montelongo, A. W. N. B. Edmund, R. B. Robinson, T. W. Tunnell, P. W. Watts and P. G. Zapata, *Proceedings of Proc Spie,* 2005.
[133]S. G. Glendinning, J. Bolstad, D. G. Braun, M. J. Edwards, W. W. Hsing, B. F. Lasinski, H. Louis, A. Miles, J. Moreno, T. A. Peyser, B. A. Remington, H. F. Robey, E. J. Turano, C. P. Verdon and Y. Zhou, Phys. Plasmas **10,** 1931 (2003).
[134]R. L. Kauffman, H. N. Kornblum, D. W. Phillion, C. B. Darrow, B. F. Lasinski, L. J. Suter, A. R. Theissen, R. J. Wallace and F. Ze, Rev. Sci. Instrum. **66,** 678 (1995).
[135]M. Takeda, H. Ina and S. Kobayashi, J. Opt. Soc. Am. **72,** 156 (1982).
[136]M. R. Charest, P. Torres, C. T. Silbernagel and D. H. Kalantar, Rev. Sci. Instrum. **79,** 10f546 (2008).
[137]J. Oh, A. J. Schmitt, M. Karasik and S. P. Obenschain, Phys. Plasmas **28,** 032704 (2021).
[138]S. J. Ali, P. M. Celliers, S. Haan, T. R. Boehly, N. Whiting, S. H. Baxamusa, H. Reynolds, M. A. Johnson, J. D. Hughes, B. Watson, H. Huang, J. Biener, K. Engelhorn, V. A. Smalyuk and O. L. Landen, Phys. Plasmas **25,** 092708 (2018).

[139]J. L. Peebles, S. X. Hu, W. Theobald, V. N. Goncharov, N. Whiting, P. M. Celliers, S. J. Ali, G. Duchateau, E. M. Campbell, T. R. Boehly and S. P. Regan, Phys. Rev. E **99,** 063208 (2019).
[140]A. M. Saunders, S. J. Ali, H. S. Park, J. Eggert, F. Najjar, C. Huntington, T. Haxhimali, B. Morgan, Y. Ping and H. G. Rinderknecht, Aip Conf Proc **2272,** (2020).
[141]R. J. Ellis, J. E. Trebes, D. W. Phillion, J. D. Kilkenny, S. G. Glendinning, J. D. Wiedwald and R. A. Levesque, Rev. Sci. Instrum. **61,** 2759 (1990).
[142].
[143]J. R. Fein, D. J. Ampleford, J. K. Vogel, B. Kozioziemski, C. C. Walton, M. Wu, C. R. Ball, A. Ames, J. Ayers, P. Bell, C. J. Bourdon, D. Bradley, R. Bruni, G. S. Dunham, P. D. Gard, D. Johnson, K. Kilaru, C. Kirtley, P. W. Lake, A. Maurer, L. Nielsen-Weber, L. A. Pickworth, M. J. Pivovaroff, B. Ramsey, O. J. Roberts, G. A. Rochau, S. Romaine and M. Sullivan, Rev. Sci. Instrum. **89,** 10g115 (2018).
[144]P. R. Champey, Rev. Sci. Instrum. (2022).
[145]G. L. Morgan, R. R. Berggren, P. A. Bradley, F. H. Cverna, J. R. Faulkner, P. L. Gobby, J. A. Oertel, F. J. Swenson, J. A. Tegtmeier, R. B. Walton, M. D. Wilke, D. C. Wilson and L. Disdier, Rev. Sci. Instrum. **72,** 865 (2001).
[146]G. P. Grim, N. Guler, F. E. Merrill, G. L. Morgan, C. R. Danly, P. L. Volegov, C. H. Wilde, D. C. Wilson, D. S. Clark, D. E. Hinkel, O. S. Jones, K. S. Raman, N. Izumi, D. N. Fittinghoff, O. B. Drury, E. T. Alger, P. A. Arnold, R. C. Ashabranner, L. J. Atherton, M. A. Barrios, S. Batha, P. M. Bell, L. R. Benedetti, R. L. Berger, L. A. Bernstein, L. V. Berzins, R. Betti, S. D. Bhandarkar, R. M. Bionta, D. L. Bleuel, T. R. Boehly, E. J. Bond, M. W. Bowers, D. K. Bradley, G. K. Brunton, R. A. Buckles, S. C. Burkhart, R. F. Burr, J. A. Caggiano, D. A. Callahan, D. T. Casey, C. Castro, P. M. Celliers, C. J. Cerjan, G. A. Chandler, C. Choate, S. J. Cohen, G. W. Collins, G. W. Cooper, J. R. Cox, J. R. Cradick, P. S. Datte, E. L. Dewald, P. Di Nicola, J. M. Di Nicola, L. Divol, S. N. Dixit, R. Dylla-Spears, E. G. Dzenitis, M. J. Eckart, D. C. Eder, D. H. Edgell, M. J. Edwards, J. H. Eggert, R. B. Ehrlich, G. V. Erbert, J. Fair, D. R. Farley, B. Felker, R. J. Fortner, J. A. Frenje, G. Frieders, S. Friedrich, M. Gatu-Johnson, C. R. Gibson, E. Giraldez, V. Y. Glebov, S. M. Glenn, S. H. Glenzer, G. Gururangan, S. W. Haan, K. D. Hahn, B. A. Hammel, A. V. Hamza, E. P. Hartouni, R. Hatarik, S. P. Hatchett, C. Haynam, M. R. Hermann, H. W. Herrmann, D. G. Hicks, J. P. Holder, D. M. Holunga, J. B. Horner, W. W. Hsing, H. Huang, M. C. Jackson, K. S. Jancaitis, D. H. Kalantar, R. L. Kauffman, M. I. Kauffman, S. F. Khan, J. D. Kilkenny, J. R. Kimbrough, R. Kirkwood, J. L. Kline, J. P. Knauer, K. M. Knittel, J. A. Koch, T. R. Kohut, B. J. Kozioziemski, K. Krauter, G. W. Krauter, A. L. Kritcher, J. Kroll, G. A. Kyrala, K. N. La Fortune, G. LaCaille, L. J. Lagin, T. A. Land, O. L. Landen, D. W. Larson, D. A. Latray, R. J. Leeper, T. L. Lewis, S. LePape, J. D. Lindl, R. R. Lowe-Webb, T. Ma, B. J. MacGowan, A. J. MacKinnon, A. G. MacPhee, R. M. Malone, T. N. Malsbury, E. Mapoles, C. D. Marshall, D. G. Mathisen, P. McKenty, J. M. McNaney, N. B. Meezan, P. Michel, J. L. Milovich, J. D. Moody, A. S. Moore, M. J. Moran, K. Moreno, E. I. Moses, D. H. Munro, B. R. Nathan, A. J. Nelson, A. Nikroo, R. E. Olson, C. Orth, A. E. Pak, E. S. Palma, T. G. Parham, P. K. Patel, R. W. Patterson, R. D. Petrasso, R. Prasad, J. E. Ralph, S. P. Regan, H. Rinderknecht, H. F. Robey, G. F. Ross, C. L. Ruiz, F. H. Seguin, J. D. Salmonson, T. C. Sangster, J. D. Sater, R. L. Saunders, M. B. Schneider, D. H. Schneider, M. J. Shaw, N. Simanovskaia, B. K. Spears, P. T. Springer, C. Stoeckl, W. Stoeffl, L. J. Suter, C. A. Thomas, R. Tommasini,

R. P. Town, A. J. Traille, B. Van Wonterghem, R. J. Wallace, S. Weaver, S. V. Weber, P. J. Wegner, P. K. Whitman, K. Widmann, C. C. Widmayer, R. D. Wood, B. K. Young, R. A. Zacharias and A. Zylstra, Phys. Plasmas **20,** 056320 (2013).
[147]J. S. Ross, P. Datte, L. Divol, J. Galbraith, D. H. Froula, S. H. Glenzer, B. Hatch, J. Katz, J. Kilkenny, O. Landen, A. M. Manuel, W. Molander, D. S. Montgomery, J. D. Moody, G. Swadling and J. Weaver, Rev. Sci. Instrum. **87,** 11e510 (2016).
[148]J. Katz, R. Boni, C. Sorce, R. Follett, M. J. Shoup and D. H. Froula, Rev. Sci. Instrum. **83,** 10e349 (2012).
[149]F. Fiuza, G. F. Swadling, A. Grassi, H. G. Rinderknecht, D. P. Higginson, D. D. Ryutov, C. Bruulsema, R. P. Drake, S. Funk, S. Glenzer, G. Gregori, C. K. Li, B. B. Pollock, B. A. Remington, J. S. Ross, W. Rozmus, Y. Sakawa, A. Spitkovsky, S. Wilks and H. S. Park, Nat. Phys. **16,** 916 (2020).
[150]J. D. Kilkenny, M. D. Cable, E. M. Campbell, L. W. Coleman, D. L. Correll, R. P. Drake, R. J. Ellis, S. G. Glendinning, C. W. Hatcher and S. P. Hatchett, *Proceedings of Presented at the 12th International Conference on Plasma Physics and Controlled Nuclear Fusion Research,* 1988.
[151]*National Ignition Facility Conceptual Design Report*, Report UCRL-PROP-117093 ES (Lawrence Livermore National Laboratory, 1994).
[152]J. D. Kilkenny, M. D. Cable, C. A. Clower, B. A. Hammel, V. P. Karpenko, R. L. Kauffman, H. N. Kornblum, B. J. Macgowan, W. Olson, T. J. Orzechowski, D. W. Phillion, G. L. Tietbohl, J. E. Trebes, B. Chrien, B. Failor, A. Hauer, R. Hockaday, J. Oertel, R. Watt, C. Ruiz, G. Cooper, D. Hebron, R. Leeper, J. Porter and J. Knauer, Rev. Sci. Instrum. **66,** 288 (1995).
[153]*National Ignition Facility Functional Requirements and Primary Criteria Revision 1.3*, Report NIF-LLNL-93-058 (Lawrence Livermore National Laboratory, 1994).
[154]R. J. Leeper, G. A. Chandler, G. W. Cooper, M. S. Derzon, D. L. Fehl, D. E. Hebron, A. R. Moats, D. D. Noack, J. L. Porter, L. E. Ruggles, C. L. Ruiz, J. A. Torres, M. D. Cable, P. M. Bell, C. A. Clower, B. A. Hammel, D. H. Kalantar, V. P. Karpenko, R. L. Kauffman, J. D. Kilkenny, F. D. Lee, R. A. Lerche, B. J. MacGowan, M. J. Moran, M. B. Nelson, W. Olson, T. J. Orzechowski, T. W. Phillips, D. Ress, G. L. Tietbohl, J. E. Trebes, R. J. Bartlett, R. Berggren, S. E. Caldwell, R. E. Chrien, B. H. Failor, J. C. Fernandez, A. Hauer, G. Idzorek, R. G. Hockaday, T. J. Murphy, J. Oertel, R. Watt, M. Wilke, D. K. Bradley, J. Knauer, R. D. Petrasso and C. K. Li, Rev. Sci. Instrum. **68,** 868 (1997).
[155]T. J. Murphy, C. W. Barnes, R. R. Berggren, P. Bradley, S. E. Caldwell, R. E. Chrien, J. R. Faulkner, P. L. Gobby, N. Hoffman, J. L. Jimerson, K. A. Klare, C. L. Lee, J. M. Mack, G. L. Morgan, J. A. Oertel, F. J. Swenson, P. J. Walsh, R. B. Walton, R. G. Watt, M. D. Wilke, D. C. Wilson, C. S. Young, S. W. Haan, R. A. Lerche, M. J. Moran, T. W. Phillips, T. C. Sangster, R. J. Leeper, C. L. Ruiz, G. W. Cooper, L. Disdier, A. Rouyer, A. Fedotoff, V. Y. Glebov, D. D. Meyerhofer, J. M. Soures, C. Stockl, J. A. Frenje, D. G. Hicks, C. K. Li, R. D. Petrasso, F. H. Seguin, K. Fletcher, S. Padalino and R. K. Fisher, Rev. Sci. Instrum. **72,** 773 (2001).
[156]J. A. Oertel, T. J. Murphy, R. R. Berggren, J. Faulkner, R. Schmell, D. Little, T. Archuleta, J. Lopez, J. Velarde and R. F. Horton, Rev. Sci. Instrum. **70,** 803 (1999).
[157]D. H. Edgell, D. K. Bradley, E. J. Bond, S. Burns, D. A. Callahan, J. Celeste, M. J. Eckart, V. Y. Glebov, D. S. Hey, G. Lacaille, J. D. Kilkenny, J. Kimbrough, A. J.

Mackinnon, J. Magoon, J. Parker, T. C. Sangster, M. J. Shoup, C. Stoeckl, T. Thomas and A. MacPhee, Rev. Sci. Instrum. **83,** 10e119 (2012).
[158]S. F. Khan, P. M. Bell, D. K. Bradley, S. R. Burns, J. R. Celeste, L. S. Dauffy, M. J. Eckart, M. A. Gerhard, C. Hagmann, D. I. Headley, J. P. Holder, N. Izumi, M. C. Jones, J. W. Kellogg, H. Y. Khater, J. R. Kimbrough, A. G. MacPhee, Y. P. Opachich, N. E. Palmer, R. B. Petre, A. J. L. Porter, R. T. Shelton, T. L. Thomas and J. B. Worden, *Proceedings of Proc Spie,* 2012.
[159]A. B. Reighard, S. G. Glendinning, P. E. Young, W. W. Hsing, M. Foord, M. Schneider, K. Lu, T. Dittrich, R. Wallace and C. Sorce, Rev. Sci. Instrum. **79,** 10e915 (2008).
[160]A. S. Moore, T. M. Guymer, J. L. Kline, J. Morton, M. Taccetti, N. E. Lanier, C. Bentley, J. Workman, B. Peterson, K. Mussack, J. Cowan, R. Prasad, M. Richardson, S. Burns, D. H. Kalantar, L. R. Benedetti, P. Bell, D. Bradley, W. Hsing and M. Stevenson, Rev. Sci. Instrum. **83,** 10e132 (2012).
[161]J. Benstead, A. S. Moore, M. F. Ahmed, J. Morton, T. M. Guymer, R. Soufli, T. Pardini, R. L. Hibbard, C. G. Bailey, P. M. Bell, S. Hau-Riege, M. Bedzyk, M. J. Shoup, S. Reagan, T. Agliata, R. Jungquist, D. W. Schmidt, L. B. Kot, W. J. Garbett, M. S. Rubery, J. W. Skidmore, E. Gullikson and F. Salmassi, Rev. Sci. Instrum. **87,** 055110 (2016).
[162]A. S. Moore, A. B. R. Cooper, M. B. Schneider, S. MacLaren, P. Graham, K. Lu, R. Seugling, J. Satcher, J. Klingmann, A. J. Comley, R. Marrs, M. May, K. Widmann, G. Glendinning, J. Castor, J. Sain, C. A. Back, J. Hund, K. Baker, W. W. Hsing, J. Foster, B. Young and P. Young, Phys. Plasmas **21,** 063303 (2014).
[163]B. Yaakobi, T. R. Boehly, D. D. Meyerhofer, T. J. B. Collins, B. A. Remington, P. G. Allen, S. M. Pollaine, H. E. Lorenzana and J. H. Eggert, Phys. Rev. Lett. **95,** 075501 (2005).
[164]J. R. Rygg, J. H. Eggert, A. E. Lazicki, F. Coppari, J. A. Hawreliak, D. G. Hicks, R. F. Smith, C. M. Sorce, T. M. Uphaus, B. Yaakobi and G. W. Collins, Rev. Sci. Instrum. **83,** 113904 (2012).
[165]L. R. Benedetti, J. H. Eggert, J. D. Kilkenny, D. K. Bradley, P. M. Bell, N. E. Palmer, R. B. Petre, B. F. Heidl, J. R. Rygg, T. R. Boehly, G. W. Collins and C. Sorce, *Proceedings of Aip Conf Proc,* 2018.
[166]S. Stoupin, D. B. Thorn, N. Ose, L. Gao, K. W. Hill, Y. Ping, F. Coppari, B. Kozioziemski, A. Krygier, H. Sio, J. Ayers, M. Bitter, B. Kraus, P. C. Efthimion and M. B. Schneider, Rev. Sci. Instrum. **92,** 053102 (2021).
[167]K. L. Baker, R. E. Stewart, P. T. Steele, S. P. Vernon and W. W. Hsing, Appl. Phys. Lett. **101,** 031107 (2012).
[168]D. A. Shaughnessy, C. A. Velsko, D. R. Jedlovec, C. B. Yeamans, K. J. Moody, E. Tereshatov, W. Stoeffl and A. Riddle, Rev. Sci. Instrum. **83,** 10d917 (2012).
[169]J. M. Gostic, D. A. Shaughnessy, K. T. Moore, I. D. Hutcheon, P. M. Grant and K. J. Moody, Rev. Sci. Instrum. **83,** 10d904 (2012).
[170]C. A. Back, J. D. Bauer, O. L. Landen, R. E. Turner, B. F. Lasinski, J. H. Hammer, M. D. Rosen, L. J. Suter and W. H. Hsing, Phys. Rev. Lett. **84,** 274 (2000).
[171]A. B. R. Cooper, M. B. Schneider, S. A. MacLaren, A. S. Moore, P. E. Young, W. W. Hsing, R. Seugling, M. E. Foord, J. D. Sain, M. J. May, R. E. Marrs, B. R. Maddox, K.

Lu, K. Dodson, V. Smalyuk, P. Graham, J. M. Foster, C. A. Back and J. F. Hund, Phys. Plasmas **20,** 033301 (2013).
[172]T. M. Guymer, A. S. Moore, J. Morton, J. L. Kline, S. Allan, N. Bazin, J. Benstead, C. Bentley, A. J. Comley, J. Cowan, K. Flippo, W. Garbett, C. Hamilton, N. E. Lanier, K. Mussack, K. Obrey, L. Reed, D. W. Schmidt, R. M. Stevenson, J. M. Taccetti and J. Workman, Phys. Plasmas **22,** 043303 (2015).
[173]A. M. Manuel, M. Millot, L. G. Seppala, G. Frieders, Z. Zeid, K. Christensen and P. M. Celliers, *Proceedings of Proc Spie,* 2015.
[174]B. Yaakobi, F. J. Marshall, T. R. Boehly, R. P. J. Town and D. D. Meyerhofer, J. Opt. Soc. Am. B **20,** 238 (2003).
[175]S. R. Nagel, K. S. Raman, C. M. Huntington, S. A. MacLaren, P. Wang, M. A. Barrios, T. Baumann, J. D. Bender, L. R. Benedetti, D. M. Doane, S. Felker, P. Fitzsimmons, K. A. Flippo, J. P. Holder, D. N. Kaczala, T. S. Perry, R. M. Seugling, L. Savage and Y. Zhou, Phys. Plasmas **24,** 072704 (2017).
[176]A. Casner, C. Mailliet, S. F. Khan, D. Martinez, N. Izumi, D. Kalantar, P. Di Nicola, J. M. Di Nicola, E. Le Bel, I. Igumenshchev, V. T. Tikhonchuk, B. A. Remington, L. Masse and V. A. Smalyuk, Plasma Phys. Contr. F. **60,** 014012 (2018).
[177]A. Do, L. A. Pickworth, B. J. Kozioziemski, A. M. Angulo, G. N. Hall, S. R. Nagel, D. K. Bradley, T. Mccarville and J. M. Ayers, Appl. Optics **59,** 10777 (2020).
[178]G. P. Grim, P. A. Bradley, T. A. Bredeweg, A. L. Keksis, M. M. Fowler, A. C. Hayes, G. Jungman, A. W. Obst, R. S. Rundberg, D. J. Vieira, J. B. Wilhelmy, L. A. Bernstein, C. J. Cerjan, R. J. Fortner, K. J. Moody, D. H. Schneider, D. A. Shaughnessy, W. Stoeffl and M. A. Stoyer, Rev. Sci. Instrum. **79,** 10e503 (2008).
[179]S. P. Vernon, M. E. Lowry, K. L. Baker, C. V. Bennett, J. R. Celeste, C. Cerjan, S. Haynes, V. J. Hernandez, W. W. Hsing, G. A. LaCaille, R. A. London, B. Moran, A. S. von Wittenau, P. T. Steele and R. E. Stewart, Rev. Sci. Instrum. **83,** 10d307 (2012).
[180]J. D. Kilkenny, P. M. Bell, D. K. Bradley, D. L. Bleuel, J. A. Caggiano, E. L. Dewald, W. W. Hsing, D. H. Kalantar, R. L. Kauffman, D. J. Larson, J. D. Moody, D. H. Schneider, M. B. Schneider, D. A. Shaughnessy, R. T. Shelton, W. Stoeffl, K. Widmann, C. B. Yeamans, S. H. Batha, G. P. Grim, H. W. Herrmann, F. E. Merrill, R. J. Leeper, J. A. Oertel, T. C. Sangster, D. H. Edgell, M. Hohenberger, V. Y. Glebov, S. P. Regan, J. A. Frenje, M. Gatu-Johnson, R. D. Petrasso, H. G. Rinderknecht, A. B. Zylstra, G. W. Cooper and C. Ruiz, Fusion Sci. Technol. **69,** 420 (2016).
[181]A. B. Zylstra, C. Yeamans, S. Le Pape, A. MacKinnon, M. Hohenberger, D. N. Fittinghoff, H. Herrmann, Y. Kim, P. B. Radha, P. W. McKenty, R. S. Craxton and M. Hoppe, Phys. Plasmas **27,** 124501 (2020).
[182]S. Le Pape, L. Divol, L. B. Hopkins, A. Mackinnon, N. B. Meezan, D. Casey, J. Frenje, H. Herrmann, J. McNaney, T. Ma, K. Widmann, A. Pak, G. Grimm, J. Knauer, R. Petrasso, A. Zylstra, H. Rinderknecht, M. Rosenberg, M. Gatu-Johnson and J. D. Kilkenny, Phys. Rev. Lett. **112,** 225002 (2014).
[183]A. M. Cok, R. S. Craxton and P. W. McKenty, Phys. Plasmas **15,** 082705 (2008).
[184]See OSTI.gov Document No. 7127515 (E. K. Storm, H. G. Ahlstrom and J. F. Holzrichter, "Exploding pusher targets illuminated using f/1 lenses at approx. 0. 4 TW", Palaiseau, France, October 5, 1976).

[185]P. M. B. S. Glenn, L.R. Benedetti, M.W. Bowers, D.K. Bradley, B. Golick, J.P. Holder, D.H. Kalantar, S.F. Khan, N. Simanovskaia,, *Proceedings of ICALEPCS2013,* San Francisco, CA, 2013, (Lawrence Livermore National Laboratory).
[186]L. F. Berzak Hopkins, N. B. Meezan, S. Le Pape, L. Divol, A. J. Mackinnon, D. D. Ho, M. Hohenberger, O. S. Jones, G. Kyrala, J. L. Milovich, A. Pak, J. E. Ralph, J. S. Ross, L. R. Benedetti, J. Biener, R. Bionta, E. Bond, D. Bradley, J. Caggiano, D. Callahan, C. Cerjan, J. Church, D. Clark, T. Döppner, R. Dylla-Spears, M. Eckart, D. Edgell, J. Field, D. N. Fittinghoff, M. Gatu Johnson, G. Grim, N. Guler, S. Haan, A. Hamza, E. P. Hartouni, R. Hatarik, H. W. Herrmann, D. Hinkel, D. Hoover, H. Huang, N. Izumi, S. Khan, B. Kozioziemski, J. Kroll, T. Ma, A. MacPhee, J. McNaney, F. Merrill, J. Moody, A. Nikroo, P. Patel, H. F. Robey, J. R. Rygg, J. Sater, D. Sayre, M. Schneider, S. Sepke, M. Stadermann, W. Stoeffl, C. Thomas, R. P. J. Town, P. L. Volegov, C. Wild, C. Wilde, E. Woerner, C. Yeamans, B. Yoxall, J. Kilkenny, O. L. Landen, W. Hsing and M. J. Edwards, Phys. Rev. Lett. **114,** 175001 (2015).
[187]J. S. Ross, D. Ho, J. Milovich, T. Döppner, J. McNaney, A. G. MacPhee, A. Hamza, J. Biener, H. F. Robey, E. L. Dewald, R. Tommasini, L. Divol, S. Le Pape, L. B. Hopkins, P. M. Celliers, O. Landen, N. B. Meezan and A. J. Mackinnon, Phys. Rev. E **91,** 021101 (2015).
[188]*2016 Inertial Confinement Fusion Program Framework*, Report DOE/NA-0044 (Department of Energy, NNSA, 2016).
[189]See OSTI.gov Document No. 1823688 (S. Ross, "The National Diagnostic Plan (NDP) for HED Science September 2021", Lawrence Livermore National Laboratory, September 2021).